Functional analysis of candidate orthologues of Synapse-Defective-1 (SYD-1) in mice

Inauguraldissertation

zur
Erlangung der Würde eines Doktors der Philosophie
vorgelegt der
Philosophisch-Naturwissenschaftlichen Fakultät
der Universität Basel

von

Corinna Wentzel
aus Aarbergen, Deutschland

Basel, 2013

genemigt von der Philosophisch-Naturwissenschaftlichen Fakultät

auf Antrag von:

Prof. Dr. Peter Scheiffele

Prof. Dr. Yves-Alain Barde

Basel, den 11.12.12

Prof. Dr. Jörg Schibler
Dekan der Philosophisch-
Naturwissenschaftlichen Fakultät

Table of Contents

Summary

Synapses are central processing units for neuronal communication. Therefore, the investigation of synapse development and the mechanisms underlying formation of pre- and postsynaptic structures are crucial for understanding directional information flow in the brain. The differentiation of presynaptic boutons encompasses a local re-organization of the actin cytoskeleton, recruitment of synaptic vesicles, and the assembly of vesicle release sites, the so-called active zones. Several trans-synaptic adhesion complexes, have been identified that can instruct this differentiation process, such as receptor tyrosine phosphatases and the neuroligin/neurexin complex. However, the intracellular mechanisms linking adhesion to the formation of mature active zones in mammalian cells have remained obscure.

Genetic screens have led to the identification of two cytoplasmic molecules, Synapse-Defective-1 and -2 (SYD-1, SYD-2) that are essential for active zone assembly downstream of cell surface receptors in *C.elegans* and *Drosophila* (Hallam et al, 2002; Owald et al, 2010; Zhen & Jin, 1999). In invertebrates, SYD-1 is required for the concentration of SYD-2/liprin-α at the presynapse where it interacts with the active zone protein ELKS-1/Bruchpilot (Dai et al, 2006). We have identified two mouse orthologues of SYD-1, which we named mSYD1A and mSYD1B (mouse Synapse-Defective-1A/B). As the invertebrate proteins, mSYD1A and mSYD1B contain a C2 and a GTPase activating (GAP) domain. mSYD1A is expressed in neurons during embryonic and postnatal development. The protein is present in synaptosomal membrane fractions, indicating that a pool of mSYD1A is associated with synapses.

Knockdown of mSYD1A in primary cultures of cerebellar granule cells leads to a decrease in synaptic vesicle clusters, which can be rescued presynaptically by re-expression of mSYD1A. Overexpression of mSYD1A increases synapse density. Using a FRET-based assay, we discovered that mSYD1A exhibits GAP activity towards the small GTPase RhoA. Intra-molecular interactions between the N-terminal domain and the GAP domain of mSYD1A inhibit GAP activity, whereas this inhibition can be released by targeting full-length mSYD1A to the plasma membrane. Using biochemical and Yeast-2-Hybrid assays, we identified mSYD1A interacting proteins that associate with the N-terminal domain and might serve as endogenous activators of mSYD1A function. Amongst these binding partners is the active zone protein liprin-α2. In a complex with liprin-α2, mSYD1A is recruited into plasma membrane clusters downstream of the synaptic receptor protein tyrosine phosphatase LAR in COS cells. Furthermore, we generated knockout mice for mSYD1A and mSYD1B and are beginning to analyze them.

Thus, we identified a novel regulator of presynaptic assembly called mSYD1A that is evolutionary conserved from *C.elegans* to mouse.

1. Introduction

1.1 General introduction

The nervous system is a complex network of billions of neurons that form a highly interconnected structure to control behavior and perception in animals (Williams & Herrup, 1988). To understand how the nervous system forms during development of the animal and how the network of nerve cells can shape and control an animal's actions is a major task of neurobiology until today. In the early 1900s, Santiago Ramón y Cajal pioneered the study of the brain by his microscopic analysis on the connection of nerve cells. Based on his observations, he established the "neuron doctrine", which postulates that the brain is composed of individual information processing units, the neurons, which are connected to each other. His doctrine contrasted the standpoint of Camillo Golgi, who believed that the brain is a continuous entity and was later proven wrong. During the last century, an amazing progress has been made and we are beginning to understand how neurons acquire their identity, how specific connections between nerve cells are formed and how synaptic transmission works. Here, especially the study of genes and their protein products has provided invaluable insight. Many of the recent advances in the field stem from the analysis of simple, genetically accessible organisms, such as the nematode *Caenorhabditis elegans* or the fruit fly *Drosophila melanogaster*. *C.elegans* hermaphrodites comprise of 302 neurons, with a stereotypic pattern of connectivity that has been completely mapped (Rankin et al, 1990), which facilitates the study of nervous system development compared to the complex neuronal network of higher organisms. Remarkably, many of the genes discovered in simple organisms have been conserved over millions of years of evolution and have been found to have similar functions in mammals. Therefore, results that have been obtained in invertebrate studies are often the starting point for the analyses of higher organisms.

1.2 Synapse formation

The correct formation of synapses is one of the most important events during brain development. Directional flow of information crucially depends on the asymmetric arrangement of synapses. In the central nervous system (CNS), synapses consist of a presynaptic terminal, a synaptic cleft and a postsynaptic accumulation of neurotransmitter receptors. The presynaptic bouton is filled with neurotransmitter-containing synaptic vesicles and possesses a proteinaceous matrix at its plasma membrane, the so-called active zone (Shen & Scheiffele, 2010; Ziv & Garner, 2004). In response to action potentials, coming into the presynaptic terminal, synaptic vesicles fuse with the presynaptic plasma membrane at the active zone and release their neurotransmitters into the synaptic cleft. Secreted neurotransmitters diffuse across the cleft and bind to postsynaptic receptors in the

postsynaptic membrane, thereby activating a signaling cascade in the receiving neuron. During development, choice of the right synaptic partner is essential for a correct wiring of the brain. Neurons have evolved several molecular mechanisms to ensure the specificity of their synaptic connections. These involve attractive signals from the future synaptic pair and inhibitory signals from surrounding neurons (Shen & Scheiffele, 2010). Furthermore, several transient connections have been reported, which serve as “synaptic placeholders” until the correct future partner has been found to establish a stable connection.

In addition to synaptic specificity, the establishment of synaptic diversity is a fundamentally important process during brain development. The properties of a neuronal circuit depend not only on the pattern of connectivity, but also on the diverse properties of individual synapses in this circuit (Abbott & Regehr, 2004).

How synaptic contacts are established and how forming synapses differentiate into mature transmission machineries with the right synaptic properties needed, has been intensely studied during the last decades. In principle, synapse formation is thought to consist of the following steps: (1) initial contact between two cells, (2) formation of a synaptic junction and (3) maturation of this junction into mature synapses with specific synaptic properties (Fox & Umemori, 2006) (figure 1).

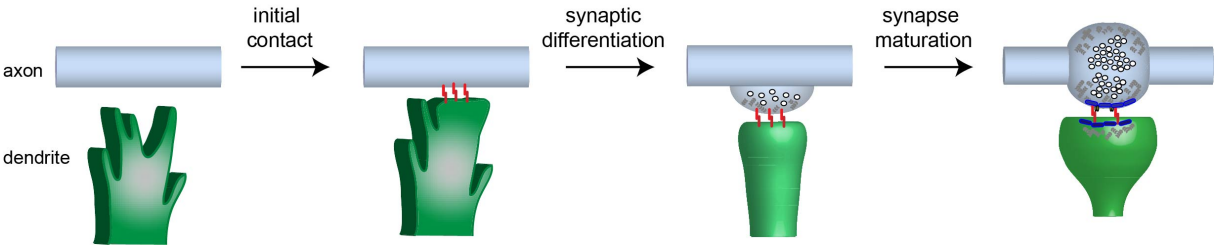

Figure 1 – Steps of synapse formation
Synapse formation is thought to consist of three steps: (1) initial contact formation between axon and dendrite, (2) formation of a synaptic junction, (3) maturation of the junction into a mature synapse (Fox & Umemori, 2006).

While the establishment of synaptic specificity and diversity are important processes during development, the focus of my work is on synaptic differentiation, which I will now concentrate on.

The coordinated differentiation of the pre- and the postsynaptic site after the initial contact founds the basis for functional synaptic transmission. Work during the last years has shown that both axon- and target-derived signals can drive this differentiation process (Shen & Scheiffele, 2010). Neuronal activity regulated pentraxin (NARP) (O'Brien et al, 1999) and ephrinB are examples for axon-derived molecules that can initiate the differentiation of the

postsynaptic terminal (Dalva et al, 2000). On the other side, Wnt7a (Hall et al, 2000) and fibroblast growth factor 22 (FGF22) (Umemori et al, 2004) have been shown to derive from the postsynaptic terminal and induce presynaptic differentiation. Furthermore, factors derived from astroglia that flank synaptic sides, have been shown to be important for this process, like for example thrombospondin (Christopherson et al, 2005). Finally, bidirectional organization by trans-synaptic adhesion complexes plays an important role for synaptic differentiation. The property to induce the process of synaptic differentiation has been referred to as "synaptogenic". Several recent reports have identified novel synaptogenic trans-synaptic adhesion molecules, which I will discuss in the next section.

1.2.1 Trans-synaptic adhesion complexes

First direct evidence for trans-synaptic adhesion complexes serving as synaptogenic molecules was provided for the neuroligin/neurexin complex (Graf et al, 2004; Scheiffele et al, 2000). Here, co-culture systems were used consisting of fibroblast cells, expressing one trans-synaptic partner, and neurons that form hemi-synapses upon contact. Expression of neuroligins in fibroblast cells is sufficient to recruit active zone components and synaptic vesicles to sites of contact in the axon of co-cultured neurons. Moreover, these presynaptic hemi-synapses contain a functional pool of neurotransmitter-containing synaptic vesicles that can be released upon depolarization (Dean et al, 2003; Fu et al, 2003). Subsequently, synaptogenic properties have been reported for several other complexes, like the homophilic interaction between SynCAMs (Biederer et al, 2002) and the heterophilic interaction between EphB and ephrinBs (Dalva et al, 2000; Kayser et al, 2006). More recently, the co-culture system has been used to search for unknown synaptogenic molecules and has revealed several novel adhesion complexes with synaptogenic activity, like LRRTM/neurexin (Linhoff et al, 2009), NGL-3/LAR (Kwon et al, 2010; Woo et al, 2009), TrkC/Ptpσ (Takahashi et al, 2011) and Slitrk3/PTPδ (Takahashi et al, 2012) (figure 2).

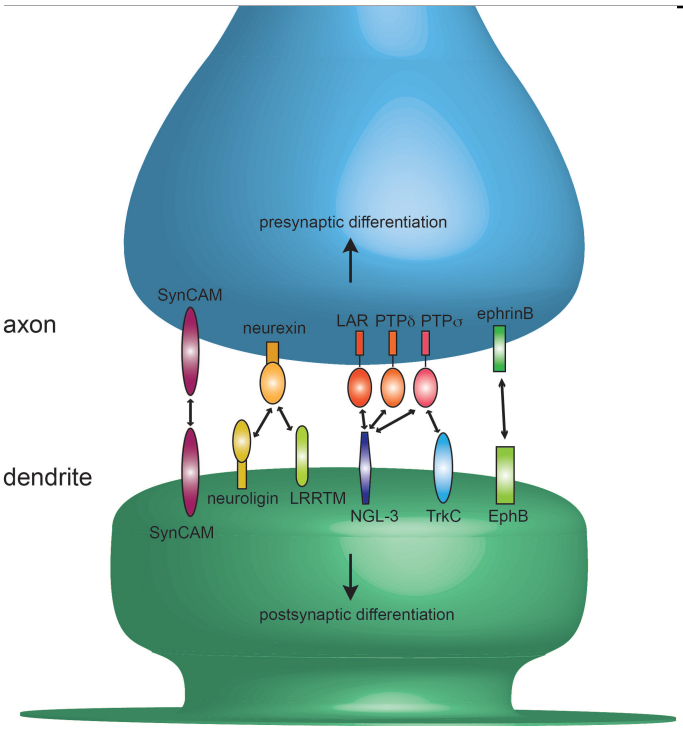

Figure 2 – Trans-synaptic adhesion complexes with synaptogenic properties Several trans-synaptic adhesion complexes with synaptogenic properties that can instruct the differentiation process of the pre- and the postsynaptic site have been identified recently. The picture shows an example of a glutamatergic synapse on a dendritic spine. While the figure summarizes several characterized synaptogenic trans-synaptic adhesion complexes, it is important to note that the exact composition of adhesion complexes at a given synapse is unknown and might consist of only a few of the displayed molecules.

Next to the trans-synaptic adhesion complexes with synaptogenic properties, a number of synaptic adhesion complexes without synaptogenic properties exist. For example, cadherins and protocadherins have been shown to be present at synaptic sites, but cannot induce pre- and postsynaptic differentiation in the co-culture assay. Especially the neuronally expressed N-cadherin has attracted a lot of attention, since it seems to be present at synaptic sites early during synaptogenesis (Benson & Tanaka, 1998). Furthermore, cooperation between N-cadherin and neuroligin1 on the postsynaptic site has been shown to be important for the trans-synaptogenic effect of neuroligin1 on synaptic vesicle clustering (Aiga et al, 2011; Stan et al, 2010). N-cadherin has a role in the modulation of the adhesive strength between cells (Shapiro et al, 1995) and is therefore thought to have a prominent function in contact formation between axons and dendrites (Arikkath & Reichardt, 2008). Furthermore, neuronal activity leads to dimerization of N-cadherin, which changes the adhesive properties of a synapse (Tanaka et al, 2000). The expression of N-cadherin, as well as of other cadherins in the brain is spatially and temporally regulated, indicating distinct functions at young and mature synapses (Elste & Benson, 2006). Presynaptically, cadherins have been shown to have an important role in the localization of synaptic vesicles to presynaptic sites via their association with the cytoplasmic proteins β-catenin, scribble and β-pix (Bamji et al, 2003; Sun et al, 2009; Sun & Bamji, 2011).

1.2.2 Active zones

During synaptic differentiation, the formation of active zones in the presynaptic terminal is a crucial step due to their importance for synaptic transmission. Active zones are specialized

sites for neurotransmitter secretion. Cell adhesion molecules on both sides of the synapse ensure their precise arrangement opposite of postsynaptic densities (figure 3). In vertebrate CNS synapses, active zones are protein-rich disc-like structures with 0.2 – 0.5 µm in diameter (Südhof, 2012). Surrounding the active zone lays a peri-synaptic zone, where synaptic vesicle endocytosis takes place.

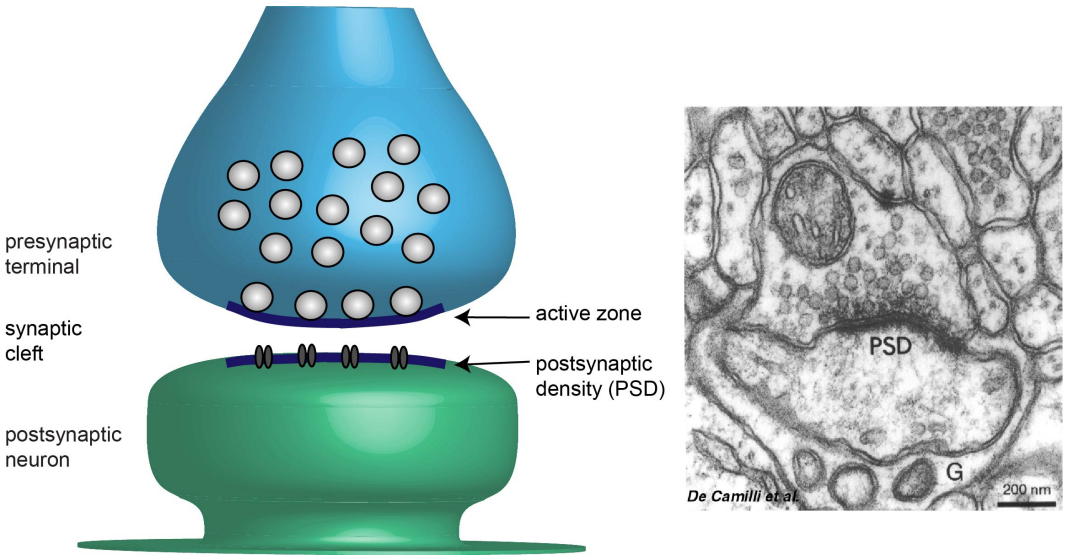

Figure 3 – Schematic drawing and electron micrograph of a glutamatergic synapse
The presynaptic terminal is filled with neurotransmitter-containing vesicles and harbors the so-called "active zone" at its plasma membrane. The postsynaptic neuron contains the postsynaptic density (PSD) and neurotransmitter receptors.

The most important role of active zones is the regulated release of neurotransmitters from synaptic vesicles that fuse with the plasma membrane. In line with this, they harbor a number of molecules important for docking and priming of synaptic vesicles (munc13, munc18) as well as the neurotransmitter release machinery (SNARE proteins). Ca^{2+} channels are localized to active zones, which are important for fast synchronous release. In addition, active zones contain a number of so-called large cytoskeletal proteins (bassoon, piccolo), and proteins that are proposed to have scaffolding functions (ELKS, liprin). Another important property of active zones is their ability to mediate short- and long-term presynaptic plasticity by recruitment of certain proteins, or by mediation of signaling cascades downstream of second messengers, such as Ca^{2+} (Südhof, 2012).

While recent discoveries have identified a plethora of trans-synaptic adhesion complexes, the intracellular signaling cascades that link synaptic adhesion molecules to the development and the formation of functional presynaptic active zones in mammals are poorly understood.

One possible mechanism of synapse assembly is that trans-synaptic complexes serve as nucleators that recruit a number of presynaptic proteins via their cytoplasmic tail, which in turn recruit more proteins and lead to the formation of a dense cytomatrix at the active zone (CAZ). Here, a linear process of active zone assembly is as conceivable as the coordinated action of several parallel pathways. Furthermore, active zone proteins could serve as nucleators that lead to the recruitment of trans-synaptic adhesion complexes and the assembly of active zones. During the last years, many of the proteins building the CAZ in mammalian synapses have been identified and a network of biochemical interactions is beginning to unfold. However, only little is known about the specific functions of most of the active zone proteins *in vitro* and *in vivo*. The temporal cascade of events that leads to synapse formation and the "nucleation question" are still unclear. This is partly due to lack of recognizable presynaptic assembly deficits in knockout mice for CAZ components (Atasoy et al, 2007; Dick et al, 2003; Kaeser et al, 2009; Mukherjee et al, 2010). In the following section, I will describe what is known about the biochemical interactions of CAZ components and then go into detail about the known function of a selection of active zone proteins.

1.2.3 Protein interactions at the active zone

In line with their synaptogenic activity, many trans-synaptic adhesion complexes contain cytoplasmic tails that directly interact with CAZ components. Based on these interactions, a nucleator function for trans-synaptic complexes has been hypothesized.

Both neurexin and SynCAM can bind directly via their cytoplasmic PDZ-domain to calcium/calmodulin-dependent serine protein kinase (CASK), whereas neurexin can additionally bind to munc18-interacting protein 1 (mint1) (Hata et al, 1996). CASK is a multi-domain scaffold protein that has been reported to support the polymerization of actin, together with protein 4.1 and spectrin (Biederer & Südhof, 2001). Furthermore, CASK has been shown to form a tripartite complex with veli and mint1 (Borg et al, 1999; Butz et al, 1998) and can bind to N-type voltage-gated calcium channels (VGCCs) (Maximov et al, 1999). From these findings, a model has emerged, in which neurexin provides the synaptogenic signal that is executed by CASK and leads to active zone protein and calcium channel recruitment, as well as the assembly of actin. However, this model has never been formally tested and still awaits validation.

The receptor protein tyrosine phosphatase LAR has been shown to bind intracellularly to liprin-α (Serra-Pagès et al, 1995). Liprin-αs in turn interact with several cytoplasmic proteins and can oligomerize, an ability that makes them ideal candidates to provide scaffolding functions and serve as a recruitment platform for CAZ proteins. The N-terminal coiled-coil

domain of liprin-α binds to RIM, ELKS, mDiaphanous and GIT1, whereas the C-terminal SAM domains bind to liprin-β, CASK and LAR. Binding of liprin-α to CASK interconnects the pathway downstream of the two synaptic adhesion molecules neurexin and LAR. Furthermore, binding of liprin-α to RIM provides another link between trans-synaptic adhesion and Ca^{2+}-channel recruitment. RIM has been shown to bind via its PDZ domain directly to VGCCs (Kaeser et al, 2011). In addition, RIM interacts with so-called RIM-binding proteins, which in turn bind Ca^{2+}-channels (Hibino et al, 2002). Furthermore, RIM can bind to Rab3 in a GTP-dependent manner (Wang et al, 2001) and to munc13, which has been shown to be essential for synaptic vesicle priming and interacts with the neurotransmitter release machinery (Brose et al, 1995). A heterotrimeric complex between RIM, Rab3 and munc13 could therefore link synaptic vesicles to active zones.

ELKS is another active zone protein that engages in multiple protein-protein interactions. In addition to binding to liprin-α, it also directly binds to RIM (Ohtsuka et al, 2002) and the two large cytoskeletal proteins piccolo and bassoon (Takao-Rikitsu et al, 2004). Piccolo and bassoon are structurally related and are the largest active zone proteins identified so far (Cases-Langhoff et al, 1996; tom Dieck et al, 1998). A link between piccolo and bassoon and synaptic vesicles has been reported via binding of piccolo/bassoon to the prenylated Rab acceptor (PRA1), which in turn interacts with Rab3 and synaptobrevin2/VAMP2 (Fenster et al, 2000). Furthermore, piccolo can bind to the filamentous-actin (F-actin) binding protein Abp1, providing a link to the actin cytoskeleton (Fenster et al, 2003). An overview of the complex protein interaction network in mammalian presynapses is given in figure 4.

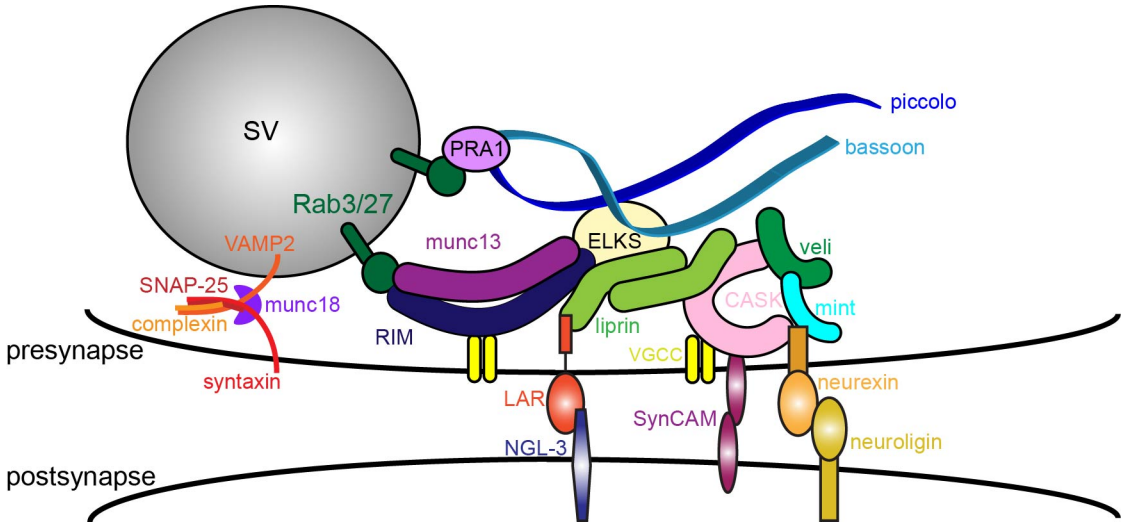

Figure 4 – The complex interaction network of presynaptic proteins in mammalian synapses
Trans-synaptic adhesion complexes are intracellularly connected with active zone proteins. Many of these have direct or indirect links to Ca^{2+}-channels (VGCC) or synaptic vesicles (SV). Detailed explanations can be found in the text.

It is apparent that the mammalian active zone consists of a tightly associated net of multiple proteins that interact with each other. In order to learn more about the specific functions of single proteins, knockout mice have been created. However, many of the proteins described above are encoded by multiple genes that may have redundant functions, which complicates the interpretation of single knockout mouse models. Informative results have therefore been obtained from *C.elegans* and *Drosophila* studies. Both invertebrate species carry only one homologue for most of the active zone proteins and creation of loss-of-function mutants is easier and faster than for mice. Furthermore forward genetic screens for genes required for synaptic differentiation have uncovered a number of formerly unknown proteins that have important roles in the formation of pre- and postsynaptic sites (Crump et al, 2001; Hallam et al, 2002; Schaefer et al, 2000; Sieburth et al, 2005; Zhen & Jin, 1999). Therefore, studies from *C.elegans* and *Drosophila* have provided invaluable insight into active zone development. In the following section I will summarize what is known about the function of a selection of active zone proteins from invertebrate studies and the analysis of knockout mice.

1.2.3.1 RIM

Vertebrates express four RIM genes (RIM1 – 4), of which RIM1 and 2 have internal promoters leading to the expression of RIM1α,β and RIM2α,β and γ isoforms. RIM3 and 4 encode only short isoforms called RIM3γ and RIM4γ (Wang & Südhof, 2003). RIMs were initially discovered as putative effectors for the small synaptic vesicle binding protein Rab3 (Wang et al, 1997). Studies from *C.elegans* and mice show that RIM proteins are essential for synaptic vesicle docking and priming. Koushika et al. report that loss-of-function of *C.elegans* unc-10, which is the worm orthologue of RIM, leads to a reduction in fusion-competent synaptic vesicles at release sites (Koushika et al, 2001). Knockout mice for RIM1α show an increase in paired-pulse facilitation at excitatory synapses, indicating a decrease in release probability (Schoch et al, 2002). Furthermore, double knockout of RIM1α and RIM2α in mice causes postnatal death due to defects in neurotransmitter release (Schoch et al, 2006).

A recent report by Kaeser et al. shows that the PDZ domain of RIMs interacts with N- and P/Q-type Ca^{2+} channels but not with L-type Ca^{2+} channels (Kaeser et al, 2011). By generating conditional knockout mice for all PDZ-domain containing isoforms, they could overcome the postnatal lethality of RIM1α and RIM2α double knockout mice. This study suggests a role for RIMs in synapse assembly, since it shows that RIMs are essential for the localization of Ca^{2+}-channels to presynaptic release sites. The assembly deficit furthermore explains the functional impairment of neurotransmitter release in RIM-deficient mice.

1.2.3.2 Munc13

Munc13 has originally been identified in *C.elegans* as UNC-13 (Maruyama & Brenner, 1991). Worm mutants for this gene exhibit an "uncoordinated" phenotype. Subsequent characterizations in mammals have shown that munc13 is localized to active zones and revealed an essential function in synaptic vesicle priming (Brose et al, 1995). The munc13 family encodes 5 genes, of which 3 (munc13-1, munc13-2, munc13-3) are primarily expressed in the brain and 2 (munc13-4 and BAP3) primarily expressed outside the brain. Knockout mice for munc13-1 die shortly after birth, do not feed and have a reduced breathing rate (Augustin et al, 1999). Synapses in munc13-1 KO mice are ultrastructurally normal with no difference in the number of vesicles per active zone, indicating that munc13-1 does not regulate synapse assembly. However, electrophysiological recordings from cultured hippocampal neurons shortly after birth show a reduction in evoked excitatory synaptic responses in mutant neurons, which is due to a selective reduction in the readily releasable vesicle pool in excitatory synapses. This suggests that munc13-1 is important for the maturation of synaptic vesicles that prepares them for fusion with the plasma membrane and neurotransmitter release. Similar findings could be obtained in *C.elegans* unc-13 and *Drosophila* dunc-13 mutant animals, although the phenotypes here seem much more severe (Aravamudan et al, 1999). Whereas synaptic transmission is completely abolished in invertebrate studies, in munc13-1 mutant mice, GABAergic transmission is unaffected and a small population of glutamatergic synapses produces fusion competent vesicles. Rosenmund et al. could later show that there are two classes of synapses that contain either munc13-1 or munc13-2 and that differ functionally in short-term plasticity properties, explaining the incomplete phenotype after KO of munc13-1 (Rosenmund et al, 2002). A recent report on the function of munc13 has shown that binding of RIM to munc13 releases munc13 homodimerization and thereby activates its priming roles (Deng et al, 2011). It is assumed that munc13 executes its priming functions by directly binding to the SNARE complex (Guan et al, 2008).

1.2.3.4 Liprin-α

Liprin-α proteins were originally identified as "LAR-interacting proteins" LIP.1a and LIP.1b (Serra-Pagès et al, 1995). Invertebrates contain only a single *liprin-α* gene, which is termed *syd-2* or *dliprin* in *C.elegans* and *Drosophila*, respectively. Mammals contain 4 liprin-α genes (liprin-α1 – 4), of which liprin-α2 and -α3 are the major isoforms expressed in the brain (Spangler et al, 2011; Zürner et al, 2011). Expression of liprin-αs is not restricted to active zones, however, studies in *C.elegans* and *Drosophila* provide evidence for the involvement of liprin-α in the formation and maintenance of active zones (Kaufmann et al, 2002; Zhen & Jin, 1999). Loss of liprin-α in both organisms leads to an increase in active zone length. In

C.elegans, SYD-2 has been placed as a central organizer of presynaptic assembly downstream of the protein SYD-1 and upstream of ELKS (Dai et al, 2006). A gain-of-function mutation in SYD-2 can overcome the defect in synapse formation caused by the absence of SYD-1. Here, the activity of the SYD-2 gain-of-function protein requires ELKS. Liprin-α has been shown to homodimerize and form large protein complexes, an ability that seems to be essential for SYD-2 function in *C.elegans* (Taru & Jin, 2011; Wei et al, 2011). A liprin homology domain (LH1) in the coiled coil segment of SYD-2, containing the homodimerization domain, is necessary and sufficient to rescue the SYD-2 loss-of-function phenotype (Taru & Jin, 2011). This study illustrates the importance of the LH1 domain and the homodimerization properties of SYD-2. Furthermore, in invertebrates, liprin-α interacts with receptor protein tyrosine phosphatases (PTP-3 and Dlar), an interaction that was validated in mouse studies between liprin-α and LAR. In the mouse, liprin-α localizes both pre- and postsynaptically (Wyszynski et al, 2002). In both axons and dendrites, liprin-α interacts with the protein GRIP. Postsynaptically, this interaction is important for the synaptic targeting and surface expression of AMPA receptors. Later, the interaction between liprin-α and GRIP and its effect on AMPA receptor distribution has been shown to be dependent on GIT1, since disruption of the liprin-α – GIT1 interaction leads to a reduction in dendritic clustering of AMPA receptors (Ko et al, 2003a). Furthermore, liprin-α has been implicated in targeting of LAR to dendrites (Dunah et al, 2005; Hoogenraad et al, 2007). Hoogenraad et al. have shown that protein levels of liprin-α are modulated by neuronal activity. Knockdown of CAMKII leads to an increase in liprin-α1 levels, whereas co-expression of constitutively active CAMKII and liprin-α1 in COS cells decreases liprin-α1 protein levels. Interestingly, liprin-α2 is not affected, suggesting an isoform-specific interaction between CAMKII and liprin-α1. Functionally, the degradation of liprin-α1 has been shown to be important for dendritic targeting of LAR and normal development of the dendritic tree.

In addition to the interactions at the active zone, liprin-α also interacts with kinesin motor proteins (Shin et al, 2003). In *Drosophila* liprin-α mutants, synaptic vesicle markers show aberrant accumulations along the length of the axon, suggesting a defect in their transport to presynaptic terminals (Miller et al, 2005).

In summary, the presynaptic assembly deficits, seen after loss-of-function of SYD-2/liprin-α in invertebrates, as well as its involvement in transport of presynaptic components, suggests a crucial role for liprin-α in synapse development. However, mouse knockout studies, to validate the *in vitro* findings, are still missing.

1.2.3.5 ELKS

Mammals contain two genes for *elks*, termed *elks1* and *elks2*, whereas only a single *elks* gene has been described in *C.elegans*. The name stems from the high content of the amino acids glutamate (E), leucine (L), lysine (K) and serine (S). The *Drosophila* orthologue of ELKS is called Bruchpilot, which resembles ELKS only in its N-terminus and additionally contains a large C-terminus, supposedly giving Bruchpilot unique functions in comparison to its mammalian orthologues (Wagh et al, 2006). In mammals, ELKS2 is exclusively expressed in the brain, whereas alternative splicing of ELKS1 results in two isoforms, ELKS1a and ELKS1b, of which ELKS1b is exclusively brain specific and ELKS1a only expressed outside the brain (Ohtsuka et al, 2002). The ELKS2 gene in mammals contains an internal promoter, giving rise to a second ELKS2 isoform termed ELKS2β (Kaeser et al, 2009). Both isoforms are expressed in the brain, with ELKS2α being the most abundant one and ELKS2β only comprising of 4 % of ELKS2α expression levels in WT mice.

Studies on Bruchpilot in *Drosophila* neuromuscular junctions (NMJ) have shown that it is an integral part of the characteristic T-bar structure of *Drosophila* active zones (Kittel et al, 2006; Wagh et al, 2006). Loss-of-function mutations lead to deficits in synapse assembly with a mislocalization of Ca^{2+}-channels, fewer individual synapses and slightly smaller NMJs but enlarged postsynaptic receptor fields. On the contrary, deletion of ELKS in *C.elegans*, does not cause a detectable phenotype (Deken et al, 2005). Knockout mice for ELKS2α have a reduction in the number of synaptic vesicles per presynaptic bouton in both excitatory and inhibitory synapses, but no change in the number of docked vesicles. Furthermore, they do not show any changes in excitatory synaptic transmission (Kaeser et al, 2009). However, the size of the readily-releasable pool (RRP) of vesicles at inhibitory synapses is increased, causing an increase in inhibitory synaptic responses. Thus, loss of ELKS2α leads to a slight defect in synapse assembly, which does not seem to have major functional consequences. While knockout of Bruchpilot in *Drosophila* leads to presynaptic assembly deficits, it is still unclear, if ELKS has a major role in presynaptic assembly in mammals. One possibility is that the C-terminus of Bruchpilot, which is not present in mammalian ELKS, is responsible for its role in presynaptic assembly in *Drosophila*, while this function might be executed by different proteins in mammals. Studies of double knockout mice of ELKS2 and ELKS1b, the other major isoform expressed in the brain, might provide a better insight into the function of ELKS in mammalian presynaptic terminals.

1.2.3.6 Piccolo and bassoon

Piccolo and bassoon are large structurally related proteins that are specific to vertebrates. Due to their large sizes, the generation of knockout mice with a complete loss of

the proteins is not straightforward. Therefore, bassoon mutant mice have been created that lack the central region of bassoon that is important for anchoring of the protein to the CAZ (Altrock et al, 2003). Analysis of these mice shows that synapses appear structurally normal, with comparable numbers of synaptic vesicles in presynaptic boutons of WT and mutant mice. However, FM-dye experiments revealed that a fraction of glutamatergic synapses is inactive. Furthermore, 50 % of homozygous mutant animals die within the first 6 months and mutant animals display spontaneous seizures. On the other hand, analysis of a specialized type of synapses in these mice, the photoreceptor ribbon synapses in the retina, has revealed presynaptic assembly deficits (Dick et al, 2003). Retinal photoreceptors are specialized glutamatergic synapses for high-frequency signaling, that need a continuous supply of synaptic vesicles to the neurotransmitter release site. This is supposedly achieved by a presynaptic ribbon, which is thought to be composed of scaffold proteins and to be equivalent to the CAZ in CNS synapses. In bassoon mutant mice, the photoreceptor ribbon is not anchored to the presynaptic active zone, a phenotype that has been termed “floating ribbons”. Functionally, this results in impaired synaptic transmission and abnormal dendritic branching patterns. A more recent study functionally analyzes the lack of bassoon in cerebellar mossy fiber – granule cell synapses in mice with a complete knockout of bassoon protein (Hallermann et al, 2010). Hallermann et al. show that basal synaptic transmission is unchanged in these mice, whereas they exhibit an enhanced depression during high-frequency stimulation. They demonstrate that the enhanced depression is due to a decrease in the rate of vesicle reloading in bassoon KO mice, suggesting that bassoon is functionally important for the fast transfer of vesicles to release sites.

Piccolo knockout mice also exhibit a slight increase in postnatal mortality, however no synaptic phenotype could be detected in these animals (Mukherjee et al, 2010). Simultaneous knockdown of bassoon in piccolo knockout animals leads to a significant decrease in the number of synaptic vesicles per presynaptic terminal, as assessed by electron microscopy. Furthermore, the number of docked vesicles is decreased, whereas the size of postsynaptic densities is slightly increased, leading to a model in which piccolo and bassoon function to recruit and tether synaptic vesicles in the presynaptic terminal. A recent study reports that knockdown of piccolo leads to an enhanced activity-dependent synapsin1a dispersion and reduced F-actin polymerization in presynaptic boutons (Leal-Ortiz et al, 2008; Waites et al, 2011). This points to a function for piccolo in the regulation of neurotransmitter release by facilitating activity-dependent F-actin assembly.

The structural overlap between the two proteins suggests that they can execute similar functions. Both single KO of bassoon or piccolo does not lead to presynaptic assembly deficits, whereas a double loss-of-function reduced the number of synaptic vesicles per

presynaptic terminal. Thus, piccolo and bassoon might have overlapping functions in presynaptic assembly, whereas both execute different functions in the synaptic vesicle cycle.

1.2.3.7 Synapse-defective-1

One active zone protein that I have not described so far, but which has emerged as a central organizer of presynaptic development in invertebrates, is Synapse-defective-1 (SYD-1). SYD-1 has originally been identified in a screen for genes required for synaptic differentiation in *C.elegans* (Hallam et al, 2002). Hallam et al. could show that *syd-1* mutant worms exhibit defects in the distribution and the number of the synaptic vesicle marker synaptobrevin. Furthermore in *syd-1* mutant worms, not only synaptic vesicle proteins, but also active zone markers, are localized to both axonal and dendritic processes, indicating a defect in polarity. SYD-1 protein is localized to presynaptic terminals and protein structure prediction analysis revealed that it contains an N-terminal PDZ, a C2 and a C-terminal Rho-GAP domain. Later studies have shown that SYD-1 acts upstream of SYD-2/liprin-α, since a gain-of-function mutation in SYD-2 can rescue the *syd-1* mutant phenotype (Dai et al, 2006). In *syd-1* mutant worms, the synaptic localization of SYD-2 is disrupted, suggesting that SYD-1 recruits SYD-2 to presynaptic terminals. The SYD-1/SYD-2 complex was placed downstream of the guidepost molecule SYG-1, which together with SYG-2 specifies the localization of synapses along *C.elegans* axons (Patel et al, 2006). In addition, SYD-1 and SYD-2 were shown to be regulated by regulator of synaptogenesis-1 (RSY-1), which is a local inhibitor of presynaptic assembly (Patel & Shen, 2009). A recent study shows that the F-actin binding protein NAB-1/neurabin acts downstream of SYG-1 and recruits SYD-1 and SYD-2 to presynaptic terminals (Chia et al, 2012).

In addition, *Drosophila* SYD-1 (DSYD-1) was identified in a mass-spectrometry analysis for proteins that co-immunoprecipitate with the active zone protein Bruchpilot (Owald et al, 2010). The authors show that *dsyd-1* mutant flies exhibit defects in locomotion and have a reduced life span. Similar to the findings in *C.elegans*, DSYD-1 is localized to the active zone in presynaptic terminals and is necessary for the presynaptic localization of Dliprin-α and the correct distribution of active zone material. At *dsyd-1* mutant NMJs, fewer release sites are formed and evoked junctional excitatory currents are significantly reduced. In addition to the presynaptic defects seen in *C.elegans* and *Drosophila syd-1* mutant animals, *dsyd-1* mutant flies also exhibit postsynaptic defects. Individual glutamate receptor fields are enlarged, which can be rescued by presynaptic re-expression of DSYD-1, suggesting that DSYD-1 acts presynaptically. Recently the same authors could show that DSYD-1 interacts with presynaptic neurexin-1 to coordinate pre- and postsynaptic assembly (Owald et al, 2012). The N-terminal PDZ domain of DSYD-1 is important for the clustering and retention of neurexin-1 at presynaptic sites. In line with this, *syd-1*, *neurexin-1* and *neuroligin-1* mutant

flies show similar phenotypes and the phenotypes of double mutants are non-additive, suggesting that all three proteins act in the same molecular pathway. Finally, *dsyd-1* mutant flies also show a change in postsynaptic clustering of neuroligin-1. This leads to a model in which presynaptic DSYD-1 clusters neurexin-1, which in turn leads to an aggregation of postsynaptic neuroligin-1, providing a mechanism to couple pre- and postsynaptic assembly. In summary, loss-of-function of SYD-1 in invertebrates, causes severe presynaptic assembly defects, which in flies furthermore result in deficits in postsynaptic formation.

No mammalian orthologues of SYD-1 have been identified so far. The aim of this study is the identification and characterization of mouse orthologues of SYD-1.

1.2.4 "Nucleation" of presynaptic assembly

Looking at the many proteins that are present in mammalian presynaptic terminals, it becomes evident that the protein composition of the active zone is well described. However, at this moment, it is still unclear what defines the position of a future synapse along the axon and which proteins serve as nucleators for presynaptic assembly in mammalian neurons. Studies that are beginning to shed light on this question were done in invertebrates and SYD-1 seems to be a major player in the nucleation process. In *Drosophila*, DSYD-1 was shown to be one of the first proteins that localizes to nascent presynaptic boutons, before other active zone proteins, including liprin-α and Bruchpilot, could be detected in presynaptic terminals (Owald et al, 2010). Furthermore, complexes of DSYD-1 and liprin-α also preceded the accumulation of neurexin (Owald et al, 2012). These findings contradict the hypothesis that trans-synaptic adhesion complexes serve as nucleators for active zone assembly. Furthermore, in cell lines, liprin-α has been shown to regulate LAR localization and clustering (Serra-Pagès et al, 1995; Serra-Pagès, 1998). In line with this, two reports suggest that liprin-α is important for trafficking and dendritic targeting of LAR in hippocampal neurons (Dunah et al, 2005; Hoogenraad et al, 2007). Likely, the targeting of LAR to axons and presynaptic terminals is also regulated by liprin-α, furthermore contradicting the hypothesis that LAR can serve as the nucleator. Several studies suggest that presynaptic assembly is regulated by interplay between positive and negative cues. In fact, several inhibitors of presynaptic assembly have been described. RSY-1 acts on SYD-1 and SYD-2 in *C.elegans* and thereby suppresses presynaptic assembly (Patel & Shen, 2009). In *rsy-1* mutant worms, an increased number of synapses are formed and a higher amount of active zone material is present at presynaptic sites. In addition, E3 ubiquitin ligases have been shown to target presynaptic proteins for degradation and therefore negatively control synapse assembly (DiAntonio et al, 2001; van Roessel et al, 2004). In order to understand how synapses form,

we need to know how presynaptic material is transported to nascent boutons and stabilized there. Active zone proteins and synaptic vesicles in mammals have been shown to be transported in pre-packaged vesicles. A recent study in *C.elegans* suggests that these vesicles possess an intrinsic property to self-assemble, which is suppressed by an arf-like small G protein, called ARL-8 (Klassen et al, 2010). In *arl-8* mutant worms, presynaptic proteins prematurely aggregate and fail to localize to the distal axon. The authors suggest that this predisposition to self-assemble is suppressed by ARL-8, which gives presynaptic cargoes a "trafficking identity". Furthermore, ARL-8 is antagonized by assembly-promoting proteins like SYD-1, SYD-2 and SAD-1, since double mutants of *arl-8* and one of the assembly-promoting proteins partially suppress the premature aggregation phenotype. However, since previous findings on human and *Drosophila* ARL-8 have shown that it affects lysosome motility (Bagshaw et al, 2006; Hofmann & Munro, 2006), the described findings on *C.elegans* ARL-8 have to be taken with care, since they might be indirect. Nevertheless, the interplay between positive and negative cues for synapse assembly could result in a signal that leads to the stalling of pre-packaged active zone proteins and the rapid assembly of presynaptic boutons, once the decision about the right location has been made. Therefore, it might be difficult to define which protein recruits which during the assembly process and who serves as the nucleator. Yet, several studies both in *C.elegans* and *Drosophila* have identified a hierarchy in the assembly process (Chia et al, 2012; Owald et al, 2010; Patel et al, 2006). In mammals, studies about the temporal events of synapse assembly are complicated by the high number of active zone proteins and the possibility of redundancy mechanisms. In the following section, I will describe what we know about the transport of presynaptic proteins in mammals and the formation of presynaptic boutons from a cellular perspective.

1.3 Development of presynaptic boutons from a cellular perspective

1.3.1 Transport of synaptic proteins

Studies on the time-course of presynaptic development have shown that new presynaptic boutons, capable of activity-evoked vesicle recycling, can form within 30 min of axo-dendritic contact (Friedman et al, 2000). Given the dense protein network in the presynapse and the distance between the soma and the tip of the axon, the question arises how transport of presynaptic components is regulated. The precursor protein transport vesicle hypothesis suggests that active zone and synaptic vesicle proteins are not transported as single proteins from the soma, but are pre-packaged into transport vesicles (Garner et al, 2002; Ziv & Garner, 2004). One of the first observations of these transport packets came from

Kraszewski and colleagues, where they used an anti-synaptotagmin1 antibody, conjugated to Cy3, to visualize synaptic vesicle dynamics in cultured hippocampal neurons (Kraszewski et al, 1995). They observed the presence of clusters of synaptic vesicles that move together both anterogradely and retrogradely. Later, Ahmari and co-workers used a similar approach (VAMP2-GFP fusion protein) to monitor synaptic vesicle movement (Ahmari et al, 2000). Here, VAMP2-GFP puncta were bigger than individual synaptic vesicles and often stalled at sites of new axo-dendritic contact. Subsequent immunocytochemistry analysis revealed the presence of other synaptic vesicle proteins (SV2, synapsin1, amphiphysin1) in these puncta. Zhai et al. reported the presence of 80 nm-dense core granulated vesicles that were concentrated in axonal growth cones (Zhai et al, 2001). Analysis of these 80 nm-dense core vesicles suggested that they might contain a number of active zone proteins, like piccolo, bassoon, syntaxin, SNAP25 and N-cadherin. Therefore, dense core vesicles were termed piccolo-bassoon transport vesicles (PTVs). Quantitative immunocytochemical analysis showed later that the number of piccolo, bassoon and RIM in presynaptic boutons is a multiple of two or three PTVs (Shapira et al, 2003). Consequentially, presynaptic material seems to be transported in two types of vesicular organelles to nascent presynaptic sites: (1) synaptic vesicle protein transport vesicles (STVs) and (2) piccolo-bassoon transport vesicles (PTVs). Both STVs and PTVs have been shown to display similar movement characteristics and to move both anterogradely and retrogradely in the axon (Dai & Peng, 1996; Kraszewski et al, 1995). Furthermore, they move in a saltatory fashion, which is thought to be important for presynaptic formation, since the sites where STVs repeatedly pause are more likely to differentiate into synapses (Bury & Sabo, 2011; Sabo et al, 2006). For anterograde transport, STVs and PTVs have been shown to move along microtubules with motors of the kinesin superfamily (Hall & Hedgecock, 1991; Okada et al, 1995; Su et al, 2004). Retrograde transport of STVs and PTVs is carried out by the minus end-directed microtubule motor protein dynein (Fejtova et al, 2009; Vallee et al, 2004). However, how is the protein composition of these transport vesicles determined and where are they assembled? A recent study by Maas and co-workers sheds some light on these questions (Maas et al, 2012). Using rat hippocampal neurons they could show that bassoon and ELKS2 exit the trans-Golgi network on a common vesicle, whereas munc13 and synaptic vesicle proteins use distinct sets of Golgi-derived transport vesicles. RIM1α seems to associate with vesicular membranes in a post-Golgi compartment. Furthermore the authors suggest that PTVs undergo several changes in protein composition before arriving at the nascent synapse. The formation of a presynaptic bouton therefore depends on the stalling of PTVs at future presynaptic sites and the anchoring of synaptic vesicles at these sites. One cytoskeletal protein that has been shown to appear at forming synaptic boutons and co-localize with synaptic vesicles is actin (Dai & Peng, 1996). Therefore, actin has been suggested to have a

role in anchoring synaptic vesicles and in the formation of presynaptic terminals (Cingolani & Goda, 2008).

1.3.2 The role of actin in presynaptic formation

Actin is highly enriched in both pre- and postsynaptic terminals and is supposed to provide a cellular scaffold that determines and maintains cell shape (Hirokawa et al, 1989; Matus et al, 1982). The dependence of nascent presynaptic boutons on actin has been nicely demonstrated in a study by Zhang and Benson (Zhang & Benson, 2001). Here, the authors exposed hippocampal neurons during the time of synapse formation to the actin depolymerizing drug lantrunculin A, resulting in a near complete loss of synapses. However, as the culture matured, synapses became more and more resistant to lantrunculin A treatment. Studies by Sankaranarayanan have shown that actin is concentrated in presynaptic terminals and surrounds presynaptic vesicle clusters (Sankaranarayanan et al, 2003). Interestingly, increases in activity can remodel the position of actin in presynaptic terminals, with actin condensing towards the periphery after stimulation (Colicos et al, 2001). Furthermore, promoting actin polymerization with jasplakinolide is sufficient to trigger the conversion of silent presynaptic boutons into functional ones (Yao et al, 2006). A recent study provides a link between actin polymerization, anchoring of synaptic vesicles and components of the presynaptic active zone. Waites et al. could demonstrate that the piccolo knockdown phenotype, which leads to enhanced exocytosis of synaptic vesicles and synapsin1a dispersion, can be rescued by F-actin stabilization with jasplakinolide (Waites et al, 2011). Furthermore, knockdown of profilin2, an ATP/ADP exchange factor that promotes F-actin assembly, phenocopies knockdown of piccolo, suggesting that both proteins function in the same molecular pathway. These studies underline the important function of actin during development, however exactly how actin polymerization contributes to presynaptic development, is not clear yet. The polymerization of actin is controlled by Rho-GTPases and their regulators. In order to understand the role of actin in presynaptic formation, we therefore need to look at its regulators, which will be discussed in the next section. Figure 5 provides an overview over what is known about the transport of precursor proteins to nascent boutons and the role of actin in presynaptic formation.

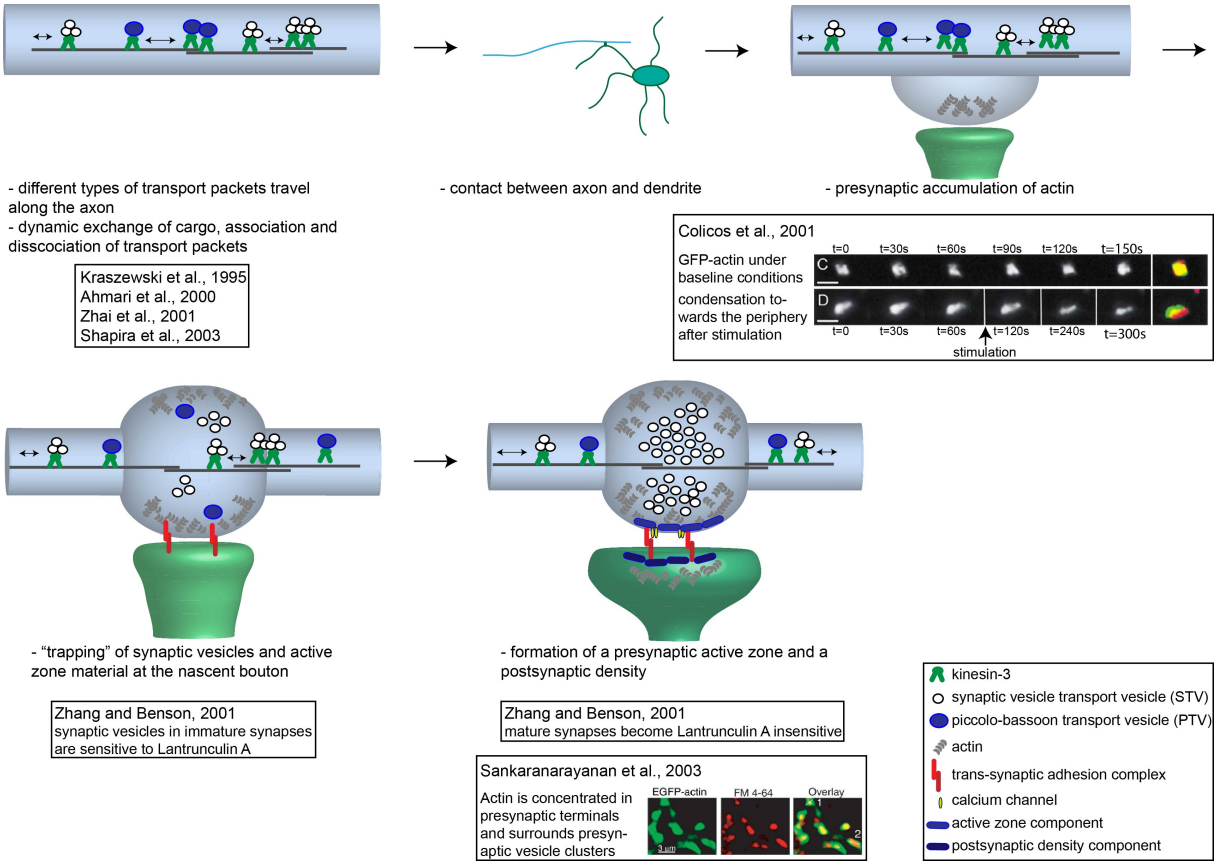

Figure 5 – Development of presynaptic terminals
Synaptic vesicle transport vesicles (STVs) and piccolo-bassoon transport vesicles (PTVs) are traveling along the axon during the time of synapse formation. After contact between axon and dendrite, F-actin condenses towards the periphery of the presynaptic bouton and several transport packets pause at this site to release their content. Subsequently, the presynaptic release site and the postsynaptic density mature.

1.4 GAP and GEF proteins in synapse formation

Rho-GTPases, a subfamily of small GTP-binding proteins, are known regulators of the actin cytoskeleton (Govek et al, 2005; Tolias et al, 2011). The best-studied ones are RhoA, Racl and Cdc42. Rho-GTPases can cycle between an active GTP- and an inactive GDP-bound state (figure 6). In the active, GTP-bound conformation, they have the ability to bind to various effector proteins and thereby initiate a number of signaling pathways. These signaling pathways range from the control of actin cytoskeleton reorganization and microtubule dynamics over gene transcription and membrane trafficking. In light of the various functions of Rho-GTPases in many cellular processes, they have to be tightly spatially and temporally regulated. The precise spatio-temporal control of Rho-GTPases is carried out by guanine nucleotide exchange factors (GEFs) and GTPase-activating proteins

(GAPs). GEFs activate Rho-GTPases by catalyzing the GDP/GTP exchange, whereas GAPs inactivate Rho-GTPases by enhancing their intrinsic GTPase activities (figure 6).

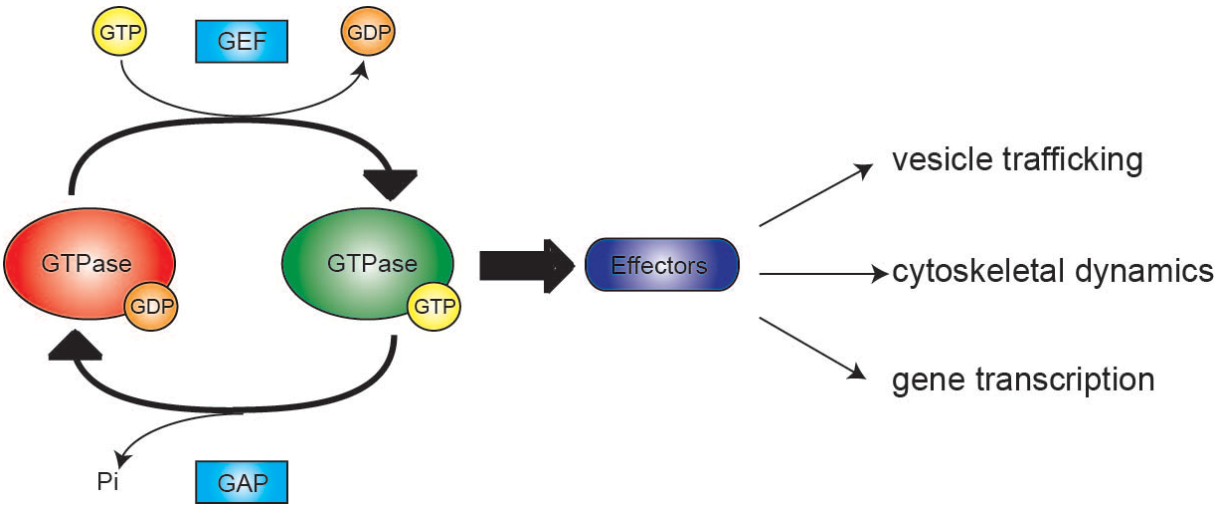

Figure 6 – Rho-GTPases and their regulators
Rho-GTPases cycle between an active GTP-bound state and an inactive GDP-bound state. Guanine nucleotide exchange factors (GEFs) and GTPase-activating proteins (GAPs) catalyze the conversions. GTPases can only interact with effector proteins in the GTP-bound state and initiate downstream signaling cascades.

In postsynaptic development, a number of GEFs and GAPs have been identified that are important for dendritic spine development, growth and plasticity (Tolias et al, 2011). It is conceivable, that GEF and GAP proteins have equally important roles in the development and plasticity of the presynapse. However, the knowledge about the role of GEFs and GAPs in presynaptic development is by far sparser. This is partly due to the fact that many GEF and GAP proteins and their Rho-GTPases have functions in neuronal polarity, axon outgrowth and guidance (Govek et al, 2005; Tahirovic & Bradke, 2009), which makes it difficult to dissect their roles in synapse development. In the following section, I will describe what is known about GEFs and GAPs in presynaptic development.

1.4.1 GEFs and GAPs in presynaptic development

Most of what is known about GEFs and GAPs in presynaptic development stems from studies in *C.elegans* and *Drosophila*.

In a recent study in *C.elegans*, Stavoe et al. investigate the presynaptic signaling cascade downstream of the netrin-receptor unc-40/DCC (Stavoe & Colon-Ramos, 2012).

They show that the Rac-GEF ced-5 (*C.elegans* orthologue for DOCK180) interacts with unc-40 and regulates signaling of the *C.elegans* Rac-GTPase ced-10. Loss-of-function of either of the three proteins leads to a defect in synaptic vesicle clustering, whereas the accumulation of active zone proteins in presynaptic terminals is not altered. Furthermore, they demonstrate that ced-10 interacts with the effector MIG-10 (*C.elegans* orthologue for RIAM and lamellipodin) to increase the accumulation of F-actin in presynaptic terminals. This study shows the importance of the Rac-GEF ced-5 for presynaptic assembly and confirms a role for F-actin in synaptic vesicle clustering during development.

In *Drosophila*, two studies have shown that the Rac-GEF trio has an important role in NMJ bouton growth and the regulation of the actin cytoskeleton. Pawson et al. show that diaphanous is necessary presynaptically for normal NMJ growth, since *dia* mutant flies show a decrease in synaptic bouton numbers (Pawson et al, 2008). In genetic experiments, they demonstrate that dia acts downstream of the receptor tyrosine phosphatase dlar and the Rac-GEF trio to control NMJ growth and F-actin accumulation in presynaptic terminals. In the second study, Ball et al. show that overexpression of the GTPase Rac leads to synaptic overgrowth and that the action of Rac requires BMP signaling (Ball et al, 2010). They demonstrate that retrograde BMP signaling directly regulates the transcription of trio, which mediates Rac signaling. In line with the data by Pawson et al., loss of trio leads to a reduction in NMJ growth.

Finally, another study in *Drosophila* provides a link between a GEF protein and the regulation of synaptic homeostasis (Frank et al, 2009). Here, the authors show that the GEF ephexin acts downstream of the Eph receptor and upstream of Cdc42 to modulate the presynaptic calcium channel $Ca_V2.1$. Regulation of $Ca_V2.1$ is important for homeostatic modulation of presynaptic release.

In vertebrates, the only study providing a direct link between a GEF and presynaptic vesicle clustering is a study by Sun and Bamji (Sun & Bamji, 2011). Here, the authors demonstrate that the Rac/Cdc42 guanine nucleotide exchange factor (GEF) β-pix forms a complex with cadherin, β-catenin and scribble at the synapse. Knockdown of β-pix leads to a reduction in actin polymerization and disrupts synaptic vesicle localization. This phenotype can be rescued by overexpression of cortactin, which stabilizes the Arp2/3 complex and thus enhances actin polymerization.

Given the important role of actin during development and maintenance of presynaptic terminals, its assembly and disassembly has to be tightly regulated. However, the knowledge about its regulation by GAP and GEF proteins as described above, is scarce. The

identification of regulators of presynaptic actin will help to shed light on the process of synapse development.

1.5 The role of actin in mature presynaptic terminals

As described above, many presynaptic active zone proteins have direct or indirect links to the actin cytoskeleton. Next to its role in the formation of presynaptic boutons, actin is also one of the major components of mature presynaptic terminals, but its exact role is debated until today. However, due to the linkage between actin and presynaptic proteins, comprehension of the role of actin in the presynapse is important for the interpretation of loss-of-function phenotypes of presynaptic components. In the following section, I will give an overview over the possible functions of presynaptic actin and the evidence for them.

Synaptic vesicles in presynaptic terminals are organized into three functionally distinct pools: the readily-releasable pool, the recycling pool and the reserve pool of synaptic vesicles (Rizzoli & Betz, 2005). The readily-releasable pool consists of synaptic vesicles that are docked and primed at the active zone and are immediately available for exocytosis. The recycling pool harbors vesicles that are released at moderate stimulation intensities, whereas the reserve pool of vesicles can only be released at very high stimulation intensities. Some presynaptic terminals contain reserve pool vesicles that are not released at all. The reserve pool constitutes the biggest pool of synaptic vesicles.

Actin has been proposed to build a topographic divide between these different pools of vesicles (Cingolani, 2008). Here, it could provide a scaffold to restrict vesicle mobility. Evidence comes from a study by Jordan et al., in which the authors show that actin depolymerization with lantrunculin A leads to an increased mobility of synaptic vesicles (Jordan et al, 2005). This and other studies also provide evidence for actin having a guiding function, helping the transfer of vesicles between the different pools. Actin is linked to synaptic vesicles via short filaments of synapsin. After increased neuronal activity, synapsin gets phosphorylated, leading to a release of the reserve pool vesicles from the actin network (Chi et al, 2003). These vesicles can then replenish the readily-releasable pool of vesicles and undergo exocytosis. Furthermore, the actin-based motor myosin-V has been shown to be associated with synaptic vesicles (Evans et al, 1998). Myosin-V associated vesicles can move along actin filaments in *in vitro* actin filament motility assays. In a more recent study, myosin-Va has been shown to interact with the t-SNARE syntaxin-1A upon increases in Ca^{2+} concentrations (Watanabe et al, 2005). This suggests that upon stimulation and Ca^{2+}

elevation, vesicles are trafficked on myosin-Va motors along actin filaments to the active zone, where they are captured by binding of myosin-Va to syntaxin.

Furthermore, actin-based transport of synaptic vesicles has been implicated in endocytotic recycling of synaptic vesicles. In electron micrographs of the lamprey reticulospinal synapse, actin-like filaments can be detected in the endocytic zone of synapses (Shupliakov et al, 2002). After stimulation, these filaments proliferate towards the synaptic vesicle cluster and have synaptic vesicles associated with them. Furthermore, a recent study in cultured hippocampal neurons demonstrates that actin-based vesicle recycling is not confined to individual presynaptic boutons (Darcy et al, 2006). Darcy et al. could show that endocytosed synaptic vesicles can be recruited into the functional pool of nearby boutons. The sharing of vesicles between boutons requires actin turnover, since treatment of cultures with jasplakinolide reduces the movement of synaptic vesicles.

At the active zone, actin has also been suggested to provide a physical barrier to prevent unwanted fusion and exocytosis of synaptic vesicles. Studies of the neuromuscular junction in frogs have shown that treatment with cytochalasin D, an actin-depolymerizing agent, do not affect acetylcholine secretion triggered by low-frequency stimulation (Wang et al, 1996). Instead, evoked secretion at higher frequency stimulations is affected by cytochalasin D treatment, with an increase in paired-pulse facilitation. The authors conclude that actin filaments do not affect the exocytosis of readily-releasable vesicles, but serve to restrain vesicles from the reserve pool to readily undergo exocytosis.

Instead, Sankaranarayanan and colleagues reduce the function of actin at presynaptic terminals to providing a scaffold to anchor synapsin1a in the terminal (Sankaranarayanan et al, 2003). In their study, they do not detect any deficits in the synaptic vesicle cycle after disruption of the actin cytoskeleton. However, actin disruption reduces the concentration of synapsin1a and leads to a dispersion of synapsin1a out of the terminal. Therefore, the authors conclude that actin may simply serve as a scaffold for retaining important molecules in the presynapse, while disruption of actin leads to a dilution of these regulatory molecules resulting in the diverse defects, seen in other studies.

In addition, several trans-synaptic adhesion complexes have indirect links to the actin cytoskeleton. For example, the cell adhesion molecule N-cadherin can form a complex with β-catenin and scribble. Scribble is important for the localization of the Rac/Cdc42 GEF β-pix at the synapse, which regulates actin polymerization (Sun & Bamji, 2011). The presynaptic cell adhesion molecule neurexin binds to CASK, which, together with protein 4.1, can nucleate local assembly of actin/spectrin filaments (Biederer & Südhof, 2001). In line with

these studies, the actin cytoskeleton might reinforce adhesion between the pre- and the postsynaptic cell, provided by cell adhesion complexes.

Many of the findings described above contrast each other. One explanation for these contradictory results might be the fact that diverse model systems, as well as different ways to disrupt the actin cytoskeleton, were used. It is conceivable that large presynaptic terminals, such as the lamprey reticulospinal synapse, may use actin in different ways than smaller terminals, in which synaptic vesicles do not have to travel such long distances to reach the presynaptic plasma membrane.

Despite of the many contradictions, the increasing number of studies on the presynaptic actin cytoskeleton shows that actin has an important role in many functional processes, both for presynaptic differentiation and in mature presynaptic terminals. Figure 7 gives an overview of the possible roles of actin in presynaptic terminals.

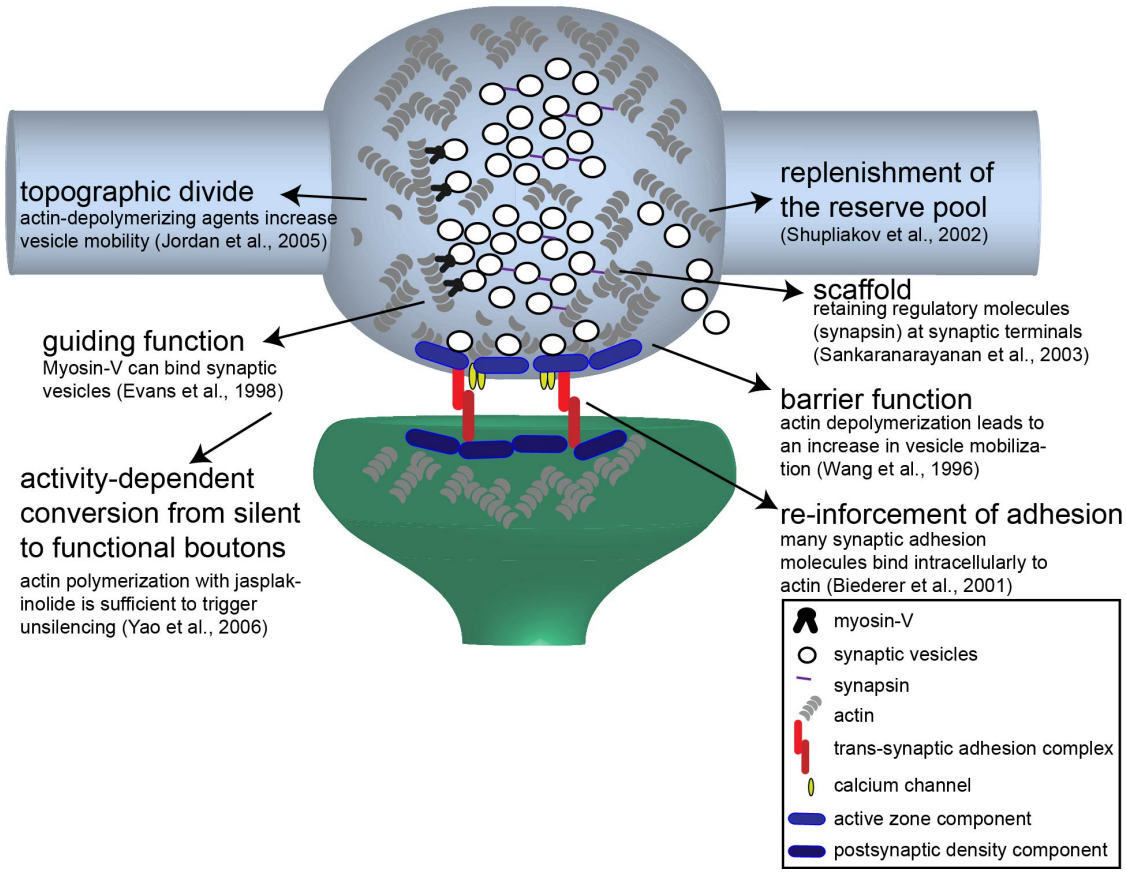

Figure 7 – The role of actin in presynaptic terminals
Actin has been proposed to have many roles in presynaptic terminals. Details are described in the text.

1.6 The dissertation project

Recent studies have identified a number of trans-synaptic adhesion complexes that induce the differentiation of pre- and postsynaptic terminals. However, the intracellular signaling cascades that link adhesion to the formation of mature active zones in mammalian cells have remained obscure. In *C.elegans* and *Drosophila*, the protein SYD-1 has emerged as a central organizer of presynaptic development (figure 8). Given the crucial role of SYD-1 for presynaptic assembly in invertebrates, the question arises, if SYD-1 exists in mammalian cells and if it executes similarly important functions. In fact, many proteins that have been shown to be important for synaptic development in *C.elegans* have mammalian orthologues with similar functions. Prominent examples are SYD-2/liprin-α (Zhen & Jin, 1999), RPM-1 (regulator of presynaptic morphology-1) (Schaefer et al, 2000) and SAD-1/SAD-A/B (synapses of the amphid defective-1) (Crump et al, 2001). Furthermore, invertebrate SYD-1 has a predicted RhoGAP domain, but its functionality has never been directly tested. Due to the important role of actin in presynaptic development, the identification and characterization of GEF and GAP proteins that act in presynaptic assembly are of major interest and will advance our understanding on presynaptic formation.

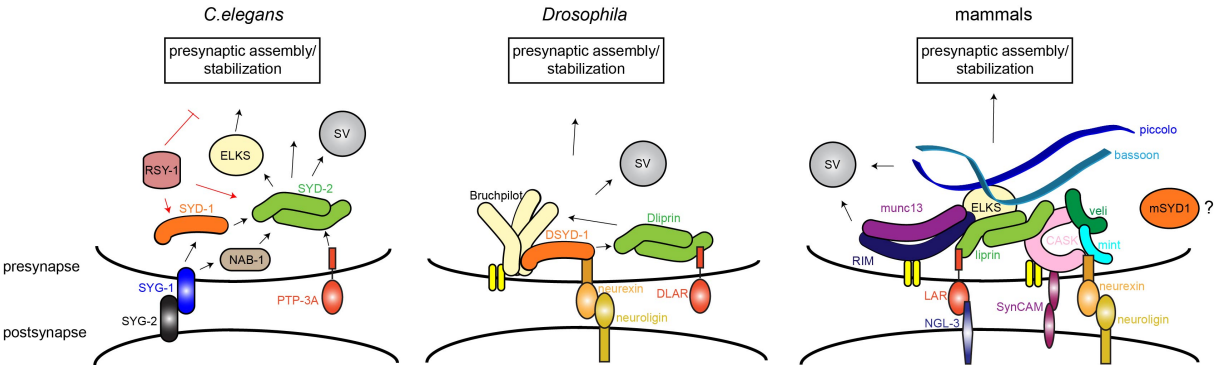

Figure 8 – Comparison of presynaptic assembly in *C.elegans*, *Drosophila* and mammals
SYD-1 has been described as a central organizer of presynaptic assembly in invertebrates. Here, SYD-1 is one of the first proteins that localizes to nascent presynaptic boutons and recruits downstream interaction partners, like SYD-2/liprin-α and ELKS/Bruchpilot. The arrows indicate genetic interactions, whereas proteins that have been shown to interact biochemically are displayed in contact with each other. RSY-1 is a negative regulator of presynaptic assembly that acts on SYD-1 and SYD-2 (red arrows). In mammals, many of the invertebrate proteins are conserved (orthologues are displayed in the same color) and a dense network of presynaptic proteins has been identified. However, how the assembly process downstream of trans-synaptic adhesion complexes is regulated, has remained obscure. No mammalian SYD-1 protein has been described yet.

No mammalian orthologues for SYD-1 have been identified so far. Therefore, the aim of this study is:

1.) Identification of vertebrate orthologues of SYD-1

2.) Investigation of mSYD1 GAP activity

3.) Identification of mSYD1 interaction partners

4.) Investigation of mSYD1 function *in vitro* and *in vivo*

2. Results

2.1 Preface

Parts of the work that I will present in the following section have been done by collaborators, whereas other parts have been joint efforts. Therefore, I herewith describe the individual contributions. The SYD-1 project was initiated by Julia Sommer, a PhD student in the lab. She identified mouse SYD1A and SYD1B in Database searches and raised and purified an antibody against mSYD1A. When I joined the project, we jointly characterized the antibody, as well as mSYD1A expression and distribution in the brain. Furthermore, Julia carried out the first analysis of the mSYD1B KO mice and evaluated the Yeast-2-Hybrid screen. The investigation of mSYD1A GAP activity, analysis of interaction partners, as well as the analysis of mSYD1A knockdown and overexpression in neurons is my work. Furthermore, I was involved in generating mSYD1A KO mice together with the Transgenic Mouse Facility of the Biozentrum, and carried out the first characterization of the mouse line. All electrophysiological recordings that are presented in this work have been done by Ramya Nair, a post-doc in the lab.

Most of the results that we have obtained on mSYD1A distribution and function are described in a submitted manuscript, which is displayed in the first part of the results section. In the second part of the results section I present additional data on mSYD1A that is relevant for the understanding and discussion of mSYD1A function, but that we have not included in the manuscript. The following part describes the creation and initial characterization of mSYD1A and mSYD1B KO mice. In the last chapter I describe our efforts to produce an additional antibody against mSYD1A.

2.2 submitted manuscript

The identification of mSYD1A and mSYD1B, as well as the characterization of mSYD1A distribution and function have resulted in a manuscript which has been submitted for publication and is displayed in the following section.

Mammalian Synapse-Defective-1 Regulates Synaptogenic Signaling

Corinna Wentzel[1,*], Julia Sommer[1,*], Ramya Nair[1], Adeline Stiefvater[1], Jean-Baptiste Sibarita[2], and Peter Scheiffele[1]

[1] Biozentrum, University of Basel, 4056 Basel, Switzerland

[2] UMR5297-CNRS, Université Bordeaux, F-33077 Bordeaux

* both authors made major contributions to this work

Correspondence: Peter Scheiffele, Biozentrum, University of Basel,

Klingelbergstrasse 50-70, 4056 Basel, Switzerland

Email: peter.scheiffele@unibas.ch

Running title: **Mammalian Synapse-Defective-1 Proteins**

Summary

Structure and function of presynaptic terminals are critical for the processing and transmission of neuronal signals. Trans-synaptic signaling systems instruct the differentiation of presynaptic sites but their downstream signaling mechanisms are poorly understood. Here, we identify a novel protein called mSYD1A (mouse Synapse-Defective-1A) as an important regulator of synaptogenic signaling in mammalian neurons. Knockdown of mSYD1A impairs synaptic vesicle clustering and reduces synaptic transmission, whereas overexpression results in an increase in synapse density. mSYD1A functions in the presynaptic cell, interacts directly with the active zone protein liprin-α2, and mediates its function via an intrinsically unstructured liprin-interaction sequence. Our work identifies an evolutionary conserved signaling module that transduces synaptogenic signaling in the presynaptic compartment.

Introduction

The transformation of an axonal plasma membrane into a presynaptic release site requires a profound re-organization of the axonal cytoskeleton and presynaptic membrane organelles (Shen & Scheiffele, 2010; Ziv & Garner, 2004). This process can be instructed by synaptogenic adhesion complexes that bridge the synaptic cleft and drive the differentiation of the synaptic terminal. Over the past decade several such synaptic organizers have been identified, including the neuroligin-neurexin complex (Graf et al, 2004; Scheiffele et al, 2000), leucine-rich repeat proteins (LRRTMs and netrin G ligands) (Linhoff et al, 2009), Ig-domain containing proteins (Biederer et al, 2002), and receptor protein tyrosine phosphatases (RPTPs) (Kwon et al, 2010; Takahashi et al, 2011). However, for none of these systems it is understood how trans-synaptic interactions instruct the morphological and functional differentiation of presynaptic terminals. Therefore, the signaling cascades that link synaptic adhesion to the formation of functional synaptic terminals in mammalian neurons are poorly understood.

Presynaptic terminals are characterized by the accumulation of synaptic vesicles and active zones, where regulated neurotransmitter release takes place (Südhof, 2012; Ziv & Garner, 2004). A multitude of protein-protein interactions links these components into highly specialized macromolecular complexes. While specific contributions of individual active zone proteins to synaptic transmission have been identified (Südhof, 2012) the current understanding of active zone assembly and the recruitment of synaptic vesicles is much more limited. Key insights into this question have been obtained in forward genetic screens

in invertebrates (Jin & Garner, 2008; Sigrist & Schmitz, 2011). From this work, two central organizers have emerged, called Synapse-defective-1 and -2 (SYD-1 and SYD-2) (Chia et al, 2012; Hallam et al, 2002; Owald et al, 2010; Sieburth et al, 2005; Zhen & Jin, 1999). *C.elegans syd-1* and *syd-2* mutants show diffuse localization of active zone components and synaptic vesicles along axonal processes (Hallam et al, 2002; Zhen & Jin, 1999). The SYD-1 and SYD-2 proteins couple to surface receptors Syg-1 and PTP-3 (a LAR-related receptor tyrosine phosphatase), respectively, and promote presynaptic assembly through ELKS-1 (Dai et al, 2006; Patel et al, 2006; Patel & Shen, 2009). Genetic experiments suggest that SYD-1 acts upstream of SYD-2. Thus, gain-of-function mutations or forced oligomerization of SYD-2 can suppress *syd-1* phenotypes, indicating that SYD-1 may regulate SYD-2 oligomeric state (Dai et al, 2006; Taru & Jin, 2011). At the *Drosophila* neuromuscular junction SYD-1 interacts via its PDZ domain with the presynaptic receptor neurexin and coordinates pre- and postsynaptic assembly through a trans-synaptic signaling link (Owald et al, 2012). In analogy to the invertebrate SYD-2 proteins, their mammalian counterparts, called liprins (for LAR-interacting proteins), form oligomeric scaffolds (Hoogenraad et al, 2007; Olsen et al, 2005) but specific functions in the presynaptic terminal are little understood. Importantly, no mammalian SYD-1 orthologues have been characterized, thus, raising the question whether an analogous SYD-1/SYD-2 signaling system exists in mammals and if so, whether it has a functional contribution to active zone assembly or synaptic vesicle recruitment.

Here, we identify two previously uncharacterized mouse SYD-1 orthologues that we name mSYD1A and mSYD1B. These mammalian SYD1 proteins share sequence homology with their invertebrate counterparts but differ significantly in domain organization and in signaling properties. Gain- and loss-of-function experiments strongly support a key role in presynaptic assembly. mSYD1A function depends on an intrinsically unstructured liprin-interaction sequence (LIS). The LIS mediates recruitment of mSYD1A to the receptor tyrosine phosphatase LAR through direct interactions with the SYD-2 orthologue liprin-α2. Finally, we demonstrate that mSYD1A down-regulation impairs multiple trans-synaptic signaling systems, establishing mSYD1A as a central regulator of presynaptic differentiation.

Results

mSYD1A is expressed during the time of synapse formation and associates with synaptic membranes

Based on sequence similarity searches we identified two candidate mouse *syd-1* orthologues: *syde1*/NP_082151.1 (in the following referred to as *msyd1a*, for mammalian

synapse-defective-1A) and *syde2*/NP_001159536 (*msyd1b*) (Figure S1A). The domain organization with *C.elegans* and *Drosophila* SYD-1 proteins is only partially conserved in the candidate mammalian orthologues. The SYD1 proteins share predicted C2 and Rho-GAP domains. However, the mammalian SYD1 proteins lack the N-terminal PDZ-domain sequences observed in the invertebrate proteins (Figure 1A), a domain critical for trans-synaptic signaling by *Drosophila* SYD-1 (Owald et al, 2012). Notably, the mouse genome contains no protein with consecutive PDZ, C2 and Rho-GAP domains. mSYD1A and mSYD1B resemble invertebrate SYD-1 most closely, followed by Bcr (breakpoint cluster region protein)(Figure S1A). However, Bcr differs significantly from SYD-1 proteins due to its more complex domain architecture with additional RhoGEF and PH domains. A remarkable feature of mSYD1A and mSYD1B is the presence of extensive stretches of N-terminal sequences that are predicted to be intrinsically unstructured (Figure 1B, S1B), a property that has been hypothesized to endow proteins with an ability to adapt to multiple specific binding partners and to contribute to the assembly of macromolecular arrays (Dyson & Wright, 2005). In summary, the mSYD1A and mSYD1B proteins do not exactly conform to the invertebrate proteins but represent the best candidate SYD-1 orthologues based on sequence information.

Expression of cDNAs encoding HA-epitope tagged mSYD1A and mSYD1B in HEK293T cells resulted in proteins with an apparent molecular weight of 100 and 150 kDa, respectively (Figure 1C, “cDNA”). An affinity-purified antibody raised against the N-terminus of mSYD1A recognized overexpressed mSYD1A but not mSYD1B. Using this mSYD1A-specific antibody we confirmed expression of endogenous mSYD1A in lysates of purified cerebellar granule cells (GC) and P5 whole brain (Figure 1C). Endogenous mSYD1A exhibited the same apparent molecular weight (100 kDa) as the protein expressed from cDNA. Notably, the deviation from the size predicted from the primary amino acid sequence (80 kDa) is a phenomenon frequently observed for intrinsically unfolded proteins (Tompa, 2002). mSYD1A was also detected in HEK293 cells (Figure 1C, “HEK”) demonstrating that the protein is also expressed in non-neuronal cells. Specificity of mSYD1A detection was confirmed by RNA interference knockdown in HEK293T cells and neuronal cultures, which strongly reduced abundance of the 100 kDa immunoreactive band (Figure 1D). Note that small double-stranded RNAs were applied conjugated to a cell membrane penetrating tag, which allows for direct delivery into cultured cells and efficient mSYD1A knockdown in the majority of cells (Figure S2A).

In mouse brain extracts, we observed significant expression of mSYD1A from E14 until adult stages (Figure 1E). Cross-reactivity of our antibody with unknown cellular proteins precludes an analysis with histological methods. Therefore, we employed subcellular fractionation to investigate the localization of endogenous mSYD1A. In P2 mouse brain

extracts mSYD1A was enriched in a membrane fraction (P2) (Figure 1F). Notably, a pool of mSYD1A was recovered in nuclear fractions (P1). To address whether mSYD1A is found at synapses, we isolated synaptosomal membranes from adult mouse brain (Figure 1G). mSYD1A was recovered in brain cytosol (S2) but also in the crude purified synaptosomal fractions (P2). After lysis of the synaptosomes, similar amounts of mSYD1A were associated with the Triton X-100 soluble and insoluble fractions. Finally, we examined the localization of epitope-tagged mSYD1A that was overexpressed in cultured cerebellar granule neurons. The tagged protein was detected throughout the cell, however, within axons immune-reactivity was observed in a punctate pattern with a significant fraction of mSYD1A accumulations also containing synaptic markers vGluT1 and PSD95 (Figure 1H). In combination, these findings demonstrate that mSYD1A is expressed in the developing brain with pools of the protein distributed between the cytoplasm, membranes and synaptic structures.

mSYD1A is required for synapse assembly

We tested a requirement for mSYD1A in presynaptic differentiation using RNA interference. To measure the density of synaptic terminals along the axon we marked synaptic vesicles in a subset of cells by transfection of a synaptophysin-mCherry fusion protein (Figure 2A). Postsynaptic elements were visualized by immunostaining for PSD95. Morphometric analysis of synaptic markers was performed by a wavelet-based segmentation method with a Multidimensional Image Analysis (MIA) module (Figure S2F) (Izeddin et al, 2012; Racine et al, 2006). This approach enables reliable quantitative assessment of synaptic markers. In mSYD1A knockdown neurons, the mean density of synaptophysin-mCherry-positive puncta was reduced by 39 ± 8 (s.e.m.) % whereas the density of PSD95-containing structures was not significantly altered (Figure 2B-D). Furthermore, the intensities of synaptophysin-mCherry-positive puncta were reduced in mSYD1A knockdown neurons, with puncta of higher intensities being less frequent (Figure 2E). When restricting the analysis to synaptophysin/PSD95 double-positive structures or when analyzing an endogenous synaptic vesicle marker a similar reduction in the accumulation of synaptic vesicles was observed (Figure 2D, and see Figure 6C). In comparison to synaptic vesicle proteins active zone markers were less severely affected. Munc13-1 distribution was not noticeably altered whereas the density of bassoon-positive clusters was slightly reduced in mSYD1A knockdown neurons (Figure 2F). Thus, in cerebellar granule cells loss of mSYD1A primarily affects the recruitment of synaptic vesicles to synaptic contacts. Notably, mSYD1A knockdown did not result in alterations in the length or branching of dendritic trees or an overall density of axonal processes in the neuronal cultures (Figure S2A-E). We tested

whether function of mSYD1A is specifically required in the presynaptic cell by introducing a human, siRNA-resistant form of SYD1A (hSYD1A) into the synaptophysin-mCherry-positive cells. Importantly, this was sufficient to rescue the presynaptic terminal and synapse density back to wild-type level (Figure 2C,D).

Recording of miniature EPSCs in mSYD1A knockdown cultures further supported a presynaptic phenotype. The mEPSC frequency in knockdown neurons was reduced by 43 ± 6.4 (s.e.m.) % as compared to controls (Figure 2G). This reduction was rescued by re-introduction of hSYD1A using lenti-viral infection. We also observed an apparent decrease in mEPSC amplitude in mSYD1A knock-down neurons, however, since this was not fully rescued by hSYD1A re-expression it remains to be explored whether mSYD1A indeed regulates postsynaptic properties. In combination with the morphological effects on synaptic vesicle distribution these experiments demonstrate that mSYD1A controls presynaptic differentiation in cultured neurons and is required specifically in the presynaptic cell.

mSYD1A exhibits GAP activity towards RhoA

To explore mechanisms of mSYD1A function we analyzed its signaling properties. Based on sequence comparisons, the invertebrate SYD-1 proteins are thought to contain inactive Rho-GAP-like domains (Hallam et al, 2002). By contrast, the mammalian SYD1 sequences show a high conservation with the Rho-GAP consensus (Figure S3A). We directly probed GAP activity of mSYD1A in intact cells using a FRET-based assay (Itoh et al, 2002) (Figure 3A). Using a RhoA sensor (Pertz et al, 2006), we observed a significant RhoA inactivation in cells expressing mSYD1A. The degree of RhoA inactivation was similar to that observed for p50rhoGAP, a well-characterized GAP (Figure 3B,C). Importantly, mutation of the arginine finger (Graham et al, 1999) in mSYD1A (R436A) strongly reduced mSYD1A activity observed in this assay and no change in FRET was observed when Lin-2/CASK, a protein lacking GAP domains, was introduced (Figure 3B,C).

We further examined the impact of sequence alterations in invertebrate Rho-GAP sequences by engineering corresponding mutations into the mammalian mSYD1A protein. R436V/N552R mimic *C.elegans* SYD-1 amino acid alterations from the Rho-GAP consensus, specifically in the arginine finger and an asparagine that stabilizes the effector loop of RhoA (Hallam et al, 2002; Scheffzek & Ahmadian, 2005). In *Drosophila* DSYD-1 the same asparagine residue is altered to alanine (corresponding mutation in mSYD1A is N552A) whereas the arginine finger is preserved (Figure S3A). Both mutant mSYD1A forms lacked GAP activity, suggesting that the mutations indeed strongly reduce activity towards RhoA

(Figure 3D,E). Therefore, mSYD1A is a functional Rho-GAP whereas amino acid substitutions render the GAP domains of invertebrate SYD-1 proteins inactive.

Neuronal cells undergo characteristic morphological changes in response to manipulation of Rho-GTPase activities (Luo, 2000). Expression of C-terminally Myc-tagged mSYD1A in cerebellar granule cells led to a significant increase in the dendritic tree of these neurons compared to GFP-transfected neurons (Figure 3F). A similar phenotype was observed in cells expressing p50rhoGAP, but not in cells expressing mSYD1A containing arginine finger mutations (R436A or ΔYRL). Furthermore, we detected a significant increase in dendritic branching. These morphological read-outs are consistent with an inactivation of endogenous RhoA-dependent contractility by mSYD1A overexpression and support the hypothesis that mSYD1A regulates RhoA in primary neuronal cells.

GAP activity of mSYD1A is auto-inhibited by its N-terminal domain

The functional and morphological differentiation of synapses requires a substantial local re-organization of the neuronal plasma membrane and the underlying cytoskeleton. We hypothesized that mechanisms should exist that impose spatial and temporal control on the GAP activity of mSYD1A during presynaptic differentiation. Therefore, we tested whether the N-terminal intrinsically unstructured sequences of mSYD1A might contribute to its functional regulation. Deletion of the N-terminal domain (NTD) and C2 domain resulted in a doubling of mSYD1A GAP activity (Figure 4A,B). A similar increase was observed when full-length mSYD1A was targeted to the plasma membrane with an N-terminal lipid modification (myr-mSYD1A) suggesting that full-length mSYD1A is in an auto-inhibitory conformation and can be activated by the displacement of N-terminal sequences (Figure 4A,B). To further dissect the potential auto-inhibitory function of mSYD1A sequences, we generated deletion constructs and tested their function in the Rho-GAP assay. These experiments revealed that the NTD was required for auto-inhibition of mSYD1A (Figure 4C). When we co-expressed NTD and GAP domains as independent polypeptides (Figure 4D), the NTD alone as well as the NTD-C2 domain supplied in *cis* where able to repress activity of the isolated mSYD1A GAP domain. In this assay, presence of the C2 domain reduced GAP activity to somewhat larger extent than the NTD construct lacking the C2 domain (Figure 4D). Finally, we tested whether the inhibition of mSYD1A GAP activity is mediated through protein-protein interactions between the NTD and GAP domains in co-immunoprecipitation experiments (Figure 4E). Myc-tagged GAP domain was co-immunoprecipitated with the HA-tagged NTD,C2 domain. Therefore, the mSYD1A GAP activity is regulated through protein-protein interactions with the intrinsically unstructured N-terminal region suggesting that full-length

mSYD1A adopts a closed, auto-inhibited conformation. Displacement of the NTD, either by truncation or membrane targeting, provides a mechanism for local activation of mSYD1A.

We tested the functional relevance of the characterized mSYD1A subdomains in synapse formation using gain-of-function experiments. Overexpression of full-length mSYD1A in cultured granule cells resulted in a 64 ± 10 (s.e.m.) % elevation in the density of synaptic vesicle clusters and a 38 ± 11 (s.e.m.) % increase in synapse density, defined as puncta containing the markers synaptophysin and PSD95. Thus, presynaptic expression of mSYD1A is sufficient to stimulate pre- and postsynaptic differentiation. Surprisingly, a construct in which the arginine finger was deleted (ΔYRL) retained the ability to elevate presynaptic terminal number (Figure 4F). Moreover, a membrane-targeted form of the NTD (that lacks the entire C2 and GAP domain sequences of mSYD1A) was sufficient to increase presynaptic terminal density and partially co-localized with the synaptic vesicle marker vGluT1 in axons (Figure 4F and S3B). While the GAP-domain was not required for driving the recruitment of synaptic vesicles it was essential for the concomitant recruitment of PSD95 (Figure 4F). Therefore, recruitment of synaptic vesicles downstream of mSYD1A is independent of its GAP activity but the further maturation of these incipient sites relies on the presence of the GAP domain, presumably through a trans-synaptic signaling mechanism.

mSYD-1A interacts with the active zone protein liprin-α2

To obtain insight into how the mSYD1A NTD may contribute to presynaptic differentiation we sought to identify proteins that interact with this domain. In pull-down assays with purified recombinant fragments of liprin-α1, α2 and α4 proteins, we uncovered selective protein-protein interactions with mSYD1A (Figure 5A-C). We first examined interactions of the N-terminal coiled-coil domains of liprin-α which was previously reported to bind to ELKS2 (Ko et al, 2003b). While we could reproduce this interaction we did not detect any binding of mSYD1A to this domain (Figure 5B). By contrast, mSYD1A interacted efficiently with the SAM-domains located in the C-terminal half of liprin-α2. The same liprin-α2 SAM-domain also exhibited robust binding to Lin-2/CASK (as previously reported (Olsen et al, 2005); Figure 4C). Interestingly, liprin-α – mSYD1A interactions were strictly isoform-specific. Liprin-α2 contains a 37 amino acid insertion located between the first and the second SAM domain that is absent in the primary liprin-α1 isoform (Wei et al, 2011; Zürner & Schoch, 2009) (Figure 5A). Deletion of these 37 amino acids (SAMΔPQ) abolished binding between mSYD1A and liprin-α2 (Figure 5C, see Figure S4A for recombinant proteins used in the pull-down). Pull-down assays with the liprin-α2 SAM domains and several deletion constructs of

mSYD1A showed that the N-terminal domain (NTD) engages in binding to liprin-α2 (Figure 5D). Interestingly, this liprin binding sequence (LIS) does not resemble any recognizable domain structure and more than 87 % of this sequence is predicted to be unstructured (protein disorder prediction; http://prdos.hgc.jp).

We confirmed direct mSYD1A-liprin-α2 protein-protein interaction with purified recombinant proteins. Beads loaded with purified liprin-α2-SAM led to a dose-dependent recovery of purified mSYD1A NTD whereas no binding was observed to a control protein (Figure 5E). In summary, these experiments demonstrate that the N-terminal LIS of mSYD1A binds directly to the SAM-domains of liprin-α2 and that these interactions require the liprin-α2-specific PQ loop insertions.

LAR/liprin-α2-nucleated scaffolding complexes recruit mSYD1A

The biochemical interactions between mSYD1A and the active zone protein liprin-α2 raise the question whether mSYD1A and liprin-α2 act in a complex downstream of synaptic cell surface receptors, in particular receptor protein tyrosine phosphatases (RPTP) that recruit liprins and contribute to synapse formation (Kwon et al, 2010; Takahashi et al, 2011; Yoshida et al, 2011). To investigate mSYD1A – liprin-α – LAR complexes in intact cells, we co-expressed the proteins in COS7 cells and analyzed their subcellular distribution. When expressed alone, liprin-α2 was distributed in clusters throughout the cell, whereas LAR was mainly found in intracellular peri-nuclear structures reminiscent of the ER-Golgi/Intermediate-compartment (Figure 5F). By contrast, mSYD1A was diffusely distributed throughout the cytoplasm. Co-expression of mSYD1A and liprin-α2 resulted in recruitment of mSYD1A into the liprin-α2 containing structures (Figure 5F). In presence of LAR, liprin-α2 and mSYD1A were found concentrated in patches of LAR at the cell surface (Pearson's coefficient, 0.85 ± 0.05 (s.d.)), suggesting that these proteins function in a signaling complex (Figure 5G, S4B,C). Deletion of the mSYD1A NTD abolished concentration of mSYD1A in the LAR-liprin-α2 complexes (Pearson's coefficient 0.19 ± 0.2 (s.d.), Figure 5G). These cellular assays demonstrate that mSYD1A is recruited to sub-membrane clusters of liprin-α2 that are associated with the cell surface receptor LAR in heterologous cells.

mSYD1A regulates presynaptic assembly downstream of multiple trans-synaptic signals

The association of mSYD1A with the active zone protein liprin-α2 and its recruitment to the receptor tyrosine phosphatase LAR suggest that mSYD1A may contribute to the assembly of presynaptic terminals specifically downstream of protein receptor tyrosine phosphatases (Woo et al, 2009). Alternatively, liprin-α2 may be a common regulator downstream of multiple neuronal cell surface receptors. To explore this, we stimulated presynaptic differentiation by overexpression of the LAR-receptor NGL-3 or neuroligin-1 (NL1, which promotes presynaptic differentiation through neurexins but does not interact with LAR). We monitored the density of vGluT-1-positive synaptic vesicle clusters and the active zone marker bassoon (Figure 6). Overexpression of NGL-3 or neuroligin-1 led to a significant elevation in the density of vGluT1 and bassoon puncta along the dendrites of transfected neurons (Figure 6A,B). Knockdown of mSYD1A significantly attenuated this increase, both for cells expressing NGL-3 as well as neuroligin-1 (Figure 6A-C). Furthermore, knockdown of mSYD1A led to a reduction in the number of vGluT1 and bassoon puncta formed onto the dendrites of GFP-transfected control neurons. Importantly, NGL-3 or NL1 expression levels were not significantly different in siSYD1A- *versus* siCNT-treated cultures (Figure 6D). These findings demonstrate that in cerebellar granule cells, mSYD1A acts in a common presynaptic pathway downstream of at least two different synaptic adhesion complexes and represents a novel regulator of presynaptic differentiation.

Discussion

While recent studies have identified a number of trans-synaptic signaling systems that promote the formation of synapses in the central nervous system, there is a significant gap of knowledge with respect to the cytoplasmic signal transducers that control synaptogenic signaling (Shen & Scheiffele, 2010). Several lines of evidence obtained in this study support a function for mSYD1A as a novel presynaptic regulator of synapse assembly: (a) Elevation of mSYD1A protein level stimulates synaptic differentiation, (b) suppression of mSYD1A impairs presynaptic differentiation and synaptic transmission; (c) mSYD1A function is required in the presynaptic neuron and endogenous mSYD1A is recovered in synaptosome fractions; (d) mSYD1A interacts directly with liprin-α proteins via an intrinsically unstructured liprin-interacting sequence (LIS), and (e) the mSYD1A LIS alone stimulates presynaptic differentiation without modifying postsynaptic scaffolds.

Considering that mammalian and invertebrate SYD-1 proteins share significant sequence homology only in their C2 and GAP domains it was a critical question whether mSYD1A can indeed be considered a functional SYD-1 orthologue. We uncovered functional and biochemical properties of mSYD1A that parallel hallmarks of SYD-1 activity deduced from genetic studies in invertebrates, thus supporting the notion that mSYD1A is indeed a bona fide orthologue. However, our analysis also reveals several striking differences between mSYD1A and invertebrate SYD-1 proteins. We identified an intrinsically unstructured LIS in mSYD1A as key determinant for presynaptic differentiation. Liprin-α binding to the LIS requires a specific PQ-loop insertion in liprin-α2. Notably, this insertion is not present in the invertebrate SYD-2s, suggesting that this biochemical interaction is unique for the vertebrate proteins. Trans-synaptic signaling by *Drosophila* SYD-1 requires the PDZ-domain of the protein (Owald et al, 2012) which is absent in mSYD1A. By contrast, for the mammalian protein trans-synaptic signaling relies on its Rho-GAP domain. Thus, in mammalian SYD1 proteins certain divergent mechanisms of synaptic function have evolved.

Identification of an intrinsically unstructured region in mSYD1A as presynaptic scaffolding regulator

Multiple Rho-GTPase regulators (GAPs and GEFs) have been previously recognized as regulators of synapse size and tethering of synaptic vesicles at presynaptic release sites (Ball et al, 2010; Frank et al, 2009; Sun & Bamji, 2011). While mSYD1A is an active GAP, regulation of presynaptic terminal differentiation downstream of mSYD1A does not require its GAP activity. Instead, the LIS is critical for mSYD1A-stimulated synapse assembly. Liprin-αs contain an N-terminal liprin-homology domain, which drives oligomerization of the protein, a key step in presynaptic terminal assembly (Taru & Jin, 2011; Zürner & Schoch, 2009). Considering that the mSYD1A LIS is sufficient to elevate presynaptic terminal density in cerebellar neurons, we hypothesize that liprin-binding through these sequences results in the displacement of the liprin-α SAM domains and subsequent liprin-homology-domain dependent oligomerization. The mSYD1A - liprin-α scaffold would then serve as an organizing platform for active zone components that interact directly with the N-terminal liprin-α coiled-coil domains, such as ELKS, GIT, and RIM (Ko et al, 2003b; Schoch et al, 2002). We observed an impairment of presynaptic vesicle recruitment to synaptic terminals as a primary defect resulting from mSYD1A loss-of-function whereas mutation of *C.elegans* SYD-1 results in severe disruption of both, synaptic vesicle clustering and active zone assembly (Dai et al, 2006; Patel et al, 2006). The more modest alterations in active zone markers in response to mSYD1A down-regulation suggest that additional pathways control active zone components in mammalian neurons.

In addition to its ability to recruit liprin-α, the LIS contributes to an auto-regulatory mechanism of the mSYD1A Rho-GAP domain, where displacement of the LIS results in an elevation of GAP activity. At least in our gain-of-function experiments, the mSYD1A Rho-GAP domain was not required for presynaptic assembly, but played a critical role in the recruitment of postsynaptic components. Thus, two different domains of mSYD1A regulate presynaptic assembly and trans-synaptic signaling.

mSYD1A is a downstream effector of multiple presynaptic receptors

Presynaptic differentiation in the mammalian central nervous system relies on multiple parallel signaling pathways that may converge on common signal mediators (Shen & Scheiffele, 2010). We probed whether loss of mSYD1A impacts the formation of presynaptic terminals downstream of two different classes of synaptogenic trans-synaptic links, the NGL-3/LAR and neurexin/neuroligin adhesion complexes. We observed a similar reduction in presynaptic differentiation in response to either synaptogenic trigger, indicating that mSYD1A is a common mediator in both trans-synaptic signaling systems. For LAR, we directly demonstrated recruitment of mSYD1A/liprin-α2 complexes in heterologous cells, whereas a mechanism for coupling of mSYD1A to mammalian neurexins (the neuroligin-1 receptor) remains to be explored. Regardless, our data indicate that mSYD1A is a common mediator of multiple synaptogenic signals that controls presynaptic differentiation in mammalian neurons.

Acknowledgements

We thank Yves Barde, Thi-Minh Nguyen, Olivier Pertz, Mingjie Zhang, Eunjoon Kim, Stephan Sigrist, Matthijs Verhage, Casper Hoogenraad, Susanne Schoch, Tim Sharpe and Dietmar Schreiner for reagents and advice. This work was supported by a fellowship from the Werner-Siemens Foundation to C.W., an award from the Boeringer Ingelheim Fund to J.E.S., funds to P.S. from the Swiss National Science Foundation, the National Institute on Drug Abuse, and the Kanton Basel-Stadt.

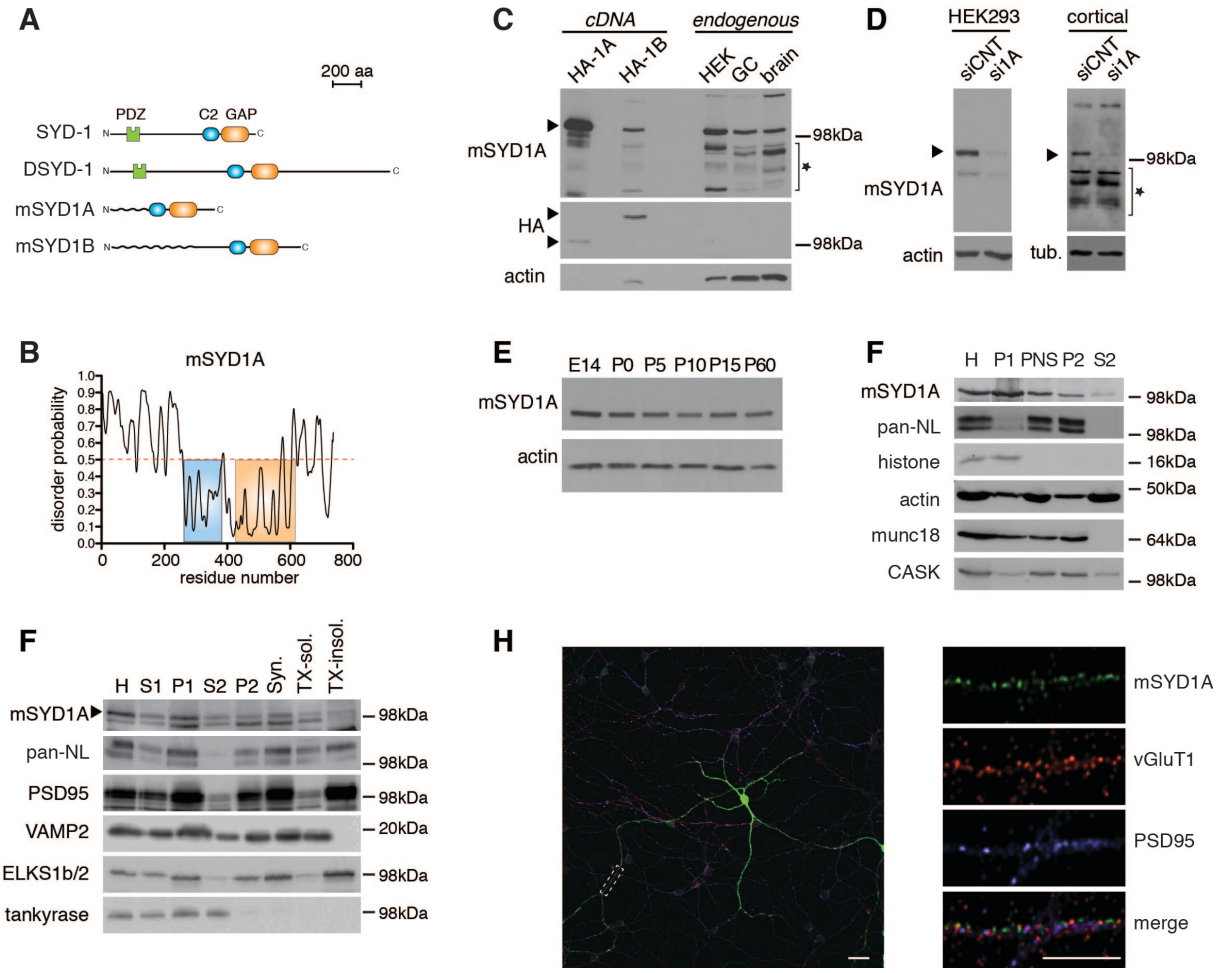

Figure 1 – Identification and characterization of mSYD1A
(A) Predicted domain structure of *C.elegans* SYD-1, *Drosophila* DSYD-1, mouse mSYD1A and mouse mSYD1B. **(B)** The N-terminal region of mSYD1A is predicted to be instrinsically unstructured (http://prdos.hgc.jp/cgi-bin/top.cgi). Residues above a threshold of 0.5 are predicted to be disordered. **(C)** Western blot with anti-mSYD1A antibodies on HA-tagged mSYD1A and mSYD1B overexpressed in HEK293T cells (HA-1A, HA-1B), untransfected HEK293T cells, cerebellar granule neurons (GC) and P5 mouse brain lysate (brain). The star marks unspecific bands. Note that higher amounts of cell lysates were loaded for detection of endogenous proteins to enable direct comparison with the protein expressed from cDNA. **(D)** The 100 kDa mSYD1A-immuno-reactive band is selectively lost after treatment of cultured HEK293T cells and cortical neurons with *syd1a* specific siRNAs (si1A) but not non-targeting control siRNAs (siCNT). **(E)** mSYD1A immune-reactivity is detected in whole brain lysate between E14 and adult. **(F)** Fractionation of P2 mouse brain lysate. H: homogenate, P1: nuclei and intact cells, PNS: post-nuclear-supernatant, P2: membrane fraction, S2: cytosolic fraction. **(G)** Synaptosome fractionation of adult mouse brain. 10 µg of proteins were loaded for each fraction. H: homogenate; Syn.: synaptosomes; TX-sol.: Triton X-100 soluble synaptic proteins; TX-insol.: Triton X-100 insoluble synaptic protein complexes. **(H)** Overexpressed mSYD1A with a C-terminal myc-epitope tag is detected in soma, axon and dendrites of cultured cerebellar granule cells. In the axon, mSYD1A shows a punctate distribution partially overlapping with vGluT1/PSD95 puncta (scalebar left = 20 µm, scalebar right = 10 µm).

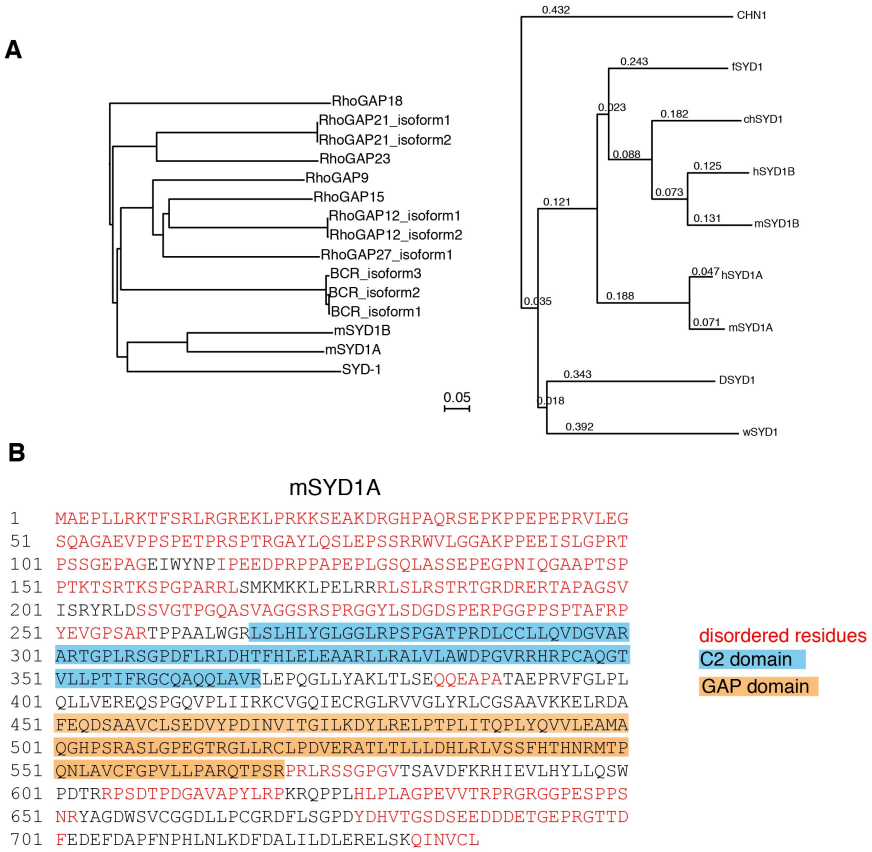

Figure S1 – Sequence alignments
(A) Phylogenetic tree of mouse proteins identified in protein homology searches with *C.elegans* SYD-1 against the non-redundant protein database NCBI. Only the proteins with the closest similarity to SYD-1 are shown. The Phylogram was created based on the ClustalW2 (http://www.ebi.ac.uk/Tools/msa/clustalw2) primary amino acid sequence alignment of SYD-1, DSYD-1, mSYD1A, mSYD1B, hSYD1A, hSYD1B, chSYD1 (chick), and fSYD1 (zebrafish). Branch lengths are proportional to inferred evolutionary change. **(B)** The N-terminal domain of mSYD1A is predicted to be instrinsically unstructured. Disordered residues are shown in red (http://prdos.hgc.jp/cgi-bin/top.cgi). C2 and RhoGAP domains are shown in blue and yellow.

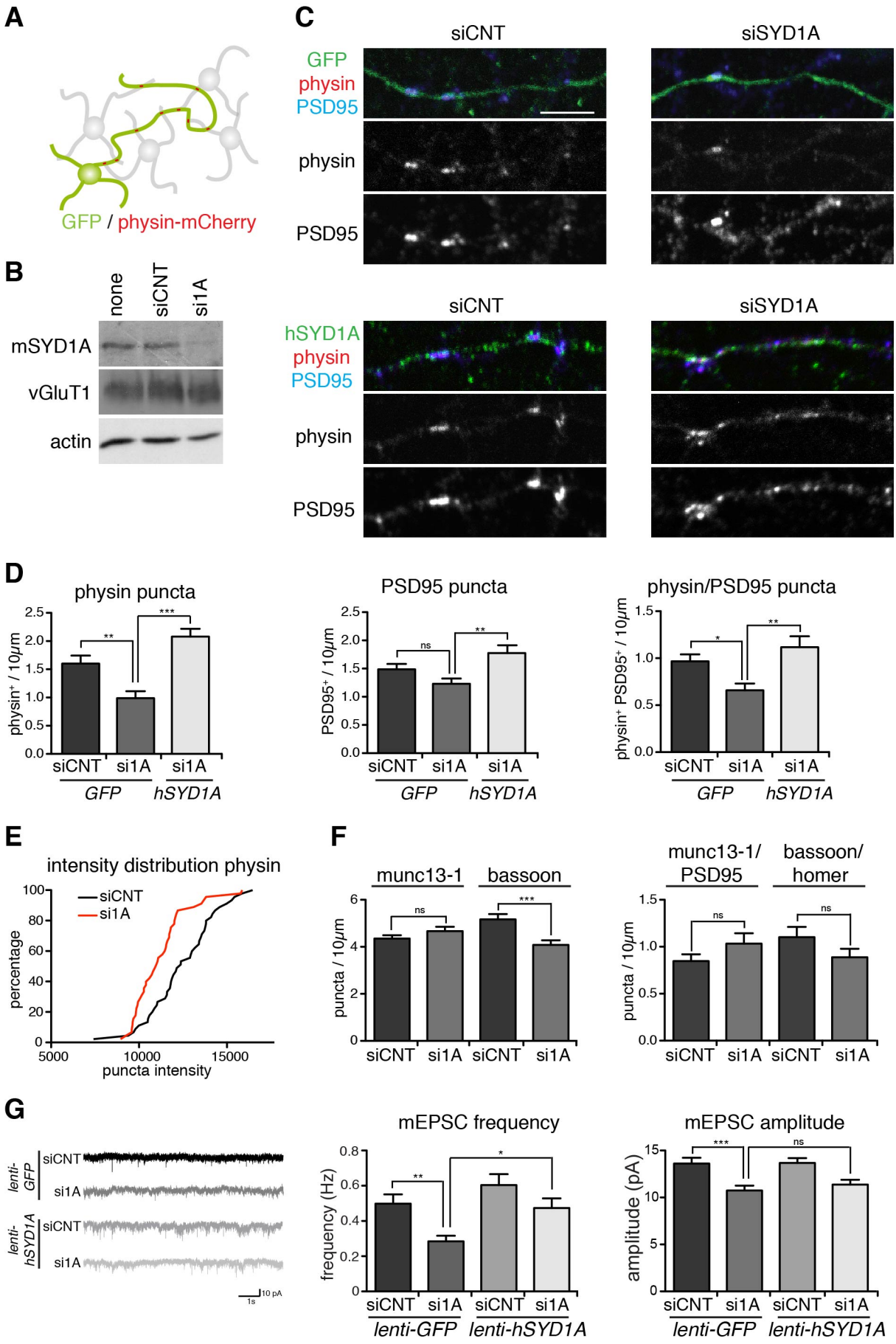
A
GFP / physin-mCherry
B
none
siCNT
si1A
mSYD1A
vGluT1
actin
C
siCNT
siSYD1A
GFP
physin
PSD95
physin
PSD95
siCNT
siSYD1A
hSYD1A
physin
PSD95
physin
PSD95
D
physin puncta
physin+ / 10µm
siCNT si1A si1A
GFP hSYD1A
PSD95 puncta
PSD95+ / 10µm
siCNT si1A si1A
GFP hSYD1A
physin/PSD95 puncta
physin+ PSD95+ / 10µm
siCNT si1A si1A
GFP hSYD1A
E
intensity distribution physin
siCNT
si1A
percentage
puncta intensity
F
munc13-1
bassoon
puncta / 10µm
siCNT si1A siCNT si1A
munc13-1/ PSD95
bassoon/ homer
puncta / 10µm
siCNT si1A siCNT si1A
G
lenti-GFP
siCNT
si1A
lenti-hSYD1A
siCNT
si1A
10 pA
1s
mEPSC frequency
frequency (Hz)
siCNT si1A siCNT si1A
lenti-GFP lenti-hSYD1A
mEPSC amplitude
amplitude (pA)
siCNT si1A siCNT si1A
lenti-GFP lenti-hSYD1A

Figure 2 – Knockdown of mSYD-1A decreases synaptic vesicle clustering
(A) Global knockdown of mSYD1A is combined with selective marking of a subset of cerebellar granule cells using eGFP and synaptophysin-mCherry. For selective presynaptic rescue of mSYD1A, siRNA-resistant hSYD1A is expressed in a subset of cells. **(B)** Knockdown of mSYD1A was verified by Western-Blot in untreated (none), control (siCNT) and mSYD1A knockdown (si1A) granule cell cultures. **(C)** Accumulation of synaptophysin-mCherry (physin) and endogenous PSD95 along transfected neurons in control (siCNT) and mSYD1A knockdown (siSYD1A) neurons. Rescue of the knockdown was achieved by transfection of the siSYD1A-resistant human SYD1A (hSYD1A) (scalebar = 10 µm). **(D)** Quantitative analysis of synaptic markers. The number of physin or PSD95-positive puncta per 10 µm axon length were counted, as well as the number of physin/PSD95 double positive puncta (n=45 cells; *: $p<0.05$; ***: $p<0.0001$; ANOVA and Tukey's multiple comparison test; mean ± s.e.m.). **(E)** Cumulative distribution of staining intensity for synaptophysin-mCherry-positive puncta in siCNT and siSYD1A-treated neurons. **(F)** Number of munc13-1^{+}, bassoon^{+} and munc13-1/PSD95, bassoon/homer double positive puncta per 10 µm axon length (n=45 cells; ns: not significant; ***: $p=0.0005$; two-tailed t-test; mean ± s.e.m.). **(G)** Recordings of miniEPSC frequency and miniEPSC amplitude from cerebellar granule cells infected with a lentivirus driving expression of GFP or GFP and hSYD1A (rescue) and treated with siCNT or siSYD1A (n=30 cells; *: $p<0.05$; **: $p<0.001$; ***: $p<0.0001$; ns: not significant; non-parametric ANOVA and Dunn's multiple comparison test; mean ± s.e.m.).

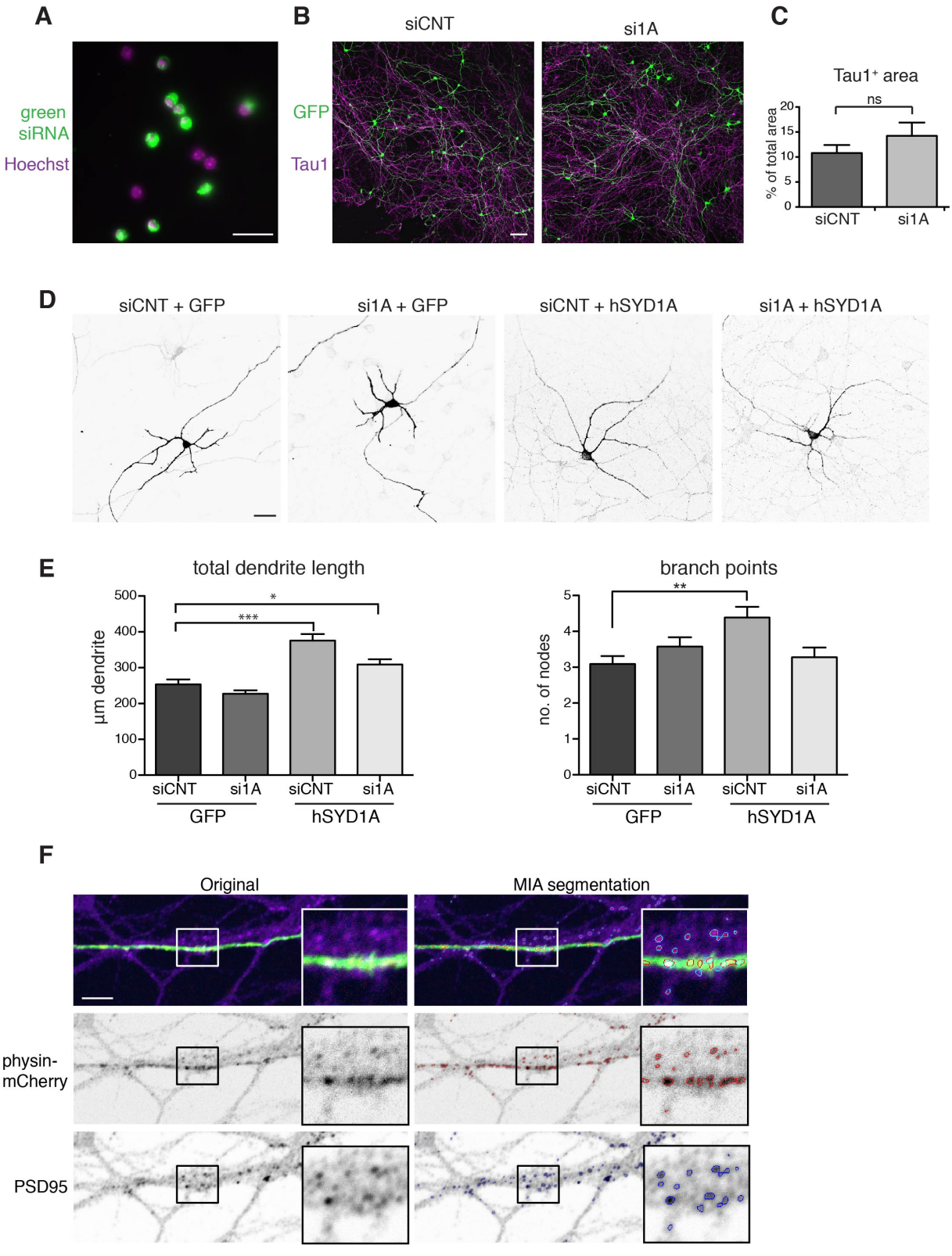

Figure S2 – Knockdown of mSYD1A with siRNA
(A) Cerebellar granule cells treated with dye-conjugated siRNAs (green) and stained with Hoechst (magenta) (scalebar = 10 µm). **(B)** Axonal density after application of control (siCNT) and SYD1A (si1A) siRNA to cerebellar granule cells transfected with GFP and stained for Tau1 (scalebar = 50 µm). **(C)** The Tau1 positive area in siRNA-treated neurons (n=20, ns: not significant; two-tailed t-test; mean ± s.e.m.). **(D)** Knockdown of mSYD1A does not change dendritic morphology (scalebar = 20 µm). **(E)** Analysis of total dendritic length and branch points in neurons treated with siCNT or siSYD1A, overexpressing GFP or hSYD1A (n=45 cells; *: p<0.05; **: p<0.001; ***: p<0.0001; ANOVA

and Tukey's multiple comparison test; mean ± s.e.m.). **(F)** Wavelet segmentation of a typical image, used for quantification of physin^{+} and PSD95^{+} puncta in figure 2. Left column displays the original images. Right column shows the result of puncta identification performed by wavelet segmentation. A threshold of 15 (synaptophysin-mCherry) or 35 (PSD95) times the noise standard deviation of the image was applied on the third wavelet map (scalebar = 10 µm).

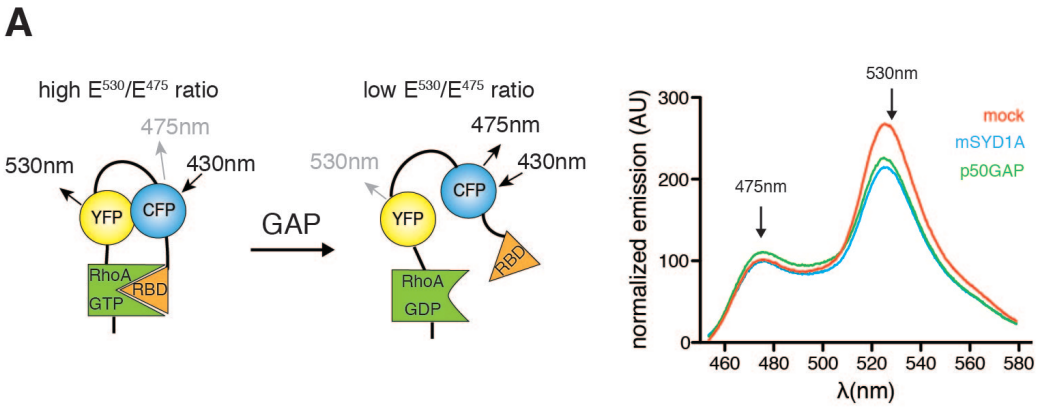
A
high E530/E475 ratio
475nm
530nm
430nm
YFP
CFP
RhoA
RBD
GTP
GAP
low E530/E475 ratio
475nm
530nm
430nm
CFP
YFP
RBD
RhoA
GDP
530nm
mock
mSYD1A
p50GAP
475nm
normalized emission (AU)
300
200
100
0
460 480 500 520 540 560 580
λ(nm)

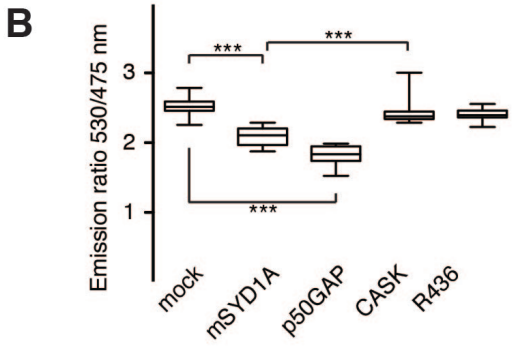
B
Emission ratio 530/475 nm
3
2
1
***
***
***
mock
mSYD1A
p50GAP
CASK
R436

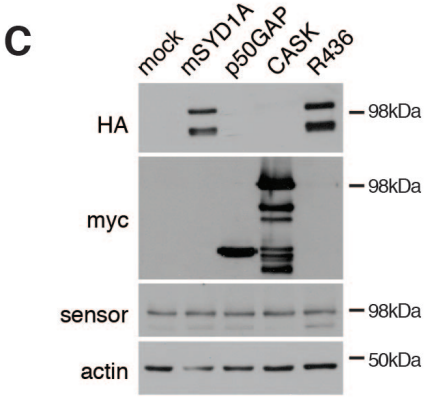
C
mock
mSYD1A
p50GAP
CASK
R436
HA
myc
sensor
actin
98kDa
98kDa
98kDa
50kDa

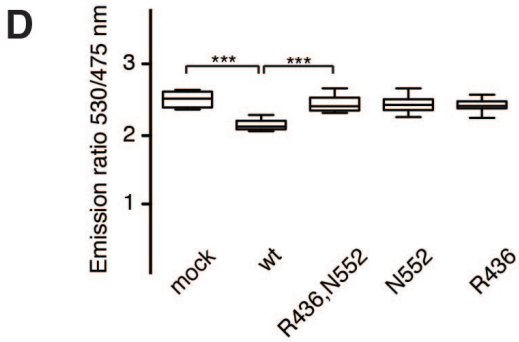
D
Emission ratio 530/475 nm
3
2
1
***
***
mock
wt
R436,N552
N552
R436

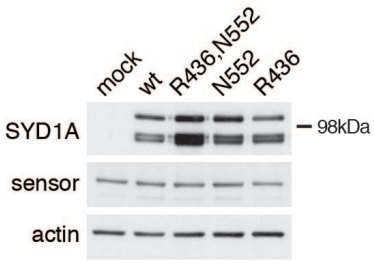
E
mock
wt
R436,N552
N552
R436
SYD1A
sensor
actin
98kDa

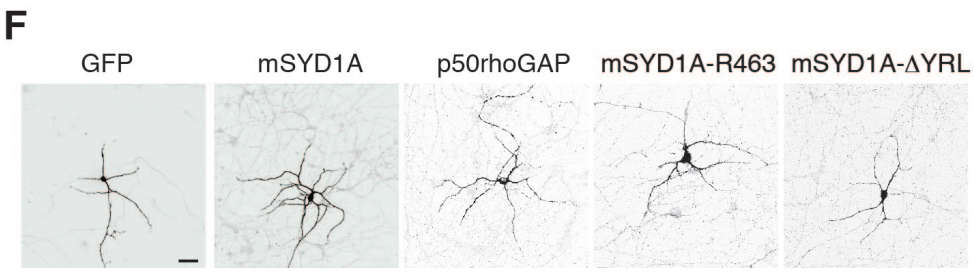
F
GFP
mSYD1A
p50rhoGAP
mSYD1A-R463
mSYD1A-ΔYRL

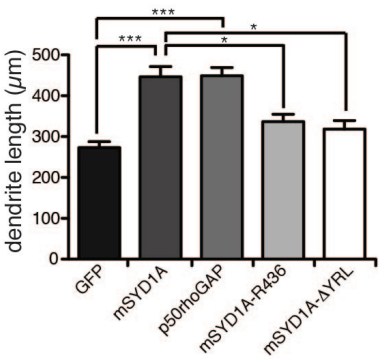
***
***
*
*
dendrite length (μm)
500
400
300
200
100
0
GFP
mSYD1A
p50rhoGAP
mSYD1A-R436
mSYD1A-ΔYRL

Figure 3 – mSYD1A shows GAP activity towards RhoA
(A) FRET sensor for the measurement of GAP activity towards RhoA. HEK293T cells were co-transfected with expression constructs for RhoA sensor and mSYD1A or p50rhoGAP. The emission spectra for excitation at 433 nm were normalized by subtraction of signals obtained with control cells lacking sensor expression. RBD: Rho-binding domain of the effector rhotekin. **(B)** Emission ratios (Intensity 530nm/Intensity 475nm) from FRET sensor assays (n=12 replicates; **: $p<0.001$; ***: $p<0.0001$; ns: not significant; ANOVA and Tukey's multiple comparison test; line at median, whiskers: min to max). **(C,E)** Expression of the RhoA sensor and the co-expressed proteins (anti-HA and anti-Myc antibodies) were verified by Western-Blotting after conducting the FRET measurements. **(D)** Emission ratio (Intensity 530 nm/Intensity 475 nm) observed for mSYD1A constructs with GAP domain mutations (n=12 replicates; ***: $p<0.0001$; ANOVA and Tukey's multiple comparison test; line at median, whiskers: min to max). **(F)** Morphology and total dendritic length of cerebellar granule cells after overexpression of GFP, C-terminally Myc-tagged mouse SYD1A or p50rhoGAP (n=40 cells; **: $p<0.001$; ***: $p<0.0001$; ANOVA and Tukey's multiple comparison test; mean ± s.e.m.; scalebar = 20 µm).

A

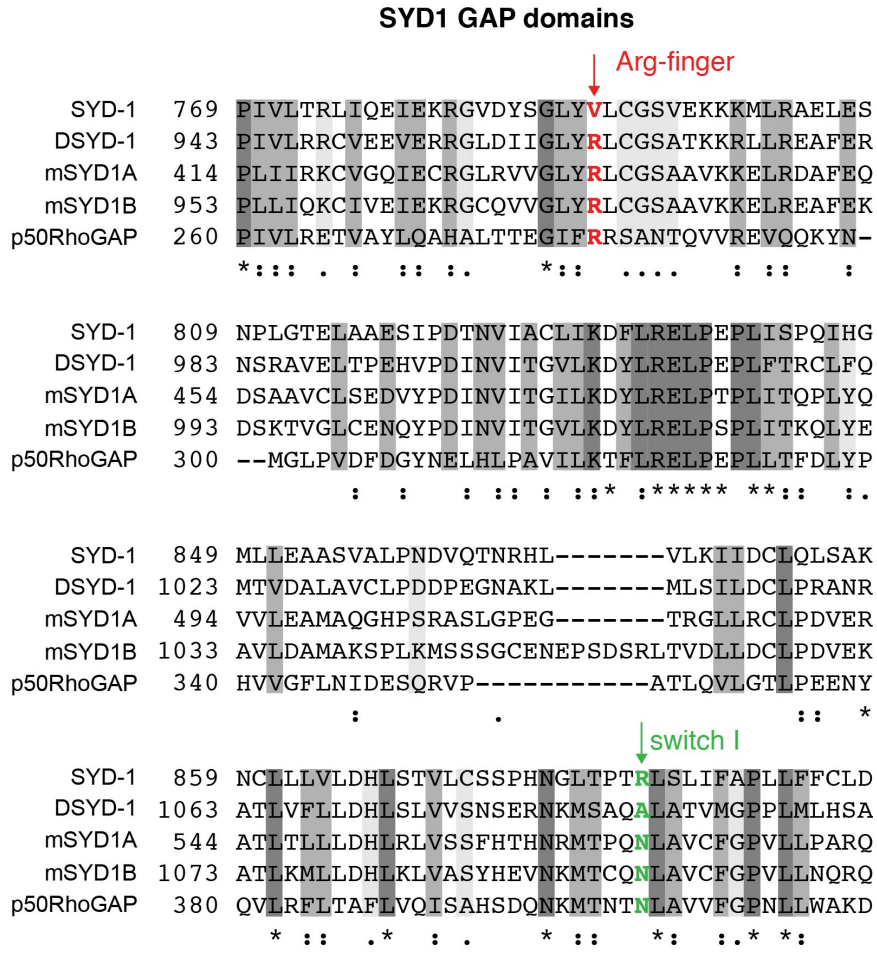

B

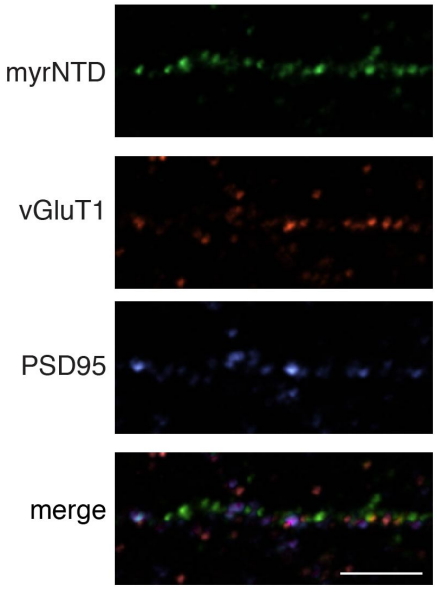

Figure S3 – Alignment of domains and localization of overexpressed mSYD1A
(A) Alignment of RhoGAP domains of SYD-1 from *C.elegans, Drosophila*, mouse mSYD1A, mSYD1B and human p50rhoGAP (ClustalW2). Arrows indicate the arginine finger (red) as well as the switch I region (green), which are critical for efficient GTP hydrolysis (Scheffzek & Ahmadian, 2005). **(B)** Overexpressed Myr-NTD(mSYD1A) in cerebellar granule cells partially overlaps with vGluT1/PSD95 puncta (scalebar = 10 µm).

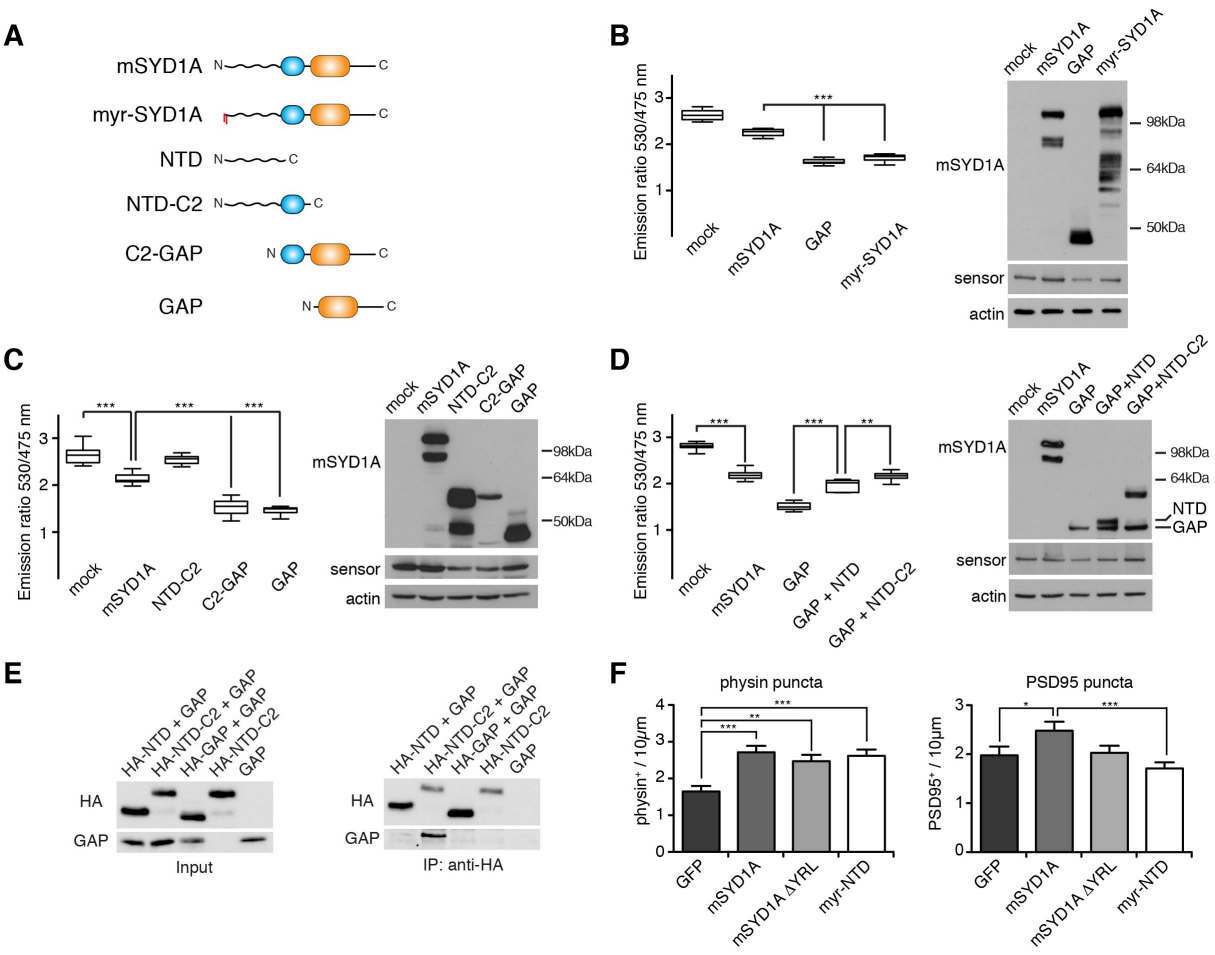

Figure 4 – mSYD1A GAP activity is auto-inhibited by its N-terminal domain
(A) mSYD1A deletion constructs. N-terminal lipid modification (myristoylation and palmitoylation) is marked in red. **(B-D)** Emission ratios (Intensity 530 nm/Intensity 475 nm) oberserved for full-length mSYD1A and deletion constructs. For GAP+NTD and GAP+NTD-C2, two mSYD1A deletion constructs were co-expressed in the same cell. (n=12 replicates; **: p<0.001; ***: p<0.0001; ANOVA and Tukey's multiple comparison test; line at median, whiskers: min to max). **(E)** Co-immunoprecipiation of proteins co-transfected in HEK293T cells. Anti-HA immunoprecipitates (IP) were probed with anti-HA and anti-Myc antibodies. **(F)** Overexpression of mSYD1A truncation constructs in neurons. Number of physin or PSD95 puncta per 10 µm axon length in cerebellar granule cells overexpressing GFP or mSYD1A constructs (n=30 cells; *: p<0.05; **: p<0.001; ***: p<0.0001, ANOVA and Tukey's multiple comparison test; mean ± s.e.m.).

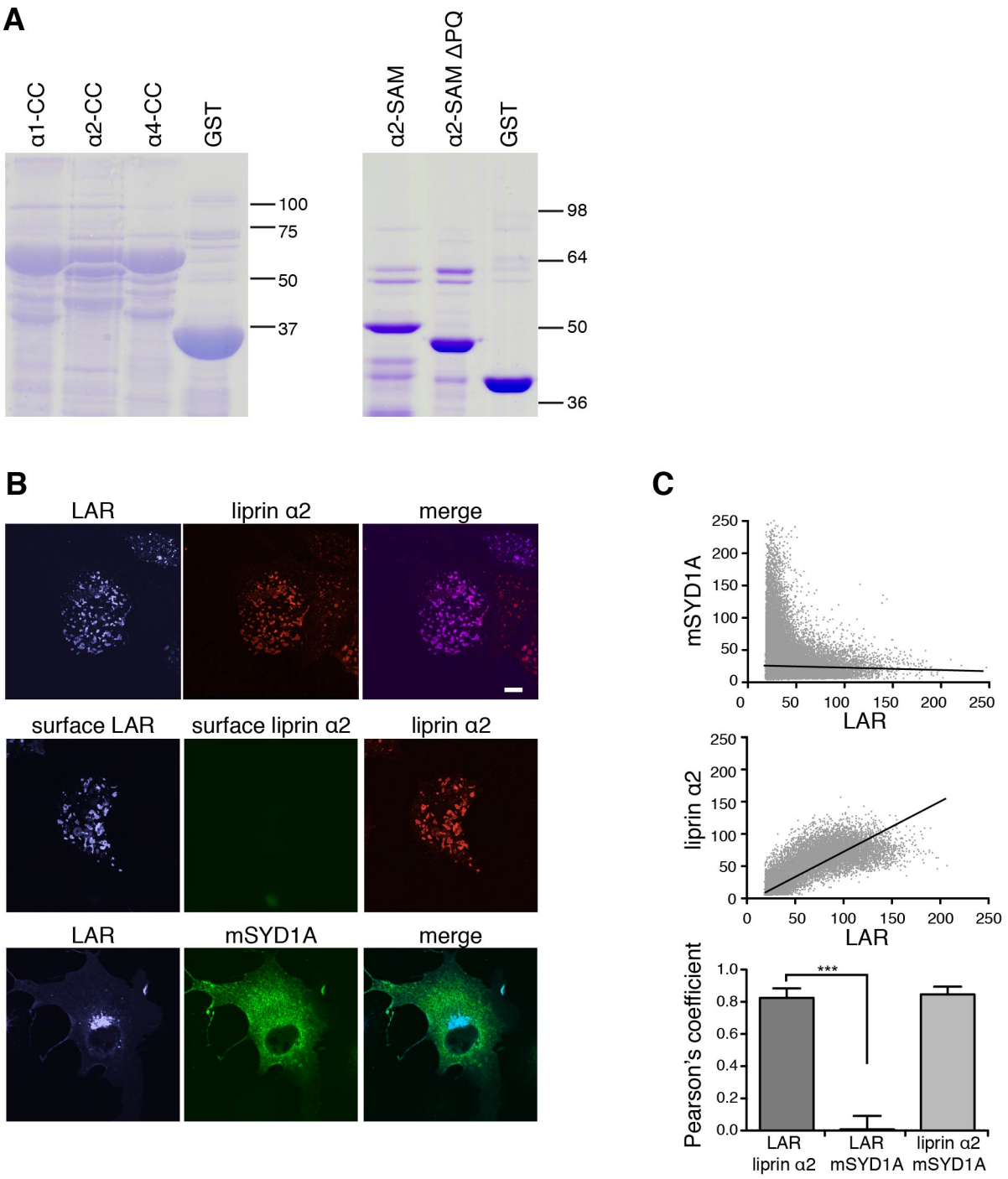

Figure S4 – Liprin α2 – mSYD1A interaction
(A) Recombinant GST- or His-tagged liprin-α proteins used in pull-down assays. **(B)** Colocalization of LAR and Myc-tagged liprin-α2 in COS7 cells. For surface staining, LAR was detected in non-permeabilized cells. In the same incubation, rabbit anti-Myc-antibody against Myc-tagged liprin-α2 was applied to confirm the integrity of the plasma membrane. Subsequently, intracellular liprin-α2 was detected after permeabilization with a mouse anti-Myc antibody. **(C)** Colocalization analysis between mSYD1A and LAR, and liprin-α2 and LAR (n=10 cells; ***: p<0.0001; ANOVA and Tukey's multiple comparison test, mean ± s.d.).

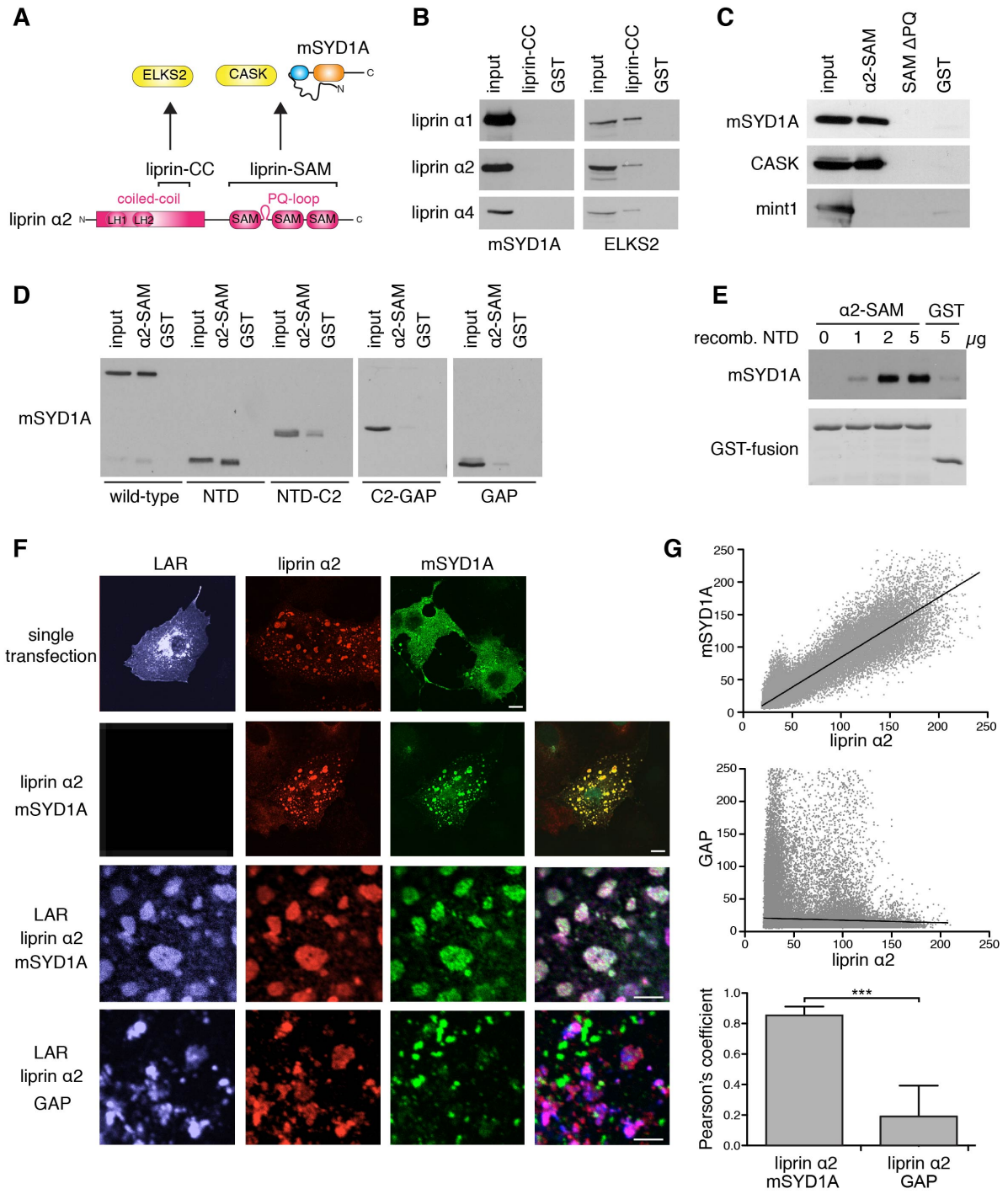

Figure 5 – mSYD1A interacts with liprin-α2

(A) Domain organization of liprin-α fragments used in pull-down assays, and protein interaction sites. LH1 and LH2 denote highly conserved liprin homology regions. Liprin-α contains an alternative splice insertion between the first and the second SAM domain (PQ-loop), which is absent from the most abundant liprin-α1 isoform. **(B)** Beads containing recombinant liprin-α1, α2, and α4 coiled-coil domain fragments (liprin-CC) were incubated with HEK293T cell lysates containing overexpressed mSYD1A or ELKS2. Recombinant GST was used as negative control (GST). Equivalent fractions of input and bound proteins were analyzed by Western blotting. **(C)** Beads containing liprin-α2 SAM domains with (α2-SAM) or without the PQ-loop (SAM DPQ) were incubated with HEK293T cell lysates containing overexpressed mSYD1A, CASK or mint1. **(D)** Beads containing liprin-α2 SAM domains were incubated with HEK293T cell lysates containing overexpressed mSYD1A deletion constructs. **(E)** Binding assay with purified recombinant liprin-α2 SAM and increasing amounts of purified recombinant N-terminal domain of mSYD1A (NTD). **(F)** COS7 cells single, double or triple transfected with

expression constructs for liprin-α2, LAR, and/or mSYD1A. Upper rows show entire cells (scalebar = 10 µm), lower rows show enlargement of sub-membrane clusters (scalebar = 5 µm). **(G)** Quantitative colocalization analysis of LAR, liprin-α2, mSYD1A co-expressing cells. Scatter plots display pixel values of liprin-α2 and mSYD1A, or liprin-α2 and mSYD1A GAP immune-reactivities. The mean Pearson's coefficient provides a quantitative measure for the distribution of the observed puncta (n=10 cells; two-tailed t-test, ***: p<0.0001; mean ± s.d.).

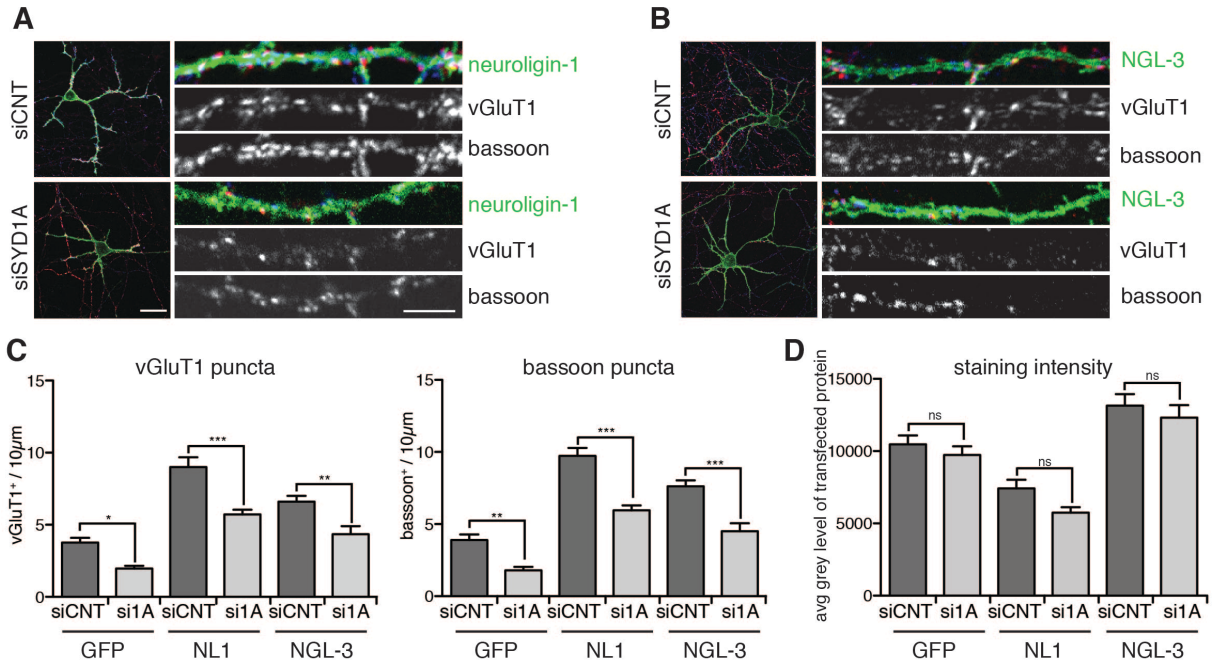

Figure 6 – mSYD1A is a general mediator of presynaptic assembly
(A,B) Cerebellar granule cells treated with control (siCNT) or mSYD1A (siSYD1A) siRNAs transfected with expression vectors for GFP, neuroligin-1 or NGL-3 (green). Presynaptic terminals are visualized by immunostaining for endogenous vGluT1 (red) and bassoon (blue). Scalebar overview = 20 µm, scalebar segment = 5 µm.m**(C)** Quantification of the density of vGluT1$^+$ and bassoon$^+$ puncta along the dendrites of GFP, neuroligin-1 (NL1) or NGL-3 expressing neurons (n = 25 cells; *: p<0.05; **: p<0.001; ***: p<0.0001; ANOVA and Tukey's multiple comparison test, mean ± s.e.m.). **(D)** The average staining intensity of the transfected proteins does not significantly change after application of siRNA against mSYD1A (n = 25 cells, ns: not significant; ANOVA and Tukey's multiple comparison test, mean ± s.e.m.).

Experimental Procedures

DNA constructs

Mammalian mSYD1A expression vectors contained the CMV enhancer and chicken beta-actin promoter (pCAGGS). For detection of overexpressed protein, either a N-terminal HA-tag or a C-terminal Myc-tag was inserted. The following mSYD1A fragments were used (in amino acids): NTD: 1-267, NTD+C2: 1-369, C2+GAP: 267-737, GAP: 411-737. Point mutations in the GAP domain were introduced with Quick Change Multi Site Directed Mutagenesis Kit (Agilent-Stratagene). In myristoylated and palmitoylated full-length mSYD1A (myr-SYD1A), the minimal MARCKS-3/4 Cys (MGCCFSKT) sequence was added to the N-terminus. For lentiviral delivery of hSYD1A, a lentiviral vector with a dual human synapsin promoter was used to express GFP and hSYD1A(Gascon et al, 2008). For HA-LAR, the transmembrane and the cytoplasmic domain of mouse LAR (amino acids: 1236 – 1898) were inserted in frame with an N-terminal HA-tag into pDisplay. The following previously published DNA constructs were used: mouse liprin-α1, -α2, -α4 coiled-coil domains (liprin-α-CC, amino acids α1: 351-673, α2: 369-696, α4: 185-419) (Ko et al, 2003b), His-tagged human liprin-α2 SAM domains (liprin-α2-SAM, amino acids: 866-1258) and liprin-α2 SAM ΔPQ (as above but lacking amino acids 976 – 1012) (Wei et al, 2011), RhoA sensor and p50rhoGAP (Pertz et al, 2006), epitope-tagged liprin-α2 (Zürner & Schoch, 2009), Myc-CASK (Borg et al, 1998) and ELKS2-Myc (Ohtsuka et al, 2002).

Antibodies

Rabbit polyclonal antibodies against mSYD-1A were raised against a synthetic peptide (MAEPLLRKTFSRLRGREK) and affinity purified on the antigen. Anti-pan-neuroligin was described previously (Taniguchi et al, 2007). Rabbit anti-munc18 was a gift from Matthijs Verhage (de Vries et al, 2000). Other antibodies were purchased from commercial sources: mouse anti-actin (clone AC-40, Sigma-Aldrich), rabbit anti-histone H3 (#96715, Cell Signaling), mouse anti-PSD95 (#73-028, Neuromab), mouse anti-VAMP2 (clone 69.1, Synaptic Systems), anti-vesicular glutamate transporter 1 (vGluT1, #1353303, Synaptic Systems), rabbit anti-GAPDH (#E1C604, Enogene), mouse anti-CASK (#75-000, Neuromab), rabbit anti-munc13-1 (#126103, Synaptic Systems), mouse anti-beta-tubulin (E7, DSHB), rabbit anti-ELKS 1b/2 (#143003, Synaptic Systems), rat anti-HA (clone 3F10, Roche Applied Science), rabbit anti-c-myc (#sc-789,Santa-Cruz), mouse anti-flag (#F1804, Sigma), rabbit anti-homer (#160003, Synaptic Systems), mouse anti-bassoon (#GTX13249, GeneTex). Secondary antibodies conjugated to cyanine dyes or Alexa 488 or 643 (Jackson ImmunoResearch and Invitrogen) were used for visualization in immunostainings.

Biochemical Fractionation Methods

Cells or brain tissues were lysed in 20 mM Tris-HCl pH 8.0, 10 % Glycerol, 150 mM NaCl, 1 % Triton X-100, 0.1 % SDS and complete protease inhibitor (Roche Applied Science) and soluble fractions were analyzed by immunoblotting. Signals were acquired using an image analyzer (LAS-3000; Fujifilm).

For fractionation brain tissue was homogenized in 10 volumes of buffer A [10 mM HEPES pH 7.4, 2 mM EDTA, 1 mM $MgCl_2$, 1 mM DTT, complete protease inhibitor (Roche Applied Science)]. The homogenate was centrifuged (2900 x g for 20 min) to yield post-nuclear supernatant (PNS) and pellet P1. PNS was centrifuged (100,000 x g, 2 h) resulting in pellet P2 and supernatant S2.

For synaptosome isolation three adult mouse brains were homogenized with a motor driven homogenizer in 0.32 M sucrose, 1 mM $NaHCO_3$, 1mM $MgCl_2$, 0.5 mM $CaCl_2$, containing complete protease inhibitor (Roche) (10 ml / 1 g of tissue). The homogenate (H) was centrifuged (1400 x g, 10 min) resulting in the pellet P1 and the supernatant S1. Centrifugation of S1 (13,800 x g, 10 min) resulted in the crude synaptosomal pellet (P2) and a cytosolic supernatant. P2 was resuspended in 1 mM $NaHCO_3$, 0.32 M sucrose and loaded on top of a sucrose gradient (0.8 M, 1 M, 1.2 M sucrose) and centrifuged at 82,500 x g for 2 h. The synaptic plasma membranes (SPM) were collected at the interface between the 1.0 M and 1.2 M sucrose layers. The SPM fraction was extracted for 15 min at 4 °C in 12 mM Tris-HCl pH 8.1, 0.32 M sucrose, 1 % Triton X-100 and centrifuged at 32,800 x g for 1 h to yield Triton X-100 soluble and insoluble fractions.

Rho-GAP Assays

Förster-resonance energy transfer (FRET) assays were performed as described previously (Itoh et al, 2002). Briefly, HEK293T cells were transfected with the RhoA sensor (Pertz et al, 2006) and expression constructs of interest. After 48 h cells were suspended in 1x PBS. The emission spectrum between 450-600 nm after excitation with 430 nm light was measured in a Fluorescence Spectrophotometer (FP-6500, Jasco). Following the measurement cells were lysed for protein expression analysis.

Pull-Down Assays

The following proteins were purified from *E. coli* and coupled to Glutathione Sepharose (GE Healthcare) or Ni-NTA (Qiagen) Agarose beads: GST-Liprin-α1-CC, GST-Liprin-α2-CC, GST-Liprin-α4-CC, 6xHis-Liprin-α2-SAM or 6xHis-Liprin-α2-SAM ΔPQ. HEK293T cell lysates containing the protein of interest were lysed in 50 mM HEPES pH 7.4, 1 % Triton X-

100, 0.1 % SDS, 10 % glycerol, 1.5 mM $MgCl_2$, 1 mM EDTA, 100 mM NaF, 1 mM Na_3VO_4, complete protease inhibitor (for pull down with liprin-CC) or 20 mM Tris-HCl pH 8.0, 1 % Triton X-100, 10 % glycerol, 100 mM NaCl and complete protease inhibitor (for pull-down with liprin-SAM). 10 µl of beads coupled to the recombinant proteins were incubated with the lysate for 5 h at 4 °C. The beads were washed and bound proteins analyzed by immunoblotting.

Cellular Assays

For co-aggregation experiments COS7 cells were transiently transfected (Fugene, Roche) and proteins were expressed for 48 h. Cells were fixed with 4 % PFA, 4 % sucrose in 100 mM sodium phosphate buffer (pH 7.4) for 15 min at room temperature. Immunostaining was done using standard procedures.

Dissociated cultures of mouse cerebellar granule cells were prepared from P5-P7 pups as previously described (Dean et al, 2003). Knockdown of *msyd-1a* was performed on day 1 (replenished at day 4) with 0.75 µM Accell SMART pool siRNA against *msyd-1a* or a non-target control siRNA (Dharmacon). At day 7, cells were fixed with 4 % paraformaldehyde, containing 4 % sucrose in 100 mM phosphate buffer (pH 7.4). After antibody staining the coverslips were mounted with ProLong (Invitrogen).

Electrophysiology

Whole cell patch clamp recordings were performed on DIV 8-11 cerebellar granule cell cultures. For rescue, the lentivirus was added at DIV 3. The extracellular solution (pH 7.3) contained the following: 145 mM NaCl, 5 mM KCl, 2 mM $CaCl_2$, 1 mM $MgCl_2$, 5 mM Glucose, 25 mM Sucrose and 5 mM HEPES. For all the experiments 300 nM TTX, 0.1 mM Picrotoxin and 0.1 mM AP5 were used in the solution. The internal solution contained the following: 130 mM CsCl, 10 mM HEPES, 10 mM EGTA, 10 mM Phosphocreatine, 2 mM MgATP, 5 mM NaCl, pH 7.25 and 298 mOsm. Data was analyzed using Axograph X software and the mEPSCs were detected using a template based detection algorithm package.

Image Acquisition and Analysis

Images were acquired on a LSM5 confocal microscope (Zeiss, Germany) and assembled using Adobe Photoshop and Illustrator software. For the analysis of dendritic arborization, soma and dendrites of the neurons were traced and analyzed with Neurolucida (MBF Bioscience).

Co-localization analysis of proteins in COS cells was performed by the Pearson's coefficient method computed on fluorograms, using the JaCOP plugin in ImageJ (Bolte & Cordelieres, 2006).

Quantification of pre- and postsynaptic proteins in granule cells was performed by a wavelet-based segmentation method, using the Multidimensional Image Analysis module (Izeddin et al, 2012; Racine et al, 2006), run in Metamorph software (Molecular Devices, USA). Puncta on different channels were segmented and counted by thresholding the third wavelet map with a value ranging from 15 to 35 times the noise standard deviation.

Some images for figures were processed by deconvolution using a theoretical PSF, a signal/noise ratio of 10 for each channel and 30 iterations of the deconvolution algorithm (Huygens remote manager v2.1.2).

Statistical Analysis

Statistical Analysis was done with Prism software (GraphPad software). Data was tested for normality using the Kolmogorov-Smirnov normality test. Normally distributed data was analyzed for statistical differences with the t-test (pairwise comparisons) or ANOVA and Tukey's for multiple comparisons. For data that was not normally distributed, non-parametric ANOVA and Dunn's multiple comparison test were used.

References

Ball, R., Warren-Paquin, M, Tsurudome, K, Liao, EH, Elazzouzi, F, Cavanagh, C, An, B-S, Wang, T-T, White, JH and Haghighi, AP (2010). Retrograde BMP signaling controls synaptic growth at the NMJ by regulating Trio expression in motor neurons. Neuron *66*, 536 - 549.

Biederer, T., Sara, Y, Mozhayeva, M, Atasoy, D, Liu, X, Kavalali, ET and Südhof, TC (2002). SynCAM, a synaptic adhesion molecule that drives synapse assembly. Science *297*, 1525 - 1531.

Bolte, S., and Cordelieres, F.P. (2006). A guided tour into subcellular colocalization analysis in light microscopy. Journal of Microscopy-Oxford *224*, 213-232.

Chia, P., Patel, MR and Shen, K (2012). NAB-1 instructs synapse assembly by linking adhesion molecules and F-actin to active zone proteins. Nature neuroscience.

Dai, Y., Taru, H, Deken, SL, Grill, B, Ackley, B, Nonet, ML and Jin, Y (2006). SYD-2 Liprin-a organizes presynaptic active zone formation through ELKS. Nature neuroscience *9*, 1479 - 1487.

de Vries, K.J., Geijtenbeek, A., Brian, E.C., de Graan, P.N., Ghijsen, W.E., and Verhage, M. (2000). Dynamics of munc18-1 phosphorylation/dephosphorylation in rat brain nerve terminals. The European journal of neuroscience *12*, 385-390.

Dean, C., Scholl, F.G., Choih, J., DeMaria, S., Berger, J., Isacoff, E., and Scheiffele, P. (2003). Neurexin mediates the assembly of presynaptic terminals. Nature neuroscience *6*, 708-716.

Dyson, H.J.a.W., P.E. (2005). Intrinsically unstructured proteins and their functions. Nature *6*, 197 - 208.

Frank, C.A., Pielage, J. and Davis, G.W. (2009). A presynaptic homeostatic signaling system composed of the Eph receptor, Ephexin, Cdc42 and Ca2.1 Calcium Channels. Neuron *61*, 556 - 569.

Graf, E., Zhang, XZ, Jin, S-X, Linhoff, MW and Craig, AM (2004). Neurexins induce differentiation of GABA and Glutamate postsynaptic specializations via neuroligins. Cell *119*, 1013 - 1026.

Graham, D., Eccleston, JF and Lowe, PN (1999). The conserved Arginine in Rho-GTPas-activating protein is essential for efficient catalysis but not for complex formation with RhoGDP and Aluminium Fluoride. Biochemistry *38*, 985 - 991.

Hallam, S., Goncharov, A, McEwen, J, Baran, R and Jin, Y (2002). SYD-1, a presynaptic protein with PDZ, C2 and rhoGAP-like domains, specifies axon identity in C.elegans. Nature neuroscience *5*, 1137 - 1146.

Hoogenraad, C.C., Feliu-Mojer, M.I., Spangler, S.A., Milstein, A.D., Dunah, A.W., Hung, A.Y. and Sheng, M. (2007). Liprina1 degradation by calcium/calmodulin-dependent protein kinase II regulates LAR receptor tyrosine phosphatase distribution and dendrite development. Developmental cell *12*, 587 - 602.

Itoh, R., Kurokawa, K, Ohba, Y, Yoshizaki, H, Mochizuki, N and Matsuda, M (2002). Activation of Rac and Cdc42 video imaged by fluorescent resonance energy transfer-

based single-molecule probes in the membrane of living cells. Molecular and Cellular Biology *22*, 6582 - 6591.

Izeddin, I., Boulanger, J., Racine, V., Specht, C.G., Kechkar, A., Nair, D., Triller, A., Choquet, D., Dahan, M., and Sibarita, J.B. (2012). Wavelet analysis for single molecule localization microscopy. Opt Express *20*, 2081-2095.

Jin, Y., and Garner, C.C. (2008). Molecular mechanisms of presynaptic differentiation. Annu Rev Cell Dev Biol *24*, 237-262.

Ko, J., Na, M, Kim, S, Lee, J-R and Kim, E (2003). Interaction of the ERC family of RIM-binding proteins with the Liprin-alpha family of multidomain proteins. Journal of Biological Chemistry *278*, 42377 - 42385.

Kwon, S.-K., Woo, J., Kim, S.-Y., Kim, H. and Kim, E. (2010). Trans-synaptic adhesions between Netrin-G Ligand-3 (NGL-3) and receptor tyrosine phosphatases LAR, protein-tyrosine phosphatase d (PTPd), and PTPs via specific domains regulate excitatory synapse formation. Journal of Biological Chemistry *285*, 13966 - 13978.

Linhoff, M., Lauren, J, Cassidy, RM, Dobie, FA, Takahashi, H, Nygaard, HB, Airaksinen, MS, Strittmatter, SM and Craig, AM (2009). An unbiased expression screen for synaptogenic proteins identifies the LRRTM protein family as synaptic organizers. Neuron *61*, 734 - 749.

Luo, L. (2000). Rho GTPases in neuronal morphogenesis. Nat Rev Neurosci *1*, 173-180.

Olsen, O., Moore, KA, Fukata, M, Kazuta, T, Trinidad, JC, Kauer, FW, Streuli, M, Misawa, H, Burlingame, AL, Nicoll, RA and Bredt, DS (2005). Neurotransmitter release regulated by a MALS-Liprin-a presynaptic complex. Journal of Cell Biology *170*, 1127 - 1134.

Owald, D., Fouquet, W, Schmidt, M, Wichmann, C, Mertel, S, Depner, H, Christiansen, F, Zube, C, Quentin, C, Körner, J, Urlaub, H, Mechtler, K and Sigrist, SJ (2010). A Syd-1 homologue regulates pre- and postsynaptic maturation in Drosophila. J Cell Biol *188*, 565 - 579.

Owald, D., Khorramshahi, O., Gupta, V.K., Banovic, D., Depner, H., Fouquet, W., Wichmann, C., Mertel, S., Eimer, S., Reynolds, E.*, et al.* (2012). Cooperation of Syd-1 with Neurexin synchronizes pre- with postsynaptic assembly. Nat Neurosci *15*, 1219-1226.

Patel, M., Lehrman, EK, Poon, VY, Crump, JG, Zhen, M, Bargmann, CI and Shen, K (2006). Hierarchical assembly of presynaptic components in defined C.elegans synapses. Nature neuroscience *9*, 1488 - 1498.

Patel, M., Shen, K (2009). RSY-1 is a local inhibitor of presynaptic assembly in C.elegans. Science *323*, 1500 - 1503.

Pertz, O., Hodgson, L, Klemke, RL and Hahn, KM (2006). Spatiotemporal dynamics of RhoA activity in migrating cells. Nature *440*, 1069 - 1072.

Racine, V., Sachse, M., Salamero, J., Fraisier, V., Trubuil, A., and Sibarita, J.-B. (2006). Visualization and quantification of vesicle trafficking on a three-dimensional cytoskeleton network in living cells. Journal of Microscopy *225*, 214 - 228.

Scheffzek, K., Ahmadian, MR (2005). GTPase activating proteins: structural and functional insights 18 years after discovery. Cell Mol Life Sci *62*, 3014 - 3038.

Scheiffele, P., Fan, J., Choih, J., Fetter, R. and Serafini, T. (2000). Neuroligin expressed in nonneuronal cells triggers presynaptic development in contacting axons. Cell *101*, 657 - 669.

Schoch, S., Castillo, P.E., Jo, T., Mukherjee, K., Geppert, M., Wang, Y., Schmitz, F., Malenka, R.C., and Südhof, T. (2002). Rim1alpha forms a protein scaffold for regulating neurotransmitter release at the active zone. Nature *415*, 321 - 326.

Shen, K., Scheiffele, P (2010). Genetics and Cell Biology of Building specific synaptic connectivity. Annu Rev Neurosci *33*, 473 - 507.

Sieburth, D., Ch'ng, Q., Dybbs, M., Tavazoie, M., Kennedy, S., Wang, D., Dupuy, D., Rual, J.-F., Hill, D.E., Vidal, M.*, et al.* (2005). Systemic analysis of genes required for synapse structure and function. Nature *436*, 510 - 517.

Sigrist, S.J., and Schmitz, D. (2011). Structural and functional plasticity of the cytoplasmic active zone. Curr Opin Neurobiol *21*, 144-150.

Sudhof, T.C. (2012). The presynaptic active zone. Neuron *75*, 11-25.

Sun, Y., and Bamji, S.X. (2011). beta-Pix modulates actin-mediated recruitment of synaptic vesicles to synapses. The Journal of neuroscience : the official journal of the Society for Neuroscience *31*, 17123-17133.

Takahashi, H., Arstikaitis, P, Prasad, T, Bartlett, TE, Wang, YT, Murphy, TH and Craig, AM (2011). Postsynaptic TrkC and Presynaptic PTPsigma function as a bidirectional excitatory synaptic organizing complex. Neuron *69*, 287 - 303.

Taniguchi, H., Gollan, L., Scholl, F.G., Mahadomrongkul, V., Dobler, E., Limthong, N., Peck, M., Aoki, C., and Scheiffele, P. (2007). Silencing of neuroligin function by postsynaptic neurexins. The Journal of neuroscience : the official journal of the Society for Neuroscience *27*, 2815-2824.

Taru, H., and Jin, Y.S. (2011). The Liprin Homology Domain Is Essential for the Homomeric Interaction of SYD-2/Liprin-alpha Protein in Presynaptic Assembly. Journal of Neuroscience *31*, 16261-16268.

Tompa, P. (2002). Intrinsically unstructured proteins. TRENDS in Biochemical Sciences *27*, 527 - 533.

Wei, Z., Zheng, S, Spangler, SA, Yu, C, Hoogenraad, CC and Zhang, M (2011). Liprin-mediated large signaling complex organization revealed by the Liprin-a/CASK and Liprin-a/Liprin-b complex structures. Molecular Cell *43*, 586 - 598.

Woo, J., Kwon, S-K, Choi, S, Kim, S, Lee, J-R, Dunah, AW, Sheng, M and Kim, E (2009). Trans-synaptic adhesion between NGL-3 and LAR regulates the formation of excitatory synapses. Nature neuroscience *12*, 428 - 437.

Yoshida, T., Yasumura, M., Uemura, T., Lee, S.-J., Ra, M., Taguchi, R., Iwakura, Y., and Mishina, M. (2011). IL-1 receptor accessory protein-like 1 associated with mental retardation an autism mediates synapse formation by trans-synaptic interaction with protein tyrosine phosphatese delta. Journal of Neuroscience *31*, 13485 - 13499.

Zhen, M., Jin, Y (1999). The liprin protein SYD-2 regulates the differentiation of presynaptic termini in C.elegans. Nature *401*, 371 - 375.

Ziv, N., Garner, CC (2004). Cellular and molecular mechanisms of presynaptic assembly. Nature Reviews Neuroscience *5*, 385 - 400.

Zürner, M., and Schoch, S. (2009). The mouse and human Liprin-alpha family of scaffolding proteins: genomic organization, expression profiling and regulation by alternative splicing. Genomics *93*, 243-253.

2.3 Additional data on mSYD1A

In the following section, I will describe additional data that we have obtained during our analysis of mSYD1A. Due to space constraints, we could not include this information in the submitted manuscript. However, the additional data relates to the results that are presented in the manuscript and is important to fully understand mSYD1A distribution and function.

2.3.1 Invertebrate SYD-1 proteins show residual GAP activity

In our analysis of the GAP activity of mSYD1A, we compared mSYD1A to its invertebrate orthologues. As shown in figure S3 in the manuscript, *C.elegans* and *Drosophila* SYD-1 sequences deviate from the consensus RhoGAP sequence in two, respectively one amino acids that are important for RhoGAP function (Scheffzek & Ahmadian, 2005). The first of these two amino acids is an arginine (termed “arginine finger”), which is important for efficient catalysis of GTP to GDP and is changed to valine in the *C.elegans* SYD-1 sequence. During RhoGAP/GTPase complex formation, the arginine finger is positioned in the active site of the GTPase and stabilizes the transition state. The second amino acid is an aspartic acid that belongs to the “switch I” region of the GAP protein, which is supposed to stabilize the RhoGAP/GTPase complex. In the *C.elegans* SYD-1 sequence, the aspartic acid is changed to arginine, whereas in *Drosophila* it is changed to alanine. To investigate the consequences of these amino acid changes, we introduced them into the mSYD1A sequence (R436V, N552R for *C.elegans* and N552A for *Drosophila*). In the FRET assay, these proteins did not show any detectable GAP activity towards RhoA (figure 9A and figure 3 of the manuscript). However, we also introduced the same amino acid changes into a deletion mutant of mSYD1A, consisting only of its GAP domain. In the WT conformation, the GAP domain alone shows stronger GAP activity than the full-length construct, which is due to the absence of the auto-inhibitory N-terminal domain. Surprisingly, the amino acid changes did not render the GAP constructs inactive. Instead, they exhibited considerable GAP activity towards RhoA (figure 9B). The level of GAP activity was reduced compared to the WT mSYD1A GAP construct, but similar to the mSYD1A full-length construct. This suggests that proteins containing these amino acid changes in their GAP domain still have the potential to act as GAP proteins.

In figure 3 of the manuscript, we had used a full-length mSYD1A construct, containing an alanine in place of the arginine finger (R436A) as a negative control, since it did not show any detectable GAP activity. However, the GAP construct containing this mutation (R436A), also showed some residual GAP activity. Former reports on p50rhoGAP have shown that the arginine is crucial for efficient hydrolysis, but residual GAP activity can still be detected after

mutation to alanine (Graham et al, 1999), which explains the GAP activity detected for GAP R436A. These results suggest that the *C.elegans* and *Drosophila* SYD-1 sequences have the potential to act as RhoGAP proteins, despite the amino acid changes and strengthens the evolutionary conservation of SYD-1 from *C.elegans* to mouse. However, if the invertebrate SYD-1 proteins are indeed functional GAPs has to be determined in a different assay.

In order to analyze the functional role of mSYD1A in neurons, we overexpressed mSYD1A in cerebellar granule cells (figure 3 of the manuscript). However, transfection of the N-terminally HA-tagged mSYD1A constructs that had been used in the FRET assay did not result in a detectable expression of the protein in neurons. Therefore, we changed the N-terminal HA-tag to a C-terminal Myc-tag. These constructs yielded significant protein expression in neurons and their overexpression led to a change in the morphology of the dendritic tree, resulting in longer and more branched dendrites (figure 3 of the manuscript). An increase in the dendritic tree is indicative for an increased inactivation of RhoA, suggesting that the GAP activity of mSYD1A is responsible for the observed phenotype. However, overexpression of the arginine finger mutation constructs (RA and ΔYRL) did not completely abolish this phenotype, but rather led to a less pronounced increase in dendrite length. To analyze if the position of the tag has an influence on mSYD1A GAP activity, we carried out another FRET assay. Surprisingly, the C-terminally tagged R436A construct exhibited detectable GAP activity (figure 9C), while the N-terminally HA-tagged R436A construct had not shown any GAP activity before (figure 9A). For the ΔYRL construct, we could not detect any significant differences compared to control, but a trend towards GAP activity was present. This result explains the intermediate phenotype for the dendritic branching and suggests that the position of the tag has an influence on the activity of the protein. Possibly, the C-terminal tag prevents a complete folding of the protein and therefore leaves mSYD1A in a more active state than with a N-terminal tag.

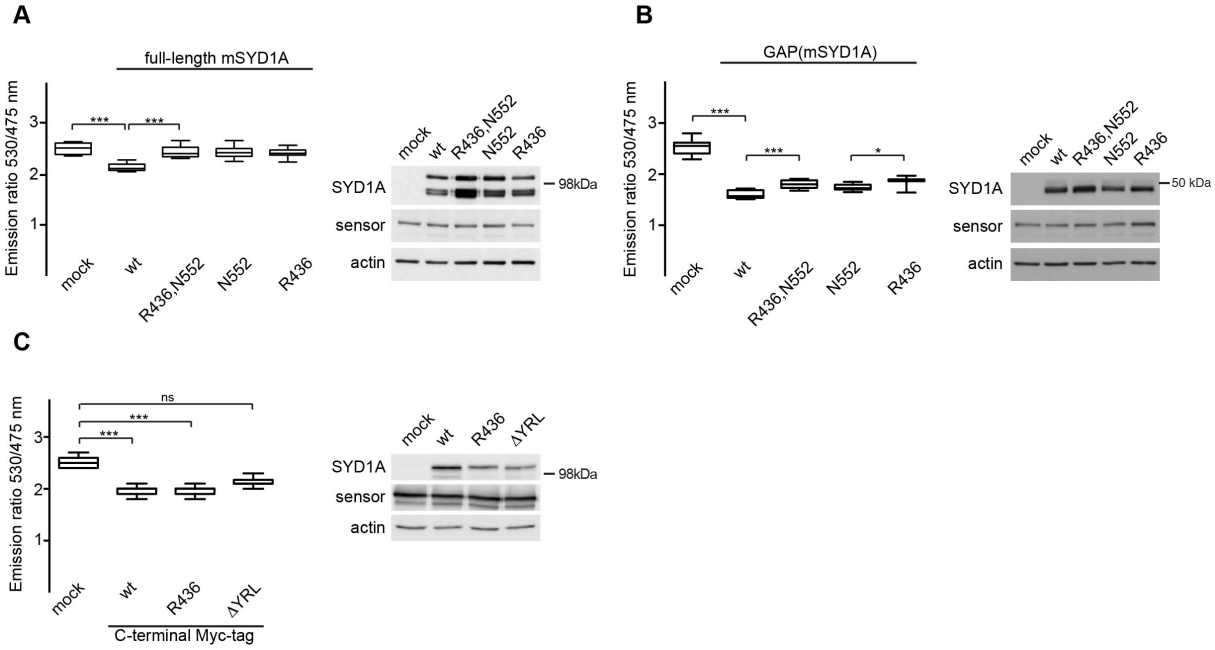

Figure 9 – GAP activity of mSYD1A mutation constructs
Emission ratios (Intensity 530nm/Intensity 475nm) for FRET assays. **(A)** Full-length constructs of mSYD1A that mimic the amino acid changes of *C.elegans* (R436,N552) and *Drosophila* (N552) GAP domains do not show any detectable GAP activity. **(B)** Deletion constructs of mSYD1A that only contain the GAP domain show GAP activity after mutation of R436 and N552. **(C)** Change oft he N-terminal HA-tag to a C-terminal Myc-tag leads to an increase in GAP activity for R436. ΔYRL: deletion of the arginine finger and the two flanking amino acids in the GAP domain of mSYD1A. Expression of the FRET sensor construct and co-expressed proteins was confirmed by Western-Blot analysis (n=12 replicates; *: p<0.05; **: p<0.001; ***: p<0.0001; ns: not significant; ANOVA and Tukey's multiple comparison test; line at median, whiskers: min to max).

2.3.2 Interaction between mSYD1A, liprin-α2 and LAR

In our search for interaction partners for mSYD1A, we could show that the N-terminal domain of mSYD1A binds to the SAM domains of liprin-α2 (figure 5 of the manuscript). Furthermore, we could show that the NTD is sufficient to increase synaptic vesicle clustering upon overexpression in neurons. The NTD of mSYD1A consists of a stretch of 267 amino acids and is predicted to be intrinsically unstructured. Mapping down the interaction site between liprin-α2 and mSYD1A, could help us to get a better insight into the mode of action of this sequence and would also enable us to use more defined deletion constructs in our overexpression experiments in neurons. Therefore, we subdivided the NTD into several parts and asked if the resulting segments are sufficient for binding to liprin-α2. Furthermore, domain prediction programs detect a 124 aa proline-rich sequence within the NTD, which we also tested for sufficiency for liprin-binding. The only deletion construct, which repeatedly showed a strong binding to the SAM domains of liprin-α2, consisted of the last two thirds of the NTD (amino acids: 88 – 267) (figure 10A,B). All other constructs did not bind to liprin-α2 in the pull-down assay. Having identified the last two thirds of the NTD to be sufficient for

liprin-binding, we next wanted to test if it is also required. Since a construct, only consisting of the first third of the NTD (aa: 1 – 87) does not yield significant protein expression in HEK293T cells, we used a construct, consisting of the NTD and the C2 domain of mSYD1A, with deletion of amino acids 124 – 262. Surprisingly, also this construct exhibited binding to liprin-α2 in the pull-down assay, suggesting that multiple sequence elements of mSYD1A, and not only amino acids 124 – 262, are involved in binding to liprin-α2 (figure 10C).

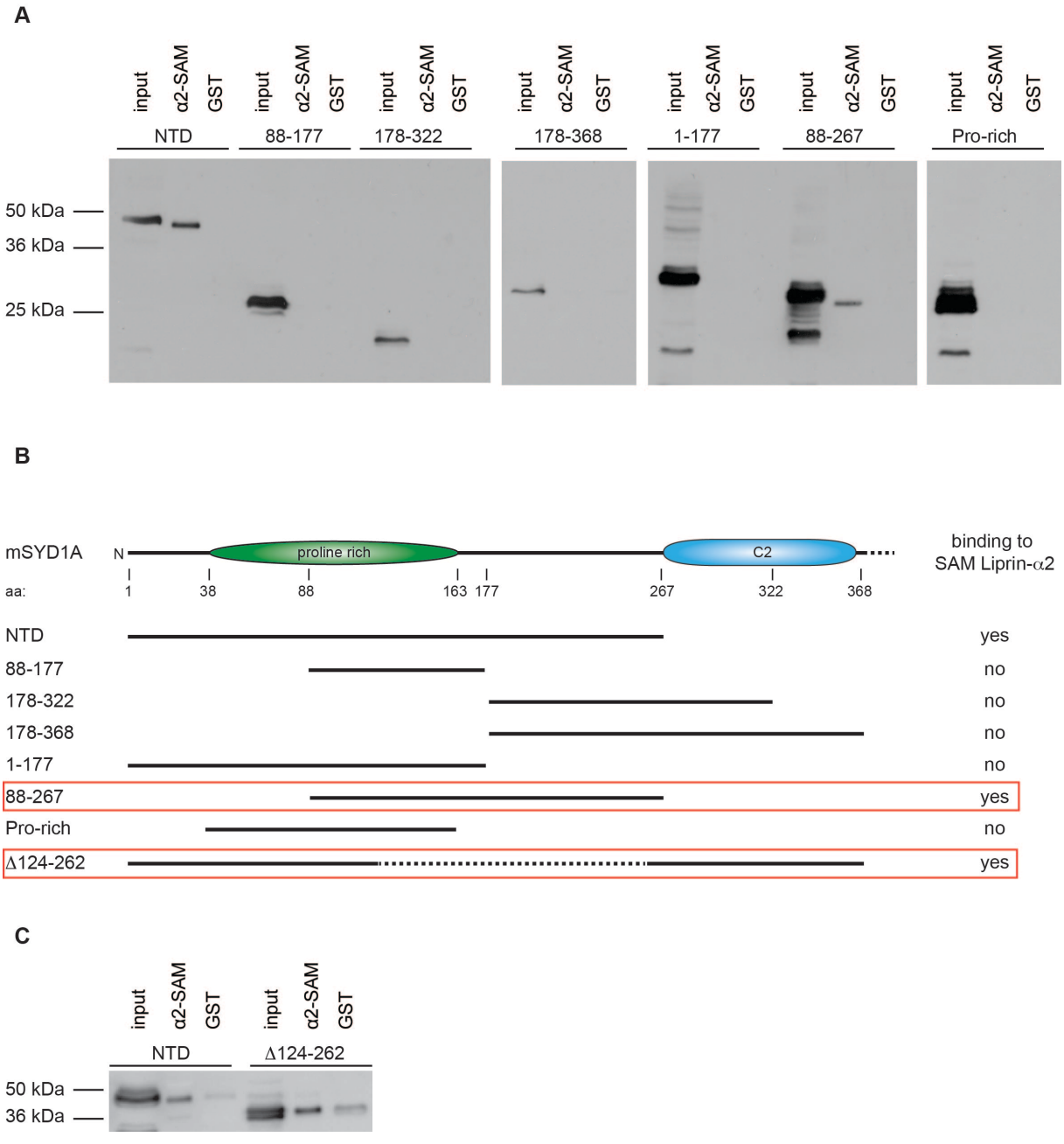

Figure 10 – Interaction between the N-terminal domain of mSYD1A and liprin-α2
(A) An N-terminal deletion construct of mSYD1A that only consists of the last two thirds of the NTD (88-267) is sufficient to bind to the SAM domains of liprin-α2. **(B)** Schematic representation of the N-terminal deletion constructs and their binding to liprin-α2. **(C)** Deletion of amino acids 124 – 262 in the NTD of mSYD1A does not abolish binding of mSYD1A to liprin-α2.

While not providing conclusive answers as to the requirement of liprin-α2 binding, this experiment indicated another interesting aspect in the interaction between mSYD1A and liprin-α2. After pull-down with liprin-α2-SAM, all of the mSYD1A truncation proteins have a smaller apparent molecular weight than the input. This small change in molecular weight could be indicative of posttranslational modifications, like phosphorylation. Indeed, several phosphorylation prediction programs predict a number of possible phosphorylation sites in the N-terminal domain of mSYD1A (NetPhos 2.0 Server) (figure 11A). A more detailed analysis shows that there are several serine and threonine residues in the mSYD1A NTD, which are predicted to be phosphorylated by the cyclin-dependent kinase Cdk5 (figure 11B). Since Cdk5 has been implicated in presynaptic development (Samuels et al, 2007; Su et al, 2012), it would be interesting to investigate further, if mSYD1A is a Cdk5 target. For example CASK has been shown to interact with liprin-α only in its dephosphorylated state, whereas phosphorylation of CASK by Cdk5 leads to a dissociation of the two proteins (Samuels et al, 2007). Similar mechanisms could exist to regulate the interaction between mSYD1A and liprin-α2.

Figure 11 – Predicted phosphorylation sites for the N-terminal domain of mSYD1A
(A) Potential phosphorylation sites in the NTD of mSYD1A are shown in red. **(B)** Potential Cdk5 phosphorylation sites are shown in green. The prediction was done with the NetPhos 2.0 Server.

The COS cell experiments showed that mSYD1A and liprin-α2 co-localize in clusters together with the receptor protein tyrosine phosphatase LAR (figure 5 of the manuscript). While the pull-down experiments indicate that mSYD1A interacts directly with liprin-α2, we were also interested in a possible direct interaction between mSYD1A and LAR. To this end, we overexpressed mSYD1A, liprin-α2 and LAR in HEK293T cells and immunoprecipitated mSYD1A (figure 12). As expected, after transfection of all three proteins, both liprin-α2 and LAR co-precipitated, suggesting again the presence of a complex of all three proteins in the

cell. Interestingly, in a double transfection of mSYD1A and LAR, LAR was repeatedly co-precipitated with mSYD1A. This result suggests the possibility of a direct interaction between mSYD1A and LAR. In COS cells, double transfection of mSYD1A and LAR did not lead to a co-localization of the proteins. On the other hand, in the absence of liprin-α2, LAR is mainly present in Golgi-intermediate compartments, leading to the fact that mSYD1A and LAR are localized to different subcompartments of the cell. This compartmentalization is broken up in co-immunoprecipitation assays, due to lysis of the cell. LAR is dependent on liprin for its recruitment to the plasma membrane, where a direct interaction with mSYD1A would be possible. Surprisingly, in this co-immunoprecipitation assay we could not co-precipitate liprin-α2 with mSYD1A after double transfection of the two proteins. The absence of an interaction in this assay suggests that LAR assists in an efficient binding between mSYD1A and liprin-α2. It is conceivable that liprin binding to LAR leads to a conformational change of liprin, resulting in an easier access for mSYD1A. Furthermore, LAR is a tyrosine phosphatase. Therefore, dephosphorylation of either mSYD1A or liprin-α2 could lead to a more efficient interaction. The fact that mSYD1A binds directly to liprin-α2 in the pull-down assay without the presence of LAR, might be due to higher amounts of purified liprin-α2 in this assay, which increases the likelihood of binding. On the other hand, for the pull-down assay liprin-α2 was purified from *E.coli* and therefore does not contain post-translational modifications. If phosphorylated liprin-α2 does not bind to mSYD1A, we would expect to see a binding in the pull-down assay, but not after overexpression of the proteins in HEK293T cells.

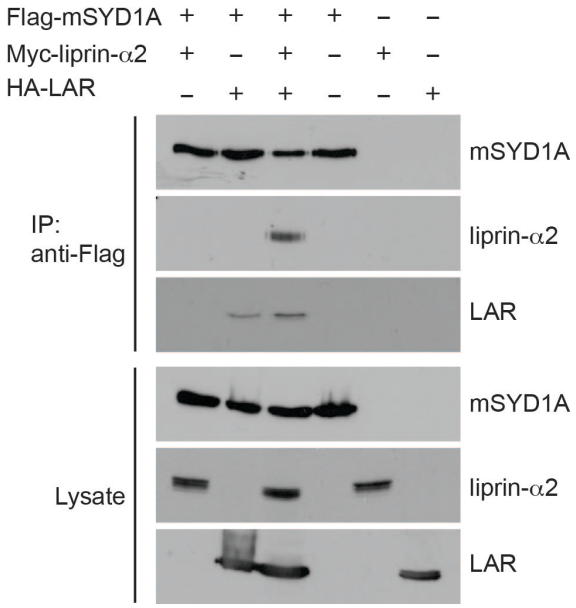

Figure 12 – mSYD1A, LAR and liprin-α2 form a complex in HEK293T cells
Liprin-α2 and LAR co-immunoprecipitate with mSYD1A after triple transfection in HEK293T cells. Double transfection of liprin-α2 and mSYD1A does not lead to co-immunoprecipitation of liprin-α2, whereas double transfection of LAR and mSYD1A results in co-immunoprecipitation of LAR with mSYD1A.

2.3.3 A possible link between mSYD1A and neurexin

Recently published work from Stephan Sigrist's laboratory (Owald et al, 2012) has shown that *Drosophila* SYD-1 interacts with neurexin via its PDZ domain. While mammalian SYD1A does not contain a PDZ domain, we were interested if an analogous interaction through different domains might exist for the mouse proteins. We carried out a pull-down assay with the purified cytoplasmic domain of neurexin and mSYD1A overexpressed in HEK293T cells. As a positive control, we used CASK (Hata et al, 1996). As has been shown before, CASK efficiently bound to neurexin, whereas we could not detect any interaction between mSYD1A and neurexin (figure 13). Surprisingly, after double transfection of both mSYD1A and CASK in HEK293T cells, we could not only detect CASK, but also mSYD1A in the pull-down with neurexin, suggesting a complex of all three proteins. Thus, the loss of the PDZ domain and therefore the loss of an interaction between mSYD1A and neurexin might be compensated for by an indirect interaction via CASK in the mouse.

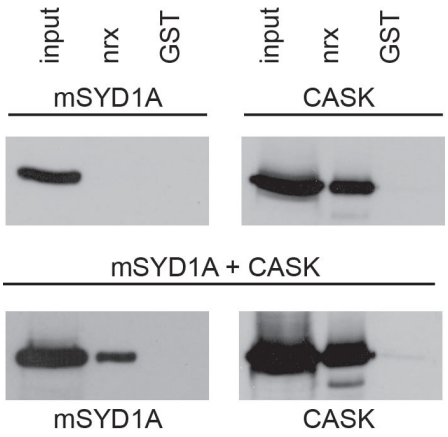

Figure 13 – Complex formation between mSYD1A, CASK and neurexin
mSYD1A, overexpressed in HEK293T cells, does not bind to the recombinant cytoplasmic domain of neurexin in the pull-down assay, whereas CASK shows binding. Co-expression of mSYD1A and CASK in HEK293T cells leads to the pull-down of both proteins with neurexin.

2.3.4 Additional interaction partners for mSYD1A

The analysis of interaction partners for mSYD1A can give insight into the cellular functions of mSYD1A, as well as its distribution patterns. Proteins that interact with mSYD1A might play a role in the activation of its GAP activity. Furthermore, the CAZ is a dense proteinacous structure and most of the proteins that form the CAZ were shown to have numerous interaction partners. Therefore, the analysis of mSYD1A function requires a careful examination of its binding properties. To get a comprehensive understanding of possible interaction partners for mSYD1A, Julia commissioned the company Hybrigenics, specialized in Yeast-2-Hybrid (Y2H) screens, to search for potential binding partners. They used two overlapping mSYD1A expression constructs (aa: 1 – 411 and aa 369 – 737) as bait

to screen an adult mouse brain cDNA library. The potential interaction partners, recovered from the screen, were evaluated for their likeliness to represent a true versus a non-specific interaction with mSYD1A. All recovered proteins were ranked from A – F, with A having the highest probability of being a true interaction partner and F the least. In our subsequent analysis, we excluded proteins in categories E and F from further analysis. The potential interaction partners have roles in different cellular pathways. Figure 14A gives an overview over proteins from categories A – D and their involvement in different cellular functions. This figure, as well as a thorough description of the Y2H screen, can be found in Julia Sommer's PhD Thesis.

A

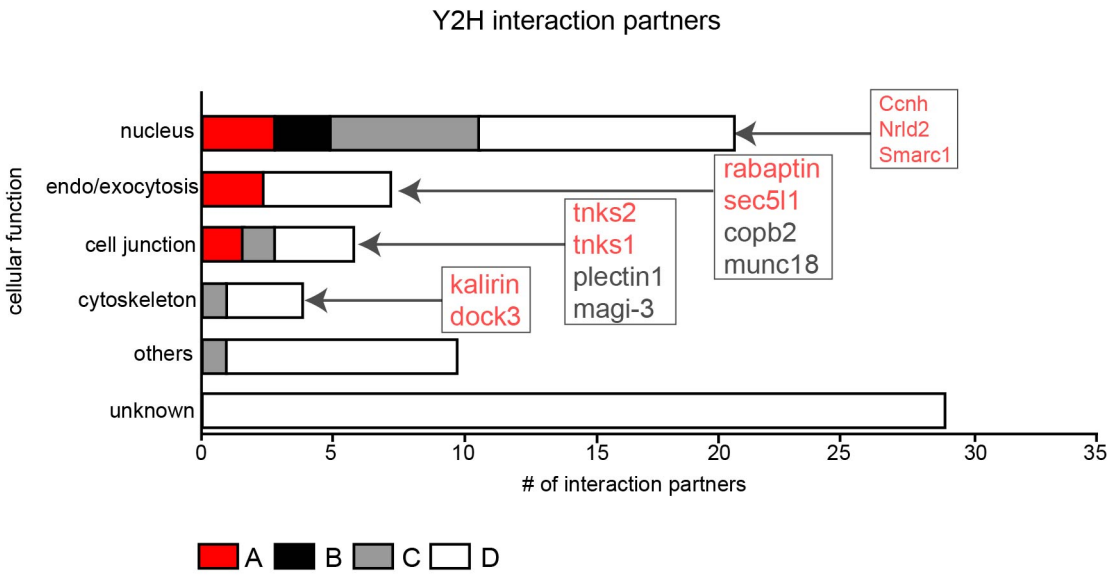

B

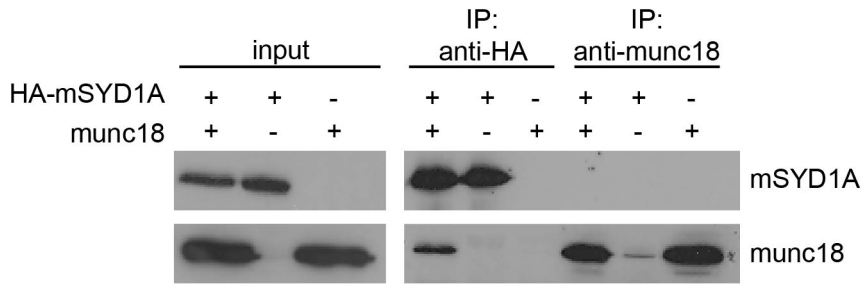

Figure 14 – Potential interaction partners for mSYD1A, identified in the Yeast-2-Hybrid screen
(A) The potential interaction partners for mSYD1A that were identified in the Yeast-2-Hybrid screen were ranked by their likelihood to present a "true" interaction partner from A – D. The potential interaction partners are arranged by their cellular function and the names of some interesting candidates are displayed in the graph. **(B)** Co-immunoprecipitation between mSYD1A and munc18, overexpressed in HEK293T cells. Munc18 co-immunoprecipitates with mSYD1A, while mSYD1A cannot be detected in an immunoprecipitation of munc18.

While we did not detect liprins in this screen, several other proteins with functions in presynaptic terminals were identified. In particular, we were interested in the protein munc18, since it is known to be present in presynaptic terminals and has a prominent role in synaptic vesicle exocytosis (Burgoyne et al, 2009). Therefore, we carried out several co-immunoprecipitation assays, to validate the potential protein interaction between mSYD1A and munc18. Whereas we could reliably co-immunoprecipitate munc18 with tagged mSYD1A, we did not succeed in detecting mSYD1A in an immunoprecipitation for munc18 with a munc18 antibody (figure 14B). Furthermore, co-immunoprecipitations with several deletion constructs of mSYD1A gave contradictory results. Therefore, this interaction still has to be validated, possibly with pull-down assays of purified proteins, which have proven to provide reliable results in the case of liprin-α2.

2.3.5 Knockdown of mSYD1A decreases mEPSC frequency

Knockdown of mSYD1A in cerebellar granule cells led to a decrease in the number of synaptic vesicle clusters per axon length, as well as the number of the active zone protein bassoon (figure 2 of the manuscript). A decrease in the number of synaptic vesicle clusters suggests a decrease in the number of functional synapses. We tested this hypothesis by recording miniEPSCs from siCNT- as well as siSYD1A-treated cultures. Indeed, we detected a decrease in the frequency of mEPSCs, which could be rescued after overexpression of a human SYD1A construct, resistant to knockdown by siRNA (figure 2 of the manuscript). In this experiment, overexpression of hSYD1A was carried out using a lentivirus to deliver the expression sequence for hSYD1A into the cells. The lentiviral delivery of hSYD1A resulted in the expression of hSYD1A in about 90 % of the cells. Consequently, we could ensure that hSYD1A is expressed in most of the presynaptic cells that formed synapses onto the postsynaptic cell that we recorded from. However, in this experiment we also observed a decrease in mEPSC amplitude after knockdown of mSYD1A, which could not be rescued with hSYD1A. Here, several explanations are possible: (1) the decrease in amplitude is an off-target effect of the siRNA, therefore it cannot be rescued by hSYD1A, (2) the decrease in amplitude is due to infection of the cells with a lentivirus, (3) the decrease in amplitude is a specific phenomenon resulting from mSYD1A knockdown, but because of technical reasons (for example rescue with hSYD1A vs mSYD1A), it cannot be rescued in these conditions. An indication for an explanation provides an experiment that we had done initially to test the effect of the siRNA. Here, we used WT cerebellar granule cell cultures that had not been infected with lentivirus and treated them with siCNT or siSYD1A. In these conditions, we could not observe any decrease in mEPSC amplitude, whereas mEPSC frequency was significantly reduced in the knockdown cultures (figure 15). Addition of the lentivirus (lenti-

GFP for control or lenti-hSYD1A for rescue) was the only difference to the later experiment, where the decrease in amplitude was observed. This suggests that the presence of the lentivirus leads to an unspecific decrease in amplitude in these cells. In fact, presence of double-stranded and single-stranded RNA molecules can lead to off-target effects (Singh et al, 2011). Since lentiviruses contain double-stranded RNA, treatment of the cells with a lentivirus and the siRNA might have led to the decrease in mEPSC amplitude and therefore might be unspecific. However, a later experiment on mSYD1A KO neurons, which is described in section 2.3.4, strengthens our conclusion that the reduction in mEPSC frequency after knockdown of mSYD1A is not an off-target effect of the siRNA.

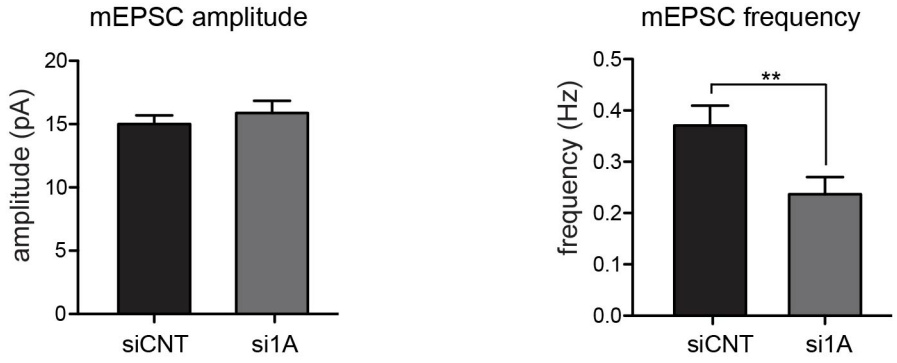

Figure 15 – Knockdown of mSYD1A reduces miniEPSC frequency
Treatment of cerebellar granule cultures with siRNA against mSYD1A leads to a reduction in miniEPSC frequency, while the miniEPSC amplitude is not changed (n = 24 cells; **: p<0.001; two-tailed t-test; mean ± s.e.m).

2.3.6 The NTD of mSYD1A localizes to the nucleus, whereas overexpression of a membrane-targeted NTD increases endogenous vGluT1 puncta

Since knockdown of mSYD1A led to a decrease in the density of synaptophysin puncta, we were interested, if mSYD1A overexpression increases synaptic vesicle clustering. Figure 4 in the manuscript shows that overexpression of mSYD1A and synatophysin-mCherry in the same cell, leads to an increase in synaptophysin puncta density in the axon. To test if the N-terminal domain of mSYD1A alone is sufficient to induce synaptic vesicle clustering, we wanted to overexpress an mSYD1A deletion construct, only consisting of the NTD. However, initial experiments in neurons showed that the NTD is localized to the nucleus after overexpression in neurons (figure 16A). To get a better insight into the subcellular localization of the different domains of mSYD1A, we overexpressed different deletion constructs of mSYD1A in HEK293T cells (figure 16B). In some cells, the NTD of mSYD1A

was localized to the nucleus, whereas in other cells, we could detect a cytoplasmic localization of the NTD. Furthermore, a subset of cells showed a perinuclear staining, suggesting that the NTD localizes to the nuclear membrane. In contrast, a deletion construct consisting of the NTD and the C2 domain of mSYD1A (NTD-C2) exhibited a mainly cytoplasmic localization, whereas we could still detect a perinuclear staining in some cells. Instead, the GAP domain of mSYD1A showed a diffuse cytoplasmic localization. These results suggest that the NTD of mSYD1A contains nuclear localization signals. In fact, the web-based prediction program PSORT (prediction of protein sorting signals and localization sites in amino acid sequences) detects several nuclear localization signals in the N-terminal domain of mSYD1A (http://psort.hgc.jp/) (figure 16C). Furthermore, our subcellular fractionation experiments in mouse brain lysates have shown that a pool of mSYD1A localizes to the nucleus and therefore strengthens the hypothesis that mSYD1A might contain a nuclear localization signal (figure 1 of the manuscript). Future experiments will have to investigate a possible role for mSYD1A in the nucleus.

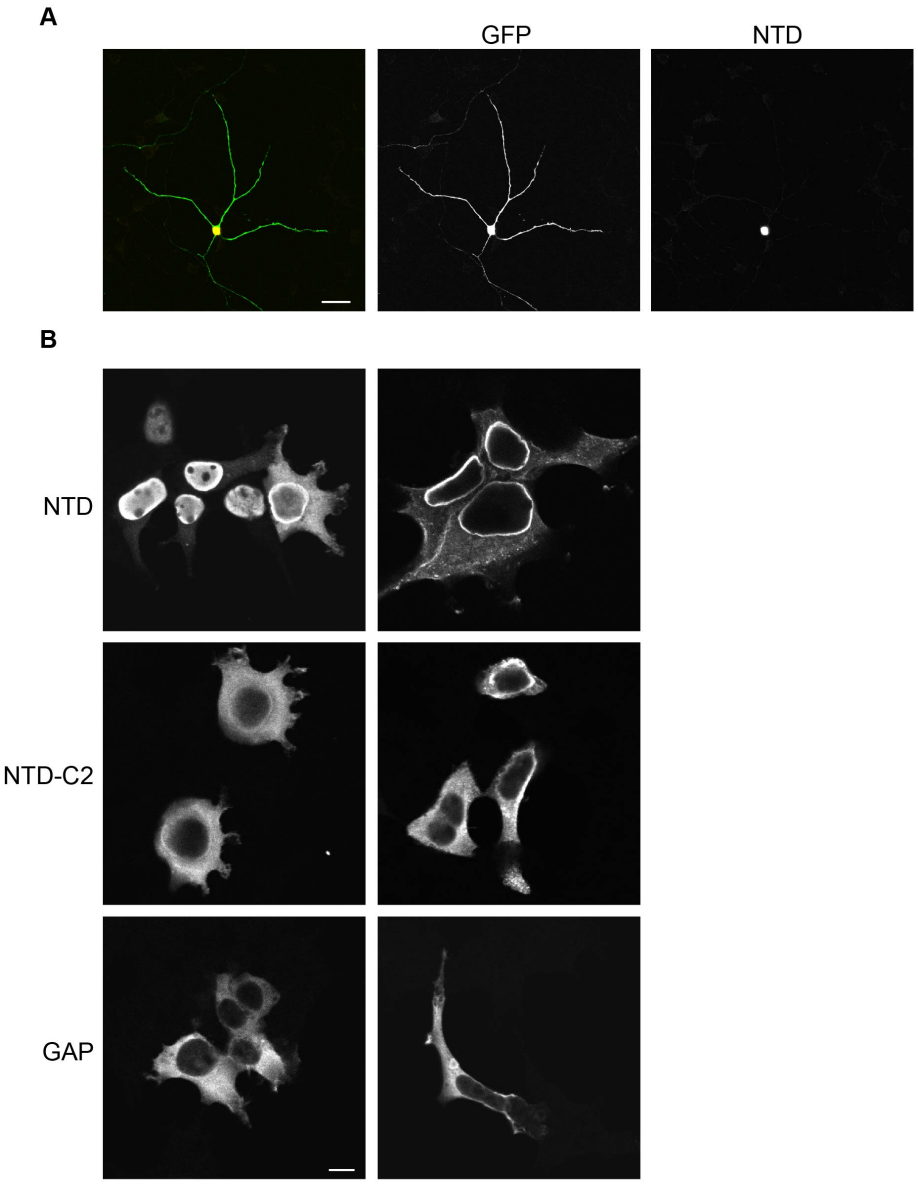

Figure 16 – Localization of mSYD1A deletion constructs
(A) The N-terminal domain (NTD) of mSYD1A is localized to the nucleus after overexpression in cerebellar granule cells. Cells were co-transfected with GFP and NTD-Myc and immunostained for GFP and Myc (scalebar = 20 µm). **(B)** The NTD of mSYD1A is localized to the nucleus, the cytoplasm and a perinuclear region in HEK293T cells. NTD-C2 (N-terminal domain and C2 domain of mSYD1A) is localized to the cytoplasm with perinuclear staining, whereas the GAP domain of mSYD1A shows a diffuse cytoplasmic localization (scalebar = 10 µm). **(C)** Several amino acids in the NTD of mSYD1A are predicted to serve as nuclear localization sequences (NLS, shown in red). Two typical NLS patterns were identified: green brackets: starting with P followed within 3 residues by a basic segment, containing 3 basic amino acids (K,R) out of 4; blue brackets: 2 basic residues, 10 residue spacer, and another basic region consisting of at least 3 basic residues out of 5 (http://psort.hgc.jp/).

Since we wanted to test if the NTD of mSYD1A is sufficient to induce synaptic vesicle clustering in neurons, it was necessary to target the NTD to the axon. Therefore, we added a myristoylation and palmitoylation tag to the NTD of mSYD1A (myr-NTD), which targets the protein to the plasma membrane. In fact, myr-NTD exhibited a punctate distribution in the soma, dendrites and the axon after overexpression in cerebellar granule neurons (figure S3 of the manuscript). Using this construct, we could show that the N-terminal domain of mSYD1A alone (myr-NTD) is sufficient to increase the density of synaptophysin-mCherry puncta. In this experiment, myr-NTD and synaptophysin-mCherry were overexpressed in the same cell. One possible concern about this experiment is that due to double-transfection, the cells have an increased expression machinery, which leads to an increase in synaptophysin puncta in the axon that might not necessarily represent a specific effect of mSYD1A on synaptic vesicle clustering. To rule that out, we also counted the density of endogenous vGluT1 puncta along axons of cells only overexpressing myr-NTD. Here as well, we could see a significant increase in the density of vGluT1 puncta, whereas the density of PSD95 puncta did not change (figure 17). This shows that overexpression of the N-terminal domain of mSYD1A alone is indeed sufficient to increase the density of synaptic vesicle clusters in the cell.

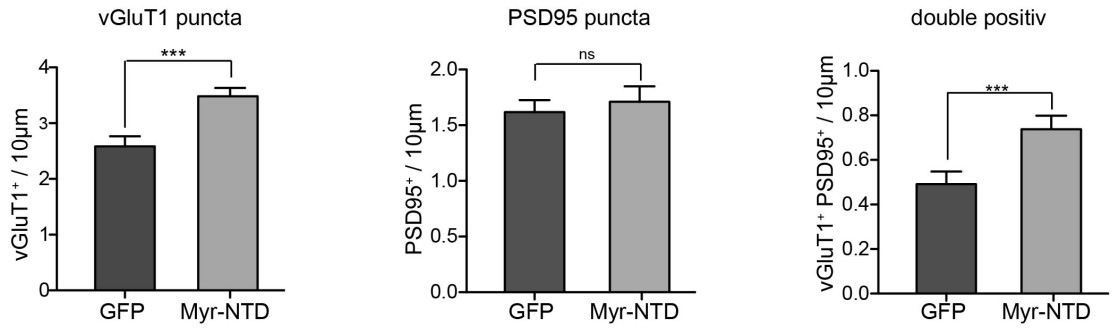

Figure 17 – Overexpression of mSYD1A increases synapse density
Overexpression of the N-terminal domain of mSYD1A (Myr-NTD) in cerebellar granule cells leads to an increase in endogenous vGluT1 compared to overexpression of GFP, while the density of PSD95 puncta is not changed. However, the number of vGluT1/PSD95 double positive puncta is significantly increased. The number of vGluT1 and PSD95 positive puncta per 10 µm axon were counted (n=45 cells; ***: $p<0.0001$; ns: not significant, two-tailed t-test; mean ± s.e.m).

2.4 Generation of mSYD1A KO mice

Our *in vitro* results show that mSYD1A is important for a coordinated assembly of presynaptic terminals. To analyze, if these results can be reproduced *in vivo* and if mSYD1A has an equally important role in neural development of the mouse, we decided to create mSYD1A knockout (KO) mice. The European Conditional Mouse Mutagenesis Program (EUCOMM) provides a large number of conditionally targeted genes that can be ordered either as mutant ES cell lines, or mutant mice (Skarnes et al, 2011). We decided to order mutant ES cell lines for mSYD1A and work together with the Transgenic Mouse Facility of the Biozentrum to create mSYD1A mutant mice.

2.4.1 mSYD1A KO mouse constructs and generation of different mouse lines

We ordered ES cell clones from EUCOMM, containing a manipulation in the gene *syde1* (Project ID: 82373). The EUCOMM vector for conditional gene targeting allows several different ways to create knockout mice. In the case of mSYD1A, an expression cassette was inserted between exon 1 and 2 of the *msyd1a* gene (figure 18). This expression cassette contains a splice acceptor (En2 SA), resulting in a gene trap and a loss-of-function of the gene after insertion. Furthermore, the presence of an internal ribosomal entry site (IRES) and a lacZ expression construct behind the splice acceptor allow for detection of cells that express mSYD1A by β-galactosidase staining. The neomycin resistance, used for selection of positive ES cell clones, is expressed under control of the human β-actin promoter. The first generation of mice that we produced, carry this cassette between exon 1 and 2 of mSYD1A and represent the first generation of mSYD1A knockout mice with the line name SYD1A-lacZ-loxP. Here, a successful insertion of the construct should result in the absence of mSYD1A in all tissues.

In addition, this construct has the potential to produce mSYD1A conditional knockout mice. The inserted cassette is flanked by FRT sites and can therefore be deleted with the Flip recombinase. Breeding of SYD1A-lacZ-loxP mice with mice containing the Flip recombinase will result in the mouse line with the name SYD1A-loxP. These mice will contain one loxP site that was inserted behind the FRT-flanked cassette between exon 1 and 2, and another loxP site, which has been inserted between exon 4 and 5. Crossing of SYD1A-loxP mice with a Cre mouse line will lead to a deletion of exon 2 – 4. Splicing of exon 1 to exon 5 results in a frame shift in the *msyd1a* sequence and therefore a loss-of-function of mSYD1A (SYD1A-del). The conditional potential is here dependent on the promoter-specific expression of the Cre recombinase.

Furthermore, mice containing the original lacZ-loxP cassette can be crossed with mice containing the Cre recombinase instead of the Flip recombinase. This will also result in a loss of the neomycin expression cassette and exon 2 – 4, but leaves the lacZ cassette between exon 1 and 5, which can be beneficial for tracing mSYD1A-expressing cells (SYD1A-lacZ-del).

The parental ES cell line (JM8A3.N1) was derived from the mouse strain C57BL/6N with the fur color agouti. In order to identify chimeric offspring by means of fur color, the manipulated ES cells were injected into blastocysts of Balb/c mice and transferred into Balb/c females, which have a white fur color.

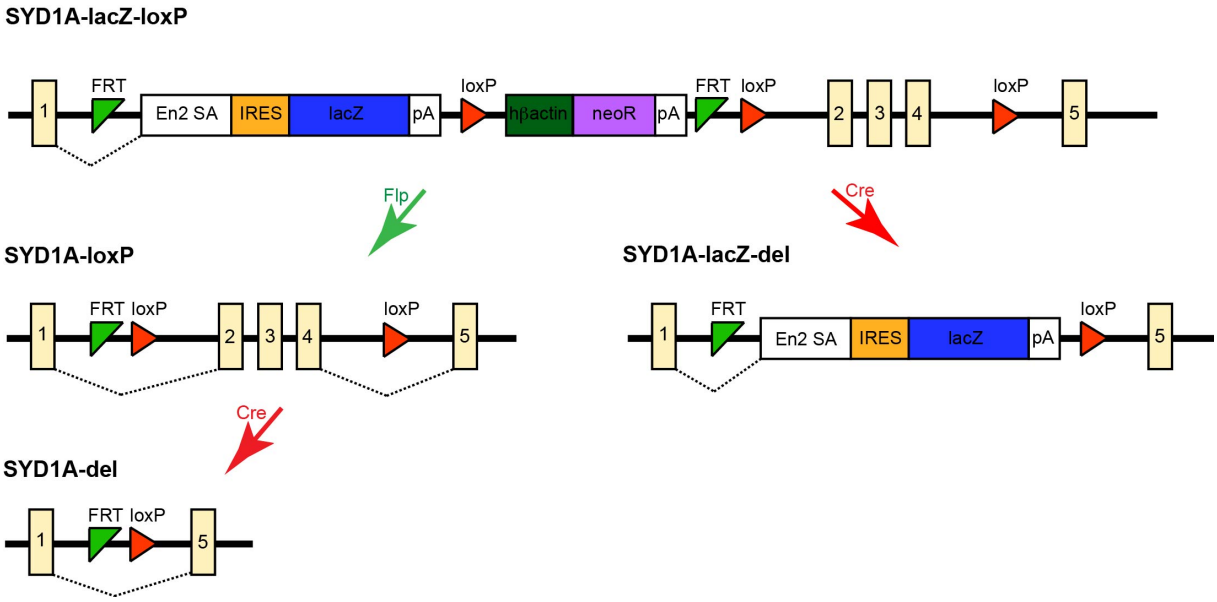

Figure 18 – Creation of mSYD1A KO mice
To create mSYD1A KO mice, a construct, containing a splice acceptor (En2 SA), an expression cassette for lacZ and the neomycin resistance, was inserted between exon 1 and 2 of mSYD1A. Insertion of this construct should result in a gene-trap and a loss-of-function of mSYD1A. Crossing of these mice with mice containing the Flip recombinase will result in a mouse line (SYD1A-loxP) that can be used for conditional, Cre-dependent deletion of exon 2 through 4 of *msyd1a* (SYD1A-del). Crossing of SYD1A-lacZ-loxP with a Cre-containing mouse line will create a deletion of exon 2 through 4 of *msyd1a* while the lacZ expression cassette is still present (SYD1A-lacZ-del).

2.4.2 mSYD1A protein expression is completely lost in mSYD1A-lacZ-loxP mice

The first mSYD1A mutant mouse line that we created (SYD1A-lacZ-loxP) contained the lacZ-neo expression cassette between exon 1 and 2. The resulting transcript of this gene should encode exon 1 of mSYD1A, which should be splice onto the splice acceptor En2 SA, followed by an internal ribosomal entry site (IRES) and a cDNA sequence encoding lacZ. To

analyze, if insertion of this cassette results in a genetrap and a loss-of-function of mSYD1A, we lysed brains of adult WT, heterozygous and homozygous littermates and carried out a Western-Blot analysis. mSYD1A protein expression was completely lost in homozygous animals, whereas heterozygous animals showed a reduction in expression compared to WT (figure 19A). Our antibody is a peptide antibody, raised against the first 18 amino acids of mSYD1A, which are encoded in exon 1. Fusion of exon 1 of mSYD1A and the splice acceptor En2 SA should result in a small protein with the molecular weight of 8 kDa. Since no mSYD1A protein of lower molecular weight could be detected on the Western-Blot, it is likely that the protein product is instable and degraded.

To investigate regional expression patterns of mSYD1A in the brain in WT and mSYD1A KO mice, we separated cortex, hippocampus and cerebellum and subjected the lysates to Western-Blot analysis. Probing for mSYD1A showed that the protein is expressed in all three brain regions with similar expression levels (figure 19B). Furthermore, we could confirm that mSYD1A is lost in all brain regions analyzed in the KO animals.

Overall brain architecture was assessed with immunostaining for NeuN (neuron specific nuclear marker) and calbindin (labels interneurons in the cortex and Purkinje cells in the cerebellum) and was found to be unchanged in the KO mice as compared to WT littermate controls (figure 19C).

Unfortunately, immunostainings for β-galactosidase in heterozygous and homozygous animals were not successful. We reasoned that the low expression levels of mSYD1A might be the cause for our difficulties to detect the presence of β-galactosidase by immunohistochemistry. Here, detection of β-galactosidase via its enzymatic reaction, or qPCR analysis might yield more successful results in the future.

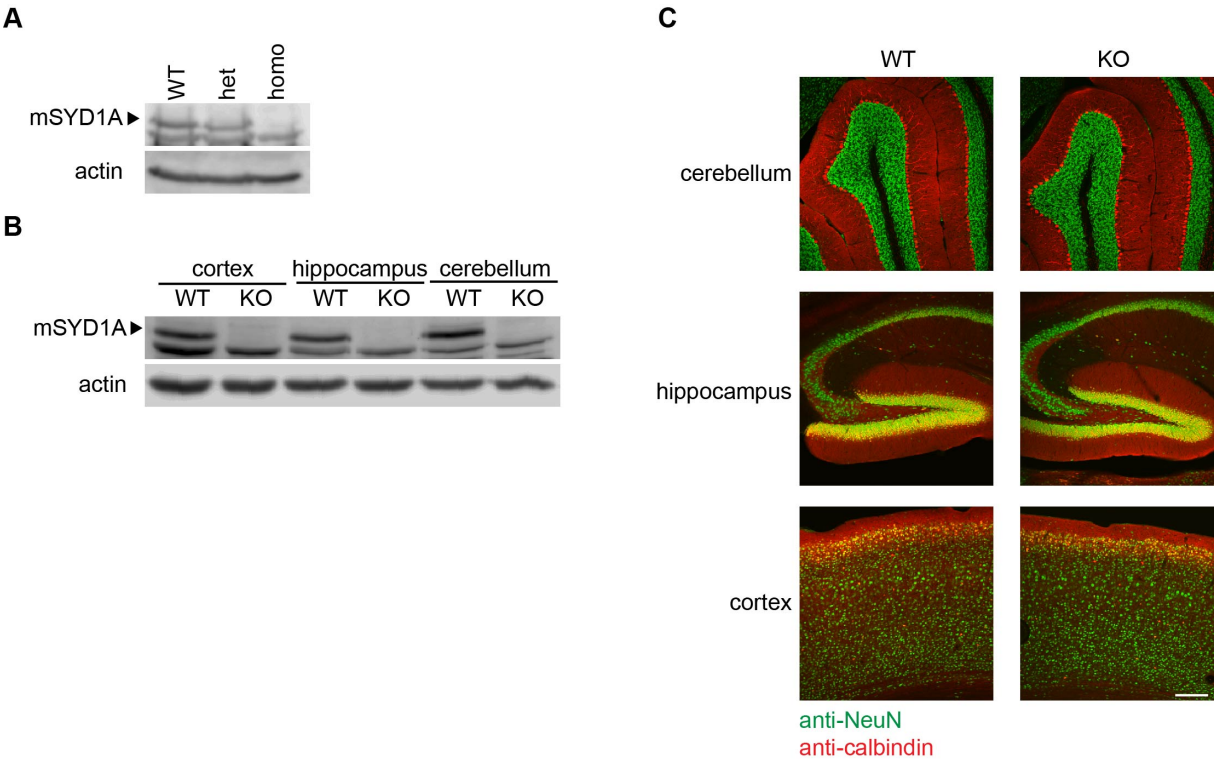

Figure 19 – Analysis of mSYD1A KO mice
(A) mSYD1A protein is completely lost in brain lysates of adult homozygous mice, whereas protein levels are reduced in heterozygous animals. **(B)** mSYD1A is expressed in cortex, hippocampus and cerebellum of P15 WT mice, and absent in homozygous KO animals. **(C)** Brain cyto-architecture of WT and homozygous mSYD1A KO mice was assessed in brain sections of adult mice by immunostaining for NeuN and calbindin (scalebar = 200 µm).

2.4.3 Increase in postnatal death in mSYD1A KO mice

To analyze if loss-of-function of mSYD1A protein has an impact on the health and survival rate of mSYD1A KO mice, we calculated the ratio of genotype distribution for each litter (figure 20A) at the time of genotyping (P5 – P7). The division of genotypes was close to Mendelian ratios, suggesting that there is no prenatal death. However, we observed an increase in postnatal death in mSYD1A heterozygous and homozygous mice (figure 20B). At 12 weeks of age, 20 % of all heterozygous and homozygous animals that were born had died, whereas only 6 % of the WT animals were dead. A closer examination revealed that most animals died between 2 and 4 weeks of age (figure 20C). However, it is important to note here that the analyzed animals have a mixed background. For the generation of the mSYD1A-lacZ-loxP mouse line, ES cells derived from C57BL/6N mice were injected into blastocysts derived from Balb/c mice. Chimeric offspring were then crossed with Balb/c mice again, yielding the heterozygous mice, which are the parents of the analyzed breedings above. A mixed background can lead to instabilities in animal health, resulting in postnatal death that might not be the result of mSYD1A loss-of-function. Therefore, these results are preliminary and have to be regarded with care. Backcrossing of these mice with C57BL

animals will be important before a thorough analysis of mSYD1A KO mice is initiated. In total, 20 litters were born from 6 different breedings, generating 61 WT, 104 heterozygous and 37 homozygous animals that were analyzed for the occurrence of postnatal death (see appendix tables 5.2.1 and 5.2.2 for more detail). Nevertheless, the number of animals is sufficient to provide a first trend, which indicates that the occurrence of postnatal death is increased in mSYD1A heterozygous and homozygous animals and peaks around week 3. Future experiments will have to be done to define the reason for the increase in postnatal death. Furthermore, it needs to be investigated why both heterozygous and homozygous animals seem to be equally affected. Our Western-Blot analysis has shown that heterozygous animals express reduced levels of mSYD1A protein compared to WT mice. If the increase in postnatal death in both heterozygous and homozygous mSYD1A KO animals after backcrossing with C57BL mice can be confirmed, it suggests that the amount of mSYD1A expression level is crucial for its function. Furthermore, we could confirm that mSYD1A homozygous KO animals are fertile.

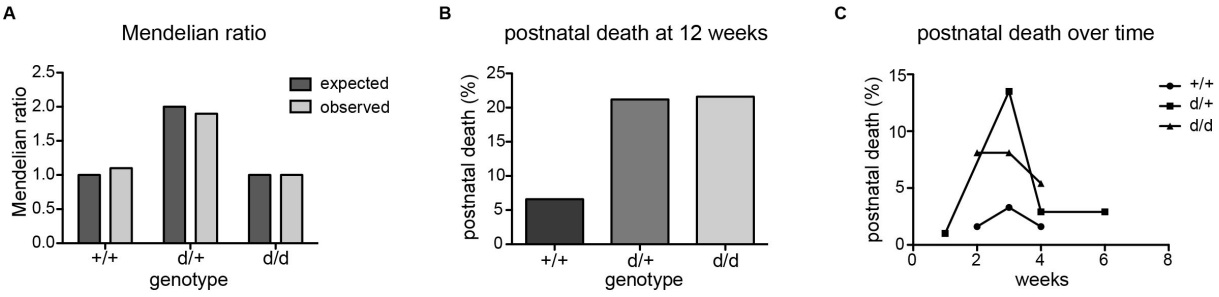

Figure 20 – Mendelian ratios and survival rate for mSYD1A KO mice
(A) The distribution of genotypes from breedings of heterozygous parents in the mSYD1A KO mouse line conforms to Mendelian ratios. The analysis was done at the time of genotyping (P5 – P7). (analysis of 13 litters; n(+/+) = 39 animals, n(d/+) = 67 animals, n(d/d) = 37 animals). **(B)** Heterozygous and homozygous animals for *msyd1a* show an increase in postnatal death. Displayed is the percentage of animals that died of the total number of animals that were born with this genotype (total number of animals analyzed: +/+: 61; d/+: 104; d/d: 37). **(C)** A closer examination of postnatal death shows that most animals die around 3 weeks of age (number of animals analyzed is the same as in B).

2.4.4 No decrease in mEPSC frequency in mSYD1A KO neurons

As a first assessment of synaptic transmission in mSYD1A KO mice and a further validation of the results obtained from knockdown of mSYD1A by siRNA, we chose to record miniEPSCs from cerebellar granule cell cultures. To this end, we prepared primary cultures from WT and KO littermate animals and compared mEPSC amplitude and frequency (figure 21A). In a first set of experiments, we could not detect any significant changes in mEPSC amplitude or frequency in the KO compared to WT animals. Thus, in mSYD1A KO mice, we

could not reproduce our data obtained from knockdown studies, showing a reduction in mEPSC frequency. To rule out that the reduction in mEPSC frequency in the knockdown studies was due to an off-target effect of the siRNA, we treated cultures, derived from mSYD1A KO mice, with siRNA against mSYD1A (figure 21B). Since no functional mSYD1A protein is present in these cells, any phenotype observed with the siRNA would be likely to represent off-target effects. We could not detect any changes in mEPSC amplitude or frequency after treatment of mSYD1A KO cultures with siSYD1A as compared to mSYD1A KO cultures treated with control siRNA. However, the effect of the siRNA against mSYD1A was validated in this experiment, since WT cultures treated with siSYD1A showed a reduction in frequency as compared to WT cultures treated with siCNT. This suggests that the reduction in mEPSC frequency after knockdown of mSYD1A is specifically due to a loss of mSYD1A and not an off-target effect. Lack of the phenotype in KO cultures can be explained by compensational effects during the development of the animal and has been seen for other presynaptic proteins (Kaeser et al, 2009; Rosenmund et al, 2002; Schoch et al, 2006).

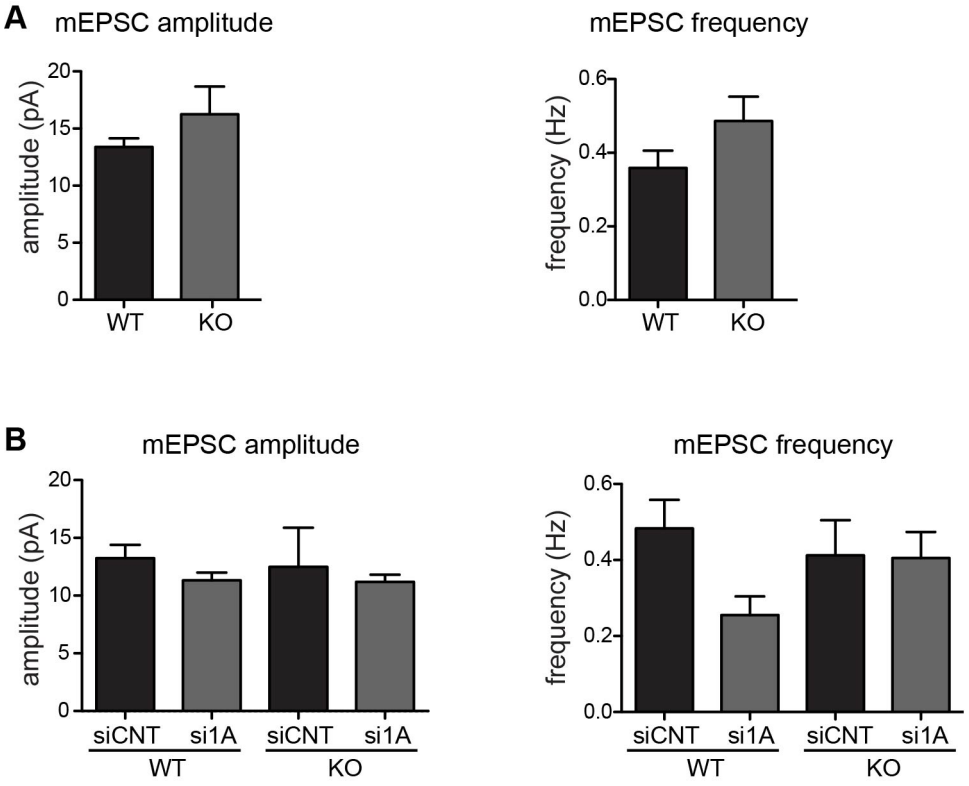

Figure 21 – mEPSC recordings from mSYD1A KO mice
(A) Cerebellar granule cell cultures were prepared from mSYD1A KO mice and miniEPSC amplitude and frequency were recorded; n(WT) = 22 cells, n(KO) = 19 cells. **(B)** Cerebellar granule cell cultures from WT and mSYD1A KO mice were treated with control siRNA (siCNT) and siRNA against mSYD1A (si1A); n = 9 cells.

2.5 mSYD1B KO mice

In our initial database search, we identified two candidate orthologues for *C.elegans* SYD-1: mSYD1A and mSYD1B. Since the amino acid sequences of the two proteins are very similar, it is likely that they execute similar functions. Therefore, potential effects resulting from loss of mSYD1A might be undetectable in mSYD1A KO mice, due to the expression of mSYD1B. Therefore, we sought to generate mSYD1B knockout mice, providing us with the possibility to create a double knockout of mSYD1A and mSYD1B. For the creation of mSYD1B knockout mice, we commissioned the Gene Targeting and Transgenic Facility of the University of Connecticut Health Center. An FRT-site-flanked Neo expression cassette, containing a loxP site at its 3'-end, was inserted between exon 3 and 4 of the *msyd1b* gene (figure 22). Furthermore, another loxP site was inserted between exon 1 and 2 of *msyd1b*. Crossing of these mice with a line containing the Flip recombinase resulted in animals containing loxP sites flanking exons 2 and 3 (SYD1B-flox). These animals were subsequently crossed with mice expressing the Cre recombinase under control of the CMV promoter (Cre-deleter), leading to excision of exons 2 and 3 in the whole organism (SYD1B-KO). Splicing of exon 1 into exon 4 results in a frame shift with a premature stop codon. However, a translational start codon in exon 5 could give rise to a truncated mSYD1B protein product, containing half of the GAP domain. Creation and analysis of these mice was part of Julia's project. She could confirm the absence of exon 2 and 3 by RT-PCR, however, she could also detect the presence of transcripts from exons 5 and 6 of *msyd1b* in the knockout animals (see PhD Thesis Julia Sommer). Quantitative PCR showed that *msyd1b* mRNA levels containing exons 5 and 6 were reduced by 44 % in the KO compared to WT levels, suggesting that the product is instable. Absence of the protein could not be evaluated, since we do not have an antibody available that recognizes endogenous mSYD1B. mSYD1B mice are viable and fertile and do not show any obvious behavioral abnormalities. Immunostaining for NeuN and calbindin suggested a normal overall brain cyto-architecture. In our future experiments, we will use these mice to create double knockouts for mSYD1A and mSYD1B. However, production of an antibody against mSYD1B protein will be important for the future analysis of mSYD1B expression and function.

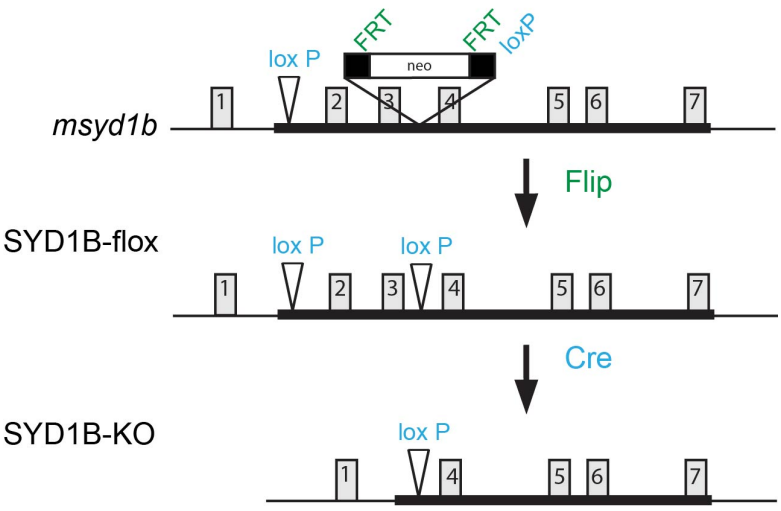

Figure 22 – Creation of mSYD1B KO mice
To create mSYD1B KO mice, a neomycin cassette, flanked with FRT sites and a loxP site was inserted between exons 3 and 4 of *msyd1b*. A second loxP site was inserted between exons 1 and 2. Crossing with mice containing the Flip recombinase led to the deletion of the neomycin cassette and creation of the line mSYD1B-flox. Subsequent crossing with Cre-deleter mice resulted in deletion of exons 2 and 3 in the line mSYD1B-KO.

2.6 Production of additional mSYD1A antibodies

The antibodies for mSYD1A that we have used throughout the study reliably detect mSYD1A on Western-Blot, but cannot be used for immunostaining of the endogenous protein. In our immunocytochemistry experiments, we could not detect a recognizable staining pattern after application of the antibody, suggesting that it does not detect native mSYD1A. Furthermore, the cross-reactivity of the antibody with several other proteins, as seen on Western-Blot, provides a second difficulty for its usage in immunostainings. Therefore, we decided to take a new approach for the production of a new mSYD1A antibody. Instead of raising antibodies against synthetic peptides, as we had done before, we chose to purify parts of mSYD1A as recombinant proteins and to use these proteins for production of an additional antibody. To this end, we generated six bacterial expression constructs covering randomly selected sequence stretches of *msyd1a*, which could serve as potential epitopes (figure 23A). In earlier studies, recombinant mSYD1A proved to be highly insoluble in bacteria and therefore difficult to purify. We encountered the same difficulties for all 6 segments of mSYD1A, with epitope 2 showing the biggest fraction of soluble protein. Therefore, we chose to use epitope 2 and to solubilize the protein in the presence of Urea. After affinity purification of the protein using IMAC (Nickel) resins, the concentration of Urea was reduced to 2 M by dialysis and the purity of the protein was analyzed by gel electrophoresis and commassie staining (figure 23B).

We commissioned Eurogentec with the immunization of three rabbits with epitope 2 of mSYD1A. Initial tests of the antisera showed that antisera from all three rabbits detected overexpressed protein on Western-Blot, whereas none detected endogenous mSYD1A in HEK293T cells or brain lysate. We purified two antisera on the antigen (purified recombinant protein). Unfortunately, the purification did not lead to a higher detection efficiency of mSYD1A (figure 23C). Thus, the new antibodies against mSYD1A detect overexpressed, but not endogenous mSYD1A on Western-Blot.

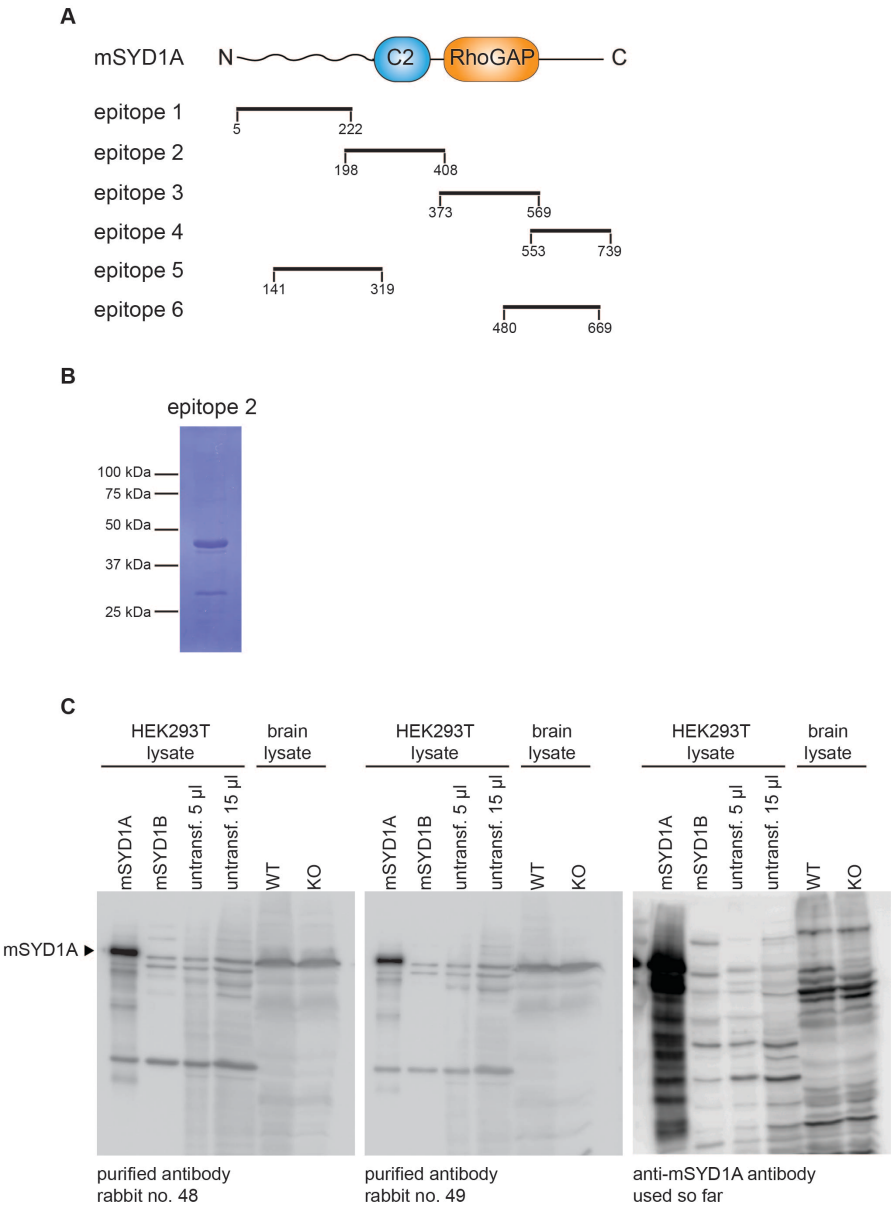

Figure 23 – Production of an additional mSYD1A antibody
(A) Constructs of mSYD1A that can be used as epitopes for the production of mSYD1A antibody from recombinant protein. **(B)** Epitope 2 of mSYD1A was purified from *E.coli,* resolved by gel-electrophoresis and stained with commassie to evaluate the purity of the protein. **(C)** Antisera from rabbits no. 48 and 49 were purified on the antigen (recombinant protein) and detection of overexpressed and endogenous mSYD1A was tested on Western-Blot. mSYD1A and mSYD1B: overexpressed protein in HEK293T cells; untransf.: untransfected HEK cell lysate. As a positive control, the anti-mSYD1A antibody that we have used so far was applied.

3. Discussion and future directions

We identified two mammalian orthologues for SYD-1 that show considerable sequence similarity and similar domain organization as the *C.elegans* SYD-1 protein. mSYD1A is expressed during the time of synapse formation and localizes to synaptic membrane fractions in synaptosome preparations. Functionally, mSYD1A acts as a GAP protein towards the small GTPase RhoA and is auto-regulated by its N-terminal domain. Knockdown of mSYD1A in cerebellar granule cells decreases synaptic vesicle clustering, whereas overexpression increases synapse density. Furthermore, the GAP domain of mSYD1A seems to contribute to trans-synaptic signaling. Thus, we identified mSYD1A as a presynaptic regulator of synapse assembly.

3.1 Is mSYD1A a true orthologue?

mSYD1A and mSYD1B show a similar domain organization as *C.elegans* and *Drosophila* SYD-1, however, they lack the N-terminal PDZ domain that is present in invertebrates. An analysis of SYD-1 in different species shows that the N-terminal PDZ domain was lost relatively early during evolution, since also predicted SYD-1 proteins for fish (*Danio rerio*) and chick (*Gallus gallus*) do not contain PDZ domains (see also Appendix, figure 25). However, all nematode (*Ascaris suum, Trichinella spiralis*) and fly species (*Aedes aegypti, Drosophila simulans, Culex quinquefasciatus*) that I have looked at contain the N-terminal PDZ domain, suggesting that it has an important function in these species. Many orthologues that have been described from *C.elegans* to mouse show the exact same domain organization, like for example SYD-2/liprin-α (Zhen & Jin, 1999). On the other hand, there are also proteins that differ considerably in domain organization from species to species. One example is ELKS, whose orthologue in *Drosophila* is called Bruchpilot. Bruchpilot contains an extensive C-terminus that is not present in *C.elegans* or mammalian ELKS (Wagh et al, 2006). By definition, orthologues are genes that diverged after a speciation event, and that encode proteins with similar functions in different species. Therefore, to define if proteins are true orthologues, we have to examine the function of these proteins. We identified mSYD1A as a GAP protein that inactivates the small GTPase RhoA. *C.elegans* and *Drosophila* SYD-1 contain amino acid changes in crucial positions in their GAP domain however it has never directly been tested, if the proteins exhibit GAP activity. Our mutation constructs that mimic the amino acid changes do not show GAP activity in the full-length conformation, however, they exhibit GAP activity after deletion of the N-terminal domain. This suggests that proteins with these amino acid changes in their GAP domain have the potential to act as GAP proteins, although the GAP activity is reduced. Yet, it has to be kept in mind that the constructs that we tested were proteins containing the mouse SYD1A sequence. Therefore, it is difficult to draw a direct conclusion about the GAP activity of the *C.elegans*

and *Drosophila* SYD-1 GAP domain. We also directly used the invertebrate proteins in the FRET assay, but due to degradation of the proteins in the human cell line, the experiment was not conclusive.

In all three species, SYD-1 is a regulator of presynaptic assembly. However, the precise role in presynaptic assembly differs slightly between species. In *C.elegans*, SYD-1 has been shown to regulate both synaptic vesicle and active zone assembly (Hallam et al, 2002). In *Drosophila*, loss-of-function of SYD-1 mainly affects active zone assembly (Owald et al, 2010), whereas in our mouse studies, mSYD1A loss-of-function mainly affected synaptic vesicle clustering. It is conceivable that during evolution, because of gene duplications and new proteins emerging, the function of a given protein becomes more specific. Therefore it is easy to explain that *C.elegans* SYD-1 has a broader spectrum of functions than *Drosophila* or mouse SYD-1. Instead, it is more difficult to explain the functional differences between *Drosophila* and mouse SYD-1. However, the number of proteins that is present in mammalian presynaptic terminals is massively increased, compared to *Drosophila*. In *Drosophila*, DSYD-1 is assumed to have “active zone nucleation activity” (Owald et al, 2010), since in the absence of DSYD-1, the number of active zones is reduced and active zone material localizes at ectopic locations. It is likely, that in the mouse the role of the “active zone nucleator” is distributed among several proteins, leading to a redundancy. This could lead to the fact that most active zone proteins still localize after knockdown of mSYD1A, but the correct downstream signaling events are perturbed, ultimately leading to a defect in synaptic vesicle assembly. On the other hand, in this study we observed a decrease in the number of bassoon puncta along axons of mSYD1A knockdown neurons. Since we have not done a comprehensive analysis of the distribution of all active zone markers, it is too early to state that mSYD1A does not affect active zone assembly.

Both *Drosophila* and mouse SYD-1 show some degree of trans-synaptic signaling. In *Drosophila*, the PDZ domain of DSYD-1 has been shown to mediate signals to the postsynapse via neurexin (Owald et al, 2012), whereas in our study we could show that the GAP domain of mSYD1A is required to increase PSD95 puncta after overexpression of mSYD1A. This suggests that different mechanisms have emerged in both species to mediate trans-synaptic signaling. In the mouse, loss of the PDZ domain and a more efficient GAP activity might have led to the difference in the signaling cascades. However, if the effect of SYD-1 on the postsynapse is similar in both species, still has to be clarified. In *Drosophila*, loss of DSYD-1 leads to an overgrowth of postsynaptic glutamate receptor fields (Owald et al, 2010), with a specific defect in GluRIIA incorporation (Owald et al, 2012). In our mouse studies, we could not detect a significant decrease in the density of PSD95 puncta after knockdown of mSYD1A, although a trend to a reduction was apparent in all experiments. On

the other hand, overexpression of mSYD1A increased the density of PSD95 puncta, only when the GAP domain was present. Therefore, it is difficult to directly compare the postsynaptic phenotypes in *Drosophila* and mouse, since different proteins and parameters have been examined.

Furthermore, it has to be considered that most studies in *C.elegans* and all studies in *Drosophila* were done at the NMJ, whereas the mouse studies were done in CNS neurons. Most likely, different protein compositions at different synapses lead to different results after loss-of-function of one of these proteins.

In our studies we could show that mSYD1A directly interacts with the SAM domains of liprin-α2. Although no biochemical interactions have been proven in *C.elegans* or *Drosophila*, SYD-1 and SYD-2/liprin-α interact genetically in both species. In *C.elegans syd-1* mutants, SYD-2 does not localize to presynaptic terminals, whereas loss of SYD-2 does not affect the localization of SYD-1 (Dai et al, 2006; Hallam et al, 2002). Furthermore, a gain-of-function mutation in SYD-2 can overcome the *syd-1* loss-of-function phenotype. This suggests that the two proteins functionally interact and that SYD-1 acts upstream of SYD-2. In *Drosophila*, DSYD-1 has been shown to recruit and anchor liprin-α to presynaptic terminals (Owald et al, 2010; Owald et al, 2012). These results indicate that SYD-1 and SYD-2/liprin-α functionally interact in all three species.

In summary, SYD-1 acts presynaptically in all three species and regulates the assembly of presynaptic terminals. Furthermore, genetic or biochemical interactions with SYD-2/liprin-α have been reported in both invertebrates and mouse. Therefore, mSYD1A can be considered a true orthologue of invertebrate SYD-1, but has evolved slightly different mechanisms of action during evolution.

3.2 Regulation of mSYD1A GAP activity

We could show that the GAP activity of mSYD1A is auto-inhibited by its N-terminal domain. For several RhoGAP proteins auto-inhibitory mechanisms have been reported. The RacI-GAP β2-chimaerin for example, is auto-inhibited by its own N-terminal domain, whereas it can be activated by phospholipid binding to its C1 domain, resulting in release of the auto-inhibition (Canagarajah et al, 2004). Furthermore, both for p50rhoGAP, as well as for p120 GAP, auto-inhibitory mechanisms have been reported (Drugan et al, 2000; Moskwa et al, 2005). GAP and GEF proteins have very specific functions during development and act

locally (Pertz, 2010; Tolias et al, 2011). Therefore it is plausible that auto-inhibitory mechanisms exist for many of them, to ensure a tight temporal and spatial regulation.

Overexpression of mSYD1A led to an increase in length and branching of the dendritic tree, whereas knockdown of mSYD1A did not result in a decrease in dendrite length. Estimating from our Western-Blot analysis, the endogenous expression levels of mSYD1A are very low, as seen for many GAP and GEF proteins. However, overexpression of mSYD1A led to a massive increase in mSYD1A protein levels globally, possibly leading to various functions that mSYD1A endogenously does not have. Since knockdown of mSYD1A did not lead to a decrease in the dendritic tree, we assume that mSYD1A does not regulate dendritic tree length and branching endogenously. However, since the FRET assay was not conclusive as to the specific Rho-GTPase that mSYD1A interacts with, the overexpression experiment was important to advance our understanding in this respect. An increase in dendrite length suggests that mSYD1A inactivates the Rho-GTPase RhoA and not RacI or Cdc42 (Luo, 2000).

3.3 mSYD1A interaction partners

We could show that mSYD1A interacts with liprin-α2 and that this interaction is dependent on a PQ-loop insertion between the first two SAM domains of liprin-α2. Similar requirements have been shown for the binding between CASK and liprin-α2 (Wei et al, 2011). The dependence of binding to liprin-α2 on the PQ-loop suggests two conclusions: first, the interaction is splice isoform specific, since liprin-α1 is alternatively spliced at this position, with the PQ-loop being either included or excluded. Second, there is probably no direct interaction of these domains between the two respective proteins in invertebrates, since invertebrate liprin-α does not contain the PQ-loop insertion. In fact, an analysis of liprin-α and SYD-1 sequences of different species has shown that the appearance of the PQ-loop insertion in liprin-α coincides with the disappearance of the PDZ domain in SYD-1 (see Appendix 5.1 figure 25). While this could be a coincidence during evolution, it offers the interesting possibility that an interaction between invertebrate SYD-1 and SYD-2/liprin-α is dependent on the PDZ domain of SYD-1. Furthermore, the PDZ domain of invertebrate SYD-1 could substitute for a direct interaction between SYD-1 and SYD-2/liprin-α in a different way. One possibility is that the PDZ domain of SYD-1 recruits active zone proteins in invertebrates, whereas a complex of mSYD1A and liprin-α forms the recruitment platform in mice. The PDZ domain of *Drosophila* DSYD-1 has for example been shown to interact with neurexin (Owald et al, 2012). While we could not reproduce this interaction between the

mouse proteins, we detected neurexin and mSYD1A together in a complex in the presence of CASK. This provides another example that the loss of an interaction domain during evolution could be substituted by the presence of another protein that links the former interaction partners. Since mSYD1A and CASK both bind to the same part of liprin-α2, it would be interesting to know if this interaction is competitive or if both proteins can bind liprin-α2 at the same time. Furthermore, the SAM domains of liprin-α have also been shown to bind to LAR (Astigarraga et al, 2010; Serra-Pagès, 1998). Liprin-α has the ability to oligomerize via its coiled-coil domain. Therefore it is possible, that mSYD1A, CASK and LAR can bind to a liprin-α oligomer at the same time. This would suggest a complex between mSYD1A, liprin-α, CASK, LAR and neurexin in mammalian presynaptic terminals. Our co-immunoprecipitation experiments have opened the possibility that mSYD1A can also directly interact with LAR. Pull-down assays with LAR and mSYD1A as purified proteins would give a definite answer to this possibility. Furthermore, it would be interesting to know if mSYD1A acts upstream of liprin-α, as it has been shown for the invertebrate proteins, or if mSYD1A is downstream of liprin-α in mammals. Here, knockdown of liprin-α and localization studies for mSYD1A could give an answer to this question. However, the interpretation of this experiment is complicated by the fact that we do not have an antibody that immunostains endogenous mSYD1A. Therefore, one would have to rely on the localization of overexpressed protein. Another possible experiment that could provide an answer to this question will be presented in section 3.8.1 of the discussion.

Our pull-down experiments between mSYD1A and liprin-α2 revealed a slight decrease in molecular weight of mSYD1A after binding to liprin-α2, possibly indicative of a dephosphorylation. Indeed, several phosphorylation sites are predicted in the N-terminal domain of mSYD1A. In particular, cyclin-dependent kinase 5 (Cdk5) has been shown to play an important role in presynaptic development. Samuels et al. report that Cdk5 regulates the subcellular distribution of CASK and its association with liprin-α (Samuels et al, 2007). Their experiments suggest that liprin-α is implicated in the trafficking of CASK to presynaptic terminals, where phosphorylation of CASK by Cdk5 leads to a dissociation of the interaction and an anchoring of CASK in the presynaptic terminal. A recent report suggests that phosphorylation of N-type calcium channels by Cdk5 increases channel open probability and facilitates the interaction with RIM (Su et al, 2012). These results suggest that Cdk5 plays an important role both in the distribution of active zone material as well as the properties of presynaptic terminals. It would be interesting to know, if Cdk5 also regulates mSYD1A phosphorylation and distribution.

The Yeast-2-Hybrid screen has provided us with a number of possible interaction partners for mSYD1A that still await validation. A possible interaction between mSYD1A and

munc18 could not be conclusively confirmed in this study. However, an interaction between these two proteins would furthermore strengthen the link between mSYD1A and active zone assembly. Munc18 is essential for regulated exocytosis of synaptic vesicles (Burgoyne et al, 2009). Since synaptic vesicle clustering is perturbed after knockdown of mSYD1A, a link between mSYD1A and a component of the vesicle release machinery is interesting to investigate further.

Several of the proteins identified in the Yeast-2-Hybrid screen are localized to or associated with the nucleus. In this study we found that overexpression of a deletion construct that only consists of the N-terminal domain (NTD) of mSYD1A in neurons leads to a nuclear localization of the truncated protein. In fact, web-based prediction programs forecast that the NTD of mSYD1A contains several potential nuclear import signals (http://psort.hgc.jp/form2.html). These results suggest the possibility that mSYD1A has a nuclear function. Future studies will have to be done to confirm this hypothesis.

3.4 Mechanism of mSYD1A regulation of synaptic vesicle clustering

Knockdown of mSYD1A has led to a decrease in synaptophysin and vGluT1 puncta density, whereas overexpression of mSYD1A increased the density of synaptic vesicle markers. This result gives rise to the question, how mSYD1A controls synaptic vesicle clustering. In *C.elegans*, a recent report suggests that SYD-1 acts by facilitating the oligomerization of SYD-2/liprin-α, leading to recruitment of downstream proteins by liprin-α oligomers (Taru & Jin, 2011). It is possible that similar mechanisms exist in mammals. Liprin-α in mice has been shown to interact with ELKS, RIM, and GIT. All three proteins have indirect links to synaptic vesicles. ELKS has been shown to bind to piccolo and bassoon, which in turn can bind to PRA1 that interacts with Rab3 and synaptobrevin in the synaptic vesicle membrane (Fenster et al, 2000). Knockout of both bassoon and piccolo leads to a perturbation of synaptic vesicle clustering in presynaptic terminals (Altrock et al, 2003; Waites et al, 2011). RIM binds in a GTP-dependent manner to Rab3, which is present in synaptic vesicle membranes and has been implicated in vesicle dynamics (Wang et al, 2001). Finally GIT proteins have been shown to interact with piccolo and β-pix (Kim et al, 2003). Knockdown of β-pix leads to a disruption in synaptic vesicle localization (Sun & Bamji, 2011). Therefore, knockdown of mSYD1A could lead to a perturbation of the coordinated recruitment of downstream signaling components, ultimately resulting in a reduction of synaptic vesicle clustering.

In addition, GAP and GEF proteins have recently been implicated in signaling events that localize synaptic vesicles and active zone proteins to presynaptic terminals (Ball et al, 2010; Pawson et al, 2008; Sun & Bamji, 2011). Therefore, we hypothesized that the GAP activity of mSYD1A is important for synaptic vesicle clustering. However surprisingly, mutant constructs that do not contain the GAP domain of mSYD1A are sufficient to increase the density of synaptic vesicle markers in axons. Thus, the GAP activity of mSYD1A does not seem to mediate synaptic vesicle clustering.

3.5 How does mSYD1A GAP activity increase PSD95 levels?

While the GAP domain was not necessary to increase presynaptic vesicle clustering, it was important for the simultaneous elevation of PSD95 puncta after overexpression of mSYD1A in neurons. How could the GAP domain mediate trans-synaptic signaling? Here, at least two modes of action are possible. Either the GAP activity itself initiates a signaling cascade that results in trans-synaptic signaling, or the GAP domain serves as a protein interaction domain for proteins that mediate trans-synaptic signaling. Overexpression of mSYD1A GAP mutation constructs that contain a non-functional GAP domain led to an intermediate phenotype in PSD95 puncta density between overexpression of the WT construct and the N-terminal domain only. However, in the FRET assay we could still detect residual GAP activity for these constructs, suggesting that also the overexpressed constructs in neurons were able to act as a GAP to a reduced extent. Since this also reduced the amount of PSD95 puncta elevation, we assume that the GAP activity is needed for trans-synaptic signaling.

In general, active RhoA destabilizes F-actin, whereas active Racl and Cdc42 lead to a stabilization of the actin cytoskeleton (Govek et al, 2005). Active RhoA can increase actin-myosin contractility through its effector, the Rho kinase ROCK. Active ROCK directly phosphorylates and activates myosin light chain (MLC), which leads to actomyosin assembly and contraction. Furthermore, active RhoA can increase actin polymerization through its effector mDia. Active mDia can bind to the barbed ends of actin filaments and therefore enhance actin nucleation. This process might involve binding of mDia to profilin, which is often associated with actin monomers. Therefore, an activation of RhoA leads to changes in the actin cytoskeleton. However, a stable F-actin network has been shown to be important for presynaptic development, since actin depolymerizing drugs like lantrunculin A lead to a loss of synapses (Zhang & Benson, 2001). A local increase of the GAP activity of mSYD1A in presynaptic terminals would lead to a local inactivation of RhoA and therefore a stabilization of the actin cytoskeleton. Trans-synaptic adhesion complexes link indirectly to

the actin cytoskeleton and actin is thought to stabilize adhesion. Therefore, it is conceivable that stabilization of the actin cytoskeleton could provide the signals for the formation of a postsynaptic density. During development, the assembly of presynaptic terminals precedes the formation of a postsynaptic density. Furthermore, it has been shown that the initial localization of active zone precursor proteins to sites along the axon does not necessarily lead to the formation of synapses. Many initial clusters of active zone proteins are later disassembled and reassembled somewhere else (Bury & Sabo, 2011; Owald et al, 2012). Therefore, it is important that the maturation of the postsynaptic density is only initiated after the presynaptic assembly process has reached a critical threshold. A stabilization of the presynaptic actin cytoskeleton could provide such a threshold. Here, the increased adhesive forces provided by actin linked to trans-synaptic adhesion molecules might lead to a maturation of postsynaptic terminals. Furthermore, increases in presynaptic F-actin could lead to the recruitment of mediators of trans-synaptic signaling. It would be possible to visualize a local inactivation of RhoA by overexpression of the RhoA sensor in neurons. Here, it would be interesting to induce synapse formation locally and image RhoA sensor activation over time. A local induction of synapse formation could for example be performed by an application of beads that are coated with a postsynaptic synaptogenic adhesion molecule, like neuroligin or NGL-3. Furthermore, it has been reported that beads coated with poly-lysine can trigger presynaptic differentiation in contacting axons (Lucido et al, 2009). This experiment would directly investigate the local regulation of Rho-GTPases during presynaptic assembly.

An increase in synapse density should be reflected by an increase in miniEPSC frequency in these cultures. However, our electrophysiological studies on neurons overexpressing human SYD1A have not shown an increase in miniEPSC frequencies. Several explanations are possible for this apparent contradiction. In the immunocytochemistry studies, we detected puncta that were double positive for synaptophysin and PSD95. However, the incorporation of the scaffolding protein PSD95 does not mean that a functional postsynaptic terminal is present. Our studies have been done with relatively young cultures that are probably still maturing. An increase in miniEPSC frequency would only be detected after incorporation of AMPA receptors into the postsynaptic membrane. On the other hand a lack of miniEPSC frequency increase could also mean that mSYD1A-mediated trans-synaptic signaling does not provide all signals necessary for the functional maturation of postsynaptic terminals. Instead, the incorporation of AMPA receptors into the postsynaptic membrane might be mediated by other signals, which are diluted due to overexpression of mSYD1A and therefore not sufficiently present. Therefore, more experiments have to be done to determine the nature of the trans-synaptic effect of mSYD1A.

3.6 Model for the role of mSYD1A in presynaptic assembly

Based on the evidence presented in this study and the knowledge of SYD-1 function in invertebrates, I would like to suggest the following model for the role of mSYD1A in presynaptic assembly (figure 24). During development, mSYD1A is transported into the axon in its closed, inactive conformation. A signal that still has to be identified, leads to the recruitment of mSYD1A to the plasma membrane, where the liprin-interaction sequence (LIS) in the N-terminal domain of mSYD1A binds to the SAM domains of liprin-α. This interaction has two functional consequences: liprin-α oligomerizes and builds a recruitment platform for other active zone proteins, leading to presynaptic assembly and synaptic vesicle recruitment. Furthermore, displacement of the N-terminal domain of mSYD1A by liprin-α leads to an open, active conformation of mSYD1A, resulting in a local increase in GAP activity. A local inactivation of RhoA leads to a stabilization of the actin cytoskeleton, providing the trans-synaptic signal for a coordinate maturation of the postsynaptic density.

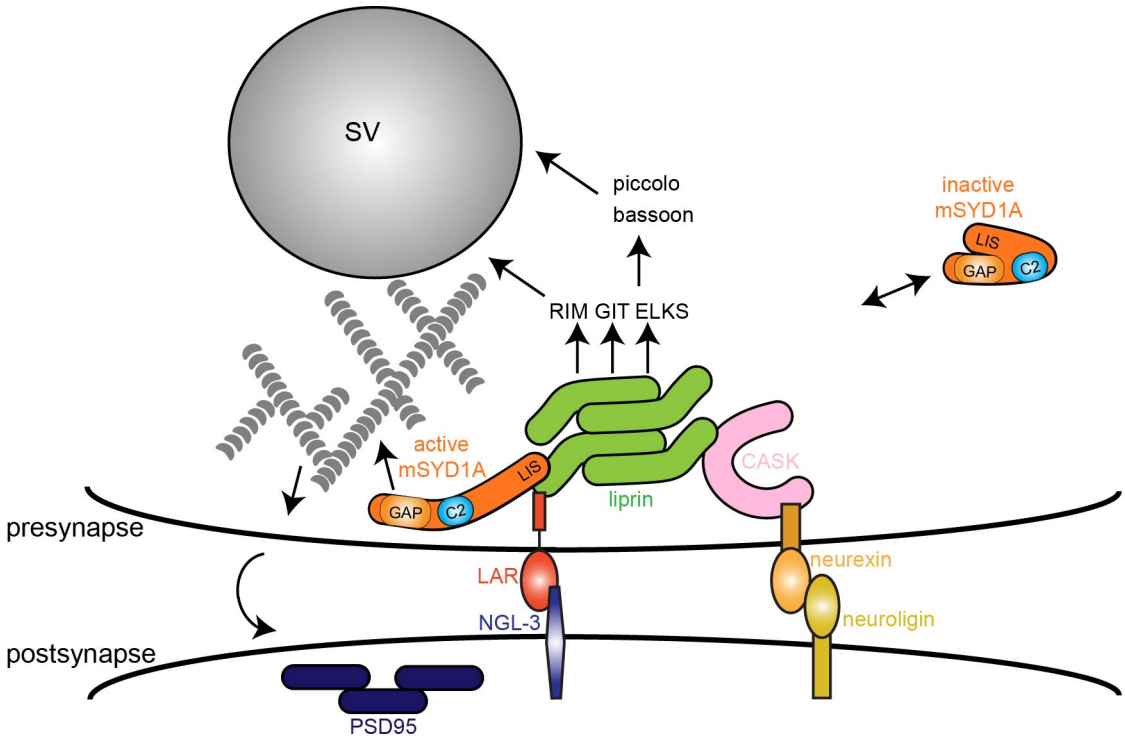

Figure 24 – Model for the role of mSYD1A in synaptic assembly
Recruitment of mSYD1A to the presynaptic plasma membrane leads to the interaction of the liprin-interaction sequence (LIS) in the N-terminal domain of mSYD1A with liprin-α. The interaction with mSYD1A activates liprin-α oligomerization, which leads to the recruitment of active zone proteins and synaptic vesicles to presynaptic terminals. At the same time, binding of mSYD1A to liprin-α changes the conformation of mSYD1A and relieves the auto-inhibition of its GAP domain, leading to a local increase in GAP activity. The resulting local inactivation of RhoA leads to a stabilization of the actin cytoskeleton, resulting in a trans-synaptic signal and the recruitment of PSD95 to the postsynaptic density.

While this model explains many of the results that have been described in this and other SYD-1 studies, it leaves several important questions unanswered that will have to be subject of future experiments: How is mSYD1A recruited to nascent presynaptic boutons? How does mSYD1A influence synaptic vesicle clustering? What is the exact nature of the synaptic vesicle clustering phenotype after knockdown of mSYD1A? Does mSYD1A play a role in synaptic vesicle docking and priming? How does mSYD1A mediate trans-synaptic signaling?

3.7 Analysis of mSYD1A function in vivo

We started our initial studies on mSYD1A KO mice with electrophysiology and tried to reproduce our *in vitro* findings that knockdown of mSYD1A leads to a reduction in miniEPSC frequency. However, we could not detect any changes in miniEPSC frequency or amplitude in the knockout cultures. One difference between the two experiments is that knockdown of mSYD1A is an acute manipulation, leading to a sudden loss of the protein, whereas in mSYD1A KO mice, mSYD1A is absent from the beginning of development. During evolution from *C.elegans* to mouse, the number of active zone proteins has massively increased. One likely explanation is that several of the proteins that are present in mammalian presynaptic terminals have similar functions, so that after loss of one protein, others can resume its function. Since the active zone is such an important structure, functional redundancies could provide a way to overcome the detrimental effect of mutations in one presynaptic protein. Therefore, our results on mSYD1A KO mice can be explained by functional redundancy between active zone proteins. The protein that most closely resembles mSYD1A is mSYD1B. Due to lack of an antibody, we have not been able to study the localization and function of mSYD1B so far. It would be interesting to know if protein expression levels of mSYD1B are upregulated in mSYD1A KO mice. However, mSYD1A protein expression levels were unchanged in mSYD1B KO mice (PhD thesis Julia Sommer). Furthermore, it will be interesting to examine protein expression levels of other active zone proteins in these mice, to determine if there are changes after KO of mSYD1A.

3.8 Future directions

One big question that we have not answered and only speculated about so far is, how exactly mSYD1A influences synaptic vesicle clustering. Therefore, a major goal of future studies will have to include a more detailed analysis of the synaptic vesicle phenotype after knockout of mSYD1A. In culture, the functionality of synapses from mSYD1A KO and knockdown neurons can be investigated by FM-dye experiments. Furthermore, mSYD1A KO mice can be used for electron microscopic analysis of synapse ultrastructure and synaptic vesicle numbers and localization *in vivo*.

In our initial observations, mSYD1A KO mice are viable and fertile and do not show an obvious phenotype. However, we could detect an increase in postnatal death in heterozygous and homozygous animals, compared to WT. Piccolo and bassoon knockout mice both show an increase in postnatal mortality rate, which for bassoon was accompanied with a decrease in fusion-competent vesicles and a reduced number of active synapses (Altrock et al, 2003; Mukherjee et al, 2010). Our data on mSYD1A knockdown studies that we have collected so far, suggests that a similar phenotype could exist in mSYD1A KO mice. The initial electrophysiological experiments on KO mice do not detect a decrease in miniEPSC frequency. However, a decrease in the number of fusion-competent vesicles will likely not be detected in miniEPSC recordings. Future studies will involve an analysis of evoked responses, paired-pulse ratio and the size of the readily-releasable pool of synaptic vesicles.

Furthermore, crossing of mSYD1A and mSYD1B KO mice to create a double KO will help us to overcome a potential redundancy between the two proteins. In addition, we could co-culture mSYD1A KO neurons with WT neurons to create a more competitive environment for synapse assembly, which might enable us to uncover a phenotype in the KO neurons that is otherwise hidden due to redundancy mechanisms. Similarly, we could overexpress postsynaptic synaptogenic adhesion molecules in mSYD1A KO cultures, similar to what we have done in WT cultures. Here, “pushing” neuronal cultures to build an increased number of synapses might help to uncover a perturbation in synapse assembly that is only revealed in a competitive environment.

3.8.1 An assay for presynaptic assembly

We could show that overexpression of mSYD1A in cerebellar granule neurons increases the density of synaptophysin puncta. This suggests that an increase of mSYD1A in axons is sufficient to induce synaptic vesicle clustering. To ultimately test this hypothesis, we would

need an assay in which we can target mSYD1A to a specific site in the axonal plasma membrane and then examine presynaptic assembly downstream of mSYD1A. Several systems have been invented during the last years that can be used to target a cytoplasmic protein to the plasma membrane after a certain stimulus (Fegan et al, 2010; Tucker, 2012). These involve chemically-induced dimerization, and more recently, light-induced dimerization systems. The first demonstration of a chemically-induced dimerization under control of a small molecule was given for the prolyl-isomerase FKBP12, which forms a homodimer after binding to rapamycin (Spencer et al, 1993). This system was subsequently used and optimized in a number of studies. Fusion of two proteins or two halves of a protein of interest to either side of the monomer, led to a temporal control of protein interaction or reconstitution after application of the small molecule. It was possible to study protein interactions, induce gene expression and recombination events and study signal transduction pathways in a temporally controlled manner (Inoue et al, 2005; Jullien et al, 2003; Nyanguile et al, 1997). However, spatial control of the induced interaction is difficult in this system, since the small molecule that induces dimerization diffuses rapidly throughout the cell. More recently, light-induced dimerization systems have been created, which provide a spatial control of dimerization by applying the light pulse only to a certain region of the cell. Here, photosensory domains from light-sensing organisms like plants and bacteria were used. The laboratory of Chandra Tucker has developed a system that employs the proteins CIB1 and cryptochrome 2 (CRY2) derived from the plant *Arabidopsis thaliana* (Kennedy et al, 2010). CRY2 is a blue light-absorbing photosensor that interacts with the helix-loop-helix protein CIB1 in its photoexcited state. An interaction between the two proteins can be induced on a timescale of 10 seconds after application of the blue light pulse, and is reversible in the dark (the dissociation of the proteins takes about 12 minutes). Fusion of CIB1 to GFP and a membrane anchor and of CRY2 to mCherry enabled the monitoring of CRY2 translocation to the plasma membrane in blue light.

We are planning to use the CIB1-CRY2 system as an assay for presynaptic assembly. Here, we will fuse mSYD1A to CRY2 and induce the translocation of mSYD1A to a defined site of the plasma membrane after application of blue light. Simultaneous transfection of the cells with synaptophysin-mCherry will then allow the visualization of synaptic vesicle clustering downstream of mSYD1A plasma membrane recruitment. Furthermore, active zone proteins, fused to a fluorescent tag, can be monitored. Using this assay, we might also be able to answer the question if mSYD1A acts upstream of and recruits liprin-α to presynaptic terminals.

3.8.2 Mediation of synaptic diversity

In our studies, we found that mSYD1A interacts with liprin-α2 and is found in a complex with liprin-α2 and LAR. Therefore, we hypothesized that mSYD1A might act specifically downstream of NGL-3/LAR induced synapse formation. However, our results in cerebellar granule cells revealed that mSYD1A does not only act downstream of NGL-3/LAR, but also of neuroligin/neurexin induced presynaptic formation. This suggests that mSYD1A acts in at least two different pathways of synapse assembly. Recently, several novel trans-synaptic adhesion complexes with synaptogenic properties have been identified (Linhoff et al, 2009; Takahashi et al, 2011; Takahashi et al, 2012; Woo et al, 2009). The fact that many different adhesion complexes with seemingly similar properties exist, has given rise to the idea that they mediate synaptic diversity (Craig & Kang, 2007; Huang & Scheiffele, 2008). It is not known, how many and which trans-synaptic adhesion complexes populate a given synapse at the same time. Furthermore, we do not know if all of the trans-synaptic complexes that a given synapse needs, are incorporated at the same time. A temporal control of receptor incorporation might provide synapses with different properties compared to their neighbors. For example, receptor protein tyrosine phosphatases and kinases have the ability to mediate protein-protein interactions, as well as changing the phosphorylation state of interacting proteins. Local control of phosphorylation at a subset of synapses might provide synapses with different properties (Dabrowski & Umemori, 2011). The picture is furthermore complicated by the fact that some adhesion complexes undergo extensive alternative splicing. Neurexins for example are encoded by three different genes, each of which has two alternative promoters. Alternative splicing at five different sites generates over 2000 potential mRNA transcripts (Baudouin & Scheiffele, 2010), possibly mediating synaptic diversity. Therefore, it will be interesting to examine if the signaling pathways that are downstream of the different adhesion complexes diverge. Does presynaptic differentiation mediated through NGL-3/LAR lead to the same CAZ composition as presynaptic differentiation mediated through neuroligin/neurexin or TrkC/PTPσ? Furthermore, do different types of synapses in different brain regions contain a different set of trans-synaptic adhesion complexes and does the adhesion complex composition change over time as synapses mature? Here, mSYD1A might play a central role, due to its importance for presynaptic assembly. Since we found that mSYD1A acts downstream of several trans-synaptic adhesion complexes, it might not only have a role in presynaptic assembly during initial synapse formation, but also mediate changes in active zone composition when the set of trans-synaptic adhesion complexes changes. Here, it will be important to investigate if mSYD1A is differentially regulated by upstream adhesion complexes. We found that mSYD1A might directly interact with the tyrosine phosphatase LAR. Therefore, LAR might have the potential to regulate the phosphorylation state of mSYD1A and consequently regulate its association with

downstream interaction partners. It will be interesting to investigate a potential phosphorylation of mSYD1A and its consequences on mSYD1A binding properties. Furthermore, liprin-αs are expressed by four different genes and it has been shown that the isoforms differ in regional distribution pattern. We found that the interaction between mSYD1A and liprin-α is splice isoform specific. Therefore, a regional difference in the expression of specific liprin-α isoforms might lead to changes in its interaction with mSYD1A and therefore in presynaptic assembly. Furthermore, we need to examine if mSYD1A is present at all types of synapses, or if a certain subset of neurons does not express mSYD1A.

3.8.3 Non-synaptic functions for mSYD1A/B

Our expression and distribution analysis of mSYD1A has shown that mSYD1A is also expressed in non-neuronal cells. An RT-PCR analysis that was done by Julia (see PhD Thesis Julia Sommer) has shown that *msyd1a* and *msyd1b* transcripts are expressed in kidney, lungs, muscle and brain tissue. Therefore, mSYD1A and mSYD1B most likely have an additional role in different cell types. The actin cytoskeleton has an important function for maintaining and changing cell shape and structure, not only in neurons. Therefore, the property of mSYD1A, and probably also mSYD1B, to act as a GAP protein, might provide it with important functions in a number of cell types. For example β-pix, a Rac/Cdc42 GEF that has been shown to have a role in presynaptic actin polymerization and synaptic vesicle localization, had previously been shown to function in the regulation of focal adhesions in various other cell types (Rosenberger & Kutsche, 2006). Possible functions of mSYD1A and mSYD1B in non-neuronal cells remain to be investigated in the future.

Furthermore, overexpressed mSYD1A in neurons localizes not only to the axon, but also to dendritic processes and the soma. While this could be an artifact of overexpression, the fact that mSYD1A can also be found in dendrites suggests a potential role for mSYD1A in dendritic development. The N-terminal domain of mSYD1A contains several nuclear localization sequences and our subcellular fractionation experiments detected a pool of mSYD1A in the nuclear fraction. In addition, several of the potential binding partners for mSYD1A, identified in the Yeast-2-Hybrid screen, are localized to the nucleus. Therefore it is likely that mSYD1A has an additional role in the nucleus, which awaits future investigation.

4. Materials and Methods

4.1 Expression constructs

Mammalian mSYD1A and mSYD1B expression constructs contained the CMV splice enhancer and the chicken beta-actin promoter (pCAGGS). mSYD1A constructs either contained an N-terminal HA- or Flag-tag, or a C-terminal Myc-tag. Point mutations in the GAP domain were introduced with Quick Change Multi Site Directed Mutagenesis Kit (Agilent-Stratagene). In myristoylated and palmitoylated mSYD1A (myr-SYD1A and myr-NTD), the minimal MARCKS-3/4 Cys (MGCCFSKT) sequence was added to the N-terminus. For lentiviral delivery of hSYD1A, a lentiviral vector with a dual human synapsin promoter was used to express GFP and hSYD1A (Gascon et al, 2008). The following previously published DNA constructs were used: mouse liprin-α1, -α2, -α4 coiled-coil domains (liprin-α-CC, amino acids α1: 351-673, α2: 369-696, α4: 185-419) (Ko et al, 2003b), His-tagged human liprin-α2 SAM domains (liprin-α2-SAM, amino acids: 866-1258) and liprin-α2 SAM ΔPQ (as above but lacking amino acids 976 – 1012) (Wei et al, 2011), RhoA sensor and p50rhoGAP (Pertz et al, 2006), epitope-tagged liprin-α2 (Zürner & Schoch, 2009), Myc-CASK (Borg et al, 1998), ELKS2-Myc (Ohtsuka et al, 2002) and Munc18 (Toonen et al, 2005). The following list provides an overview of all expression constructs that were used in this study.

Table 1 – List of constructs, used in this study

name	tag	contains amino acids	promoter	vector	species
mSYD1A					
HA-mSYD1A	HA (N-terminal)	1 - 737 (full-length)	β-actin	pCAG	mouse
HA-NTD(mSYD1A)	HA (N-terminal)	1 - 267	β-actin	pCAG	mouse
HA-NTD-C2(mSYD1A)	HA (N-terminal)	1 - 368	β-actin	pCAG	mouse
HA-C2-GAP(mSYD1A)	HA (N-terminal)	267 - 737	β-actin	pCAG	mouse
HA-GAP(mSYD1A)	HA (N-terminal)	410 - 737	β-actin	pCAG	mouse
HA-NTD 532-966(mSYD1A)	HA (N-terminal)	178 - 322	β-actin	pCAG	mouse
HA-NTD-C2 532-1104(mSYD1A)	HA (N-terminal)	178 - 368	β-actin	pCAG	mouse
HisGST-epitope1(mSYD1A)	6xHis/GST (N-terminal)	5 - 222	T7	pET9d	mouse
HisGST-epitope2(mSYD1A)	6xHis/GST (N-terminal)	198 - 408	T7	pET9d	mouse
HisGST-epitope3(mSYD1A)	6xHis/GST (N-terminal)	198 – 408	T7	pET9d	mouse
HisGST-epitope4(mSYD1A)	6xHis/GST (N-terminal)	373 – 569	T7	pET9d	mouse
HisGST-epitope5(mSYD1A)	6xHis/GST (N-terminal)	553 – 739	T7	pET9d	mouse
HisGST-epitope6(mSYD1A)	6xHis/GST (N-terminal)	480 - 669	T7	pET9d	mouse
HA-mSYD1A N552A	HA (N-terminal)	1 - 737	β-actin	pCAG	mouse
HA-mSYD1A R436A	HA (N-terminal)	1 - 737	β-actin	pCAG	mouse
HA-mSYD1A R436V N552R	HA (N-terminal)	1 - 737	β-actin	pCAG	mouse
HA-GAP N552A	HA (N-terminal)	410 - 737	β-actin	pCAG	mouse
HA-GAP R436A	HA (N-terminal)	410 - 737	β-actin	pCAG	mouse
HA-GAP R436V N552R	HA (N-terminal)	410 - 737	β-actin	pCAG	mouse
mSYD1A R436A-Myc	Myc (C-terminal)	1 - 737	β-actin	pCAG	mouse
mSYD1A ΔYRL-Myc	Myc (C-terminal)	1 - 737 Δ435 - 437	β-actin	pCAG	mouse
FLAG-mSYD1A	FLAG (N-terminal)	1 - 737	β-actin	pCAG	mouse
FLAG-GAP(mSYD1A)	FLAG (N-terminal)	410 - 737	β-actin	pCAG	mouse
FLAG-NTD(mSYD1A)	FLAG (N-terminal)	1 - 267	β-actin	pCAG	mouse
HA-NTD prorich(mSYD1A)	HA (N-terminal)	38 - 163	β-actin	pCAG	mouse
HA-NTD 1-531(mSYD1A)	HA (N-terminal)	1 - 177	β-actin	pCAG	mouse

HA-NTD 265-531(mSYD1A)	HA (N-terminal)	88 - 177	β-actin	pCAG	mouse
HA-NTD 265-801(mSYD1A)	HA (N-terminal)	88 - 267	β-actin	pCAG	mouse
Myr-SYD1A-HA	Myr (N-term) HA (C-term)	1 - 737	β-actin	pCAG	mouse
mSYD1A-Myc	Myc (C-terminal)	1 - 737	β-actin	pCAG	mouse
GAP(mSYD1A)-Myc	Myc (C-terminal)	410 - 737	β-actin	pCAG	mouse
NTD(mSYD1A)-Myc	Myc (C-terminal)	1 - 267	β-actin	pCAG	mouse
lenti Syn-hSYD1A-SYD-GFP		1 - 668	hSynapsin	LenLox 3.7	human
Myr-NTD(mSYD1A)-Myc	Myc (C-terminal)	1 - 267	β-actin	pCAG	mouse
Myr-NTD-C2(ΔLB)-Myc	Myc (C-terminal)	1 - 368 Δ124 - 262	β-actin	pCAG	mouse
hSYD1A-Myc	Myc (C-terminal)	1 - 668	β-actin	pCAG	human
mSYD1B					
HA-mSYD1B pCAG	HA (N-terminal)	1 - 1314 (full-length)	β-actin	pCAG	mouse
Liprins					
Myc-Liprin-α2	Myc (N-terminal)	full-length	β-actin	pCAG	mouse
GST-Liprina1 351-673	GST (N-terminal)	351 - 673	tac	pGEX-4T-1	mouse
GST-Liprin-α2 369-696	GST (N-terminal)	369 - 696	tac	pGEX-4T-1	mouse
GST-Liprin-α4 185-419	GST (N-terminal)	185 - 419	tac	pGEX-4T-1	mouse
6xHis Liprin-α2 SAM	6xHis (N-terminal)	866 - 1193	T7	pET.32 M.3C	human
6xHis Liprin-α2 SAM ΔPQ	6xHis (N-terminal)	866 - 1193 Δ976 - 1012	T7	pET.32 M.3C	human
others					
pMunc18-IRES2EGFP		full-length	CMV		rat
RhoA biosensor pTriEX		full-length	CMV	pTriEX	
p50rhoGAP	Myc	full-length	CMV	pTriEX	
EGFP		full-length	β-actin	pCAG	
NGL-3-Myc	Myc (C-terminal)	full-length	β-actin	pCAG	rat
HA-LAR	HA (N-terminal)	1236 - 1898	CMV	pDisplay	mouse
HA-Neuroligin1	HA (N-terminal)	full-length	β-actin	pCAG	
Synaptophysin-mCherry	mCherry (C-terminal)	full-length	CMV	pNICE	
ELKS2-Myc-His	Myc/His (C-terminal)	full-length	CMV	pcDNA3 -1	rat

4.2 Antibodies

4.2.1 Production of mSYD1A antibodies

4.2.1.1 mSYD1A antibody used in this study

The rabbit polyclonal antibody against mSYD-1A that was used in this study, was raised against a synthetic peptide (MAEPLLRKTFSRLRGREK) and affinity purified on the antigen. A description of the purification procedure can be found in Julia Sommer's PhD Thesis.

4.2.1.2 Production of an additional antibody against mSYD1A

For production of a new mSYD1A antibody, several constructs, covering different parts of the mSYD1A sequence were expressed in *E.coli*. The construct named "epitope 2", consisting of amino acids 198 – 408 of the mSYD1A sequence, showed the best protein

expression and highest solubility in *E.coli* and was purified as recombinant protein. For protein purification, the expression of epitope 2 was induced with 0.1 mM IPTG and bacteria were grown at 22 °C for 3 h. After centrifugation (1000 x g, 15 min, 4 °C), bacteria were resuspended in buffer A (20 mM Tris-HCl pH 9.0, 10 mM imidazole, 300 mM NaCl, 0.5 mM AEBSF) and lysed in the French press. After passing the bacteria through the French press twice, 1 % Triton X-100 was added to the suspension, followed by incubation at 4 °C for 30 min with overhead rotation. The cell suspension was centrifuged (17000 x g, 30 min, 4 °C) and the supernatant was saved. The pellet was resuspended in buffer A, containing 8 M urea and lysed for 45 min at 4 °C with overhead rotation. The urea-containing cell suspension was centrifuged (17000 x g, 30 min, 4 °C) and the supernatant was saved. An aliquot of all supernatants and pellets was loaded on SDS-Gel and analyzed by coommassie staining. Subsequently, the first supernatant was adjusted to 8 M urea and combined with the urea-containing supernatant. Ni-NTA (Qiagen) columns were washed with PBS and buffer A and the combined supernatant was loaded onto the column. The column was incubated with the bacterial supernatant for 30 min at 4 °C with overhead rotation and the flow-through was collected and saved. In subsequent wash steps with buffer B (20 mM Tris-HCl pH 9.0, 5 mM imidazole, 1 M NaCl, 0.1 % Triton X-100, 8 M urea) and buffer A (containing 6 M or 4 M urea), the urea concentration was reduced to 4 M. The elution was done with buffer A containing 2 M urea and 200 mM imidazole. The concentration of the eluted protein was measured with Bradford Reagent (Bio-Rad) and the purity was confirmed by SDS-PAGE, before the eluted fractions were pooled. The eluted protein was dialyzed against 20 mM Tris-HCl pH 9.0, 300 mM NaCl, 2 M urea, 2 mM EDTA, 2 mM DTT, 10 % glycerol and subsequently the protein concentration was measured again. 3 mg of protein (epitope 2 of mSYD1A) was sent to Eurogentec for the immunization of three rabbits.

4.2.1.3 Purification of the additional mSYD1A antibodies

The final bleeds of all three rabbits, immunized with epitope 2 of mSYD1A, were tested for the detection of mSYD1A on Western-Blot. Two of the three antisera were subsequently purified on nitrocellulose strips. Here, 80 µg of recombinant epitope 2 mSYD1A protein was loaded on SDS-PAGE (1 big lane) and transferred to a nitrocellulose membrane by Western-Blotting. The membrane was transiently stained with Ponceaus S and the band for epitope 2 of mSYD1A was cut out and destained with water. The membrane strip was transferred to a 15 ml Falcon tube, washed twice with 100 mM glycine-HCl pH 2.5, 100 mM NaCl for 30 sec and rinsed once in a large volume of 1x TBS-Tween. Subsequently, the membrane was blocked with 2 mg/ml BSA in 1x TBS-Tween for 1 h at room temperature. 1.5 ml of the antiserum was diluted with 10 ml 1x TBS-Tween and then added to the strip after removing the blocking solution. The incubation was performed overnight at room temperature, slowly shaking. The next day, the antibody solution was removed and the strip was washed three

times for 10 minutes with 10 ml 1x TBS-Tween. Subsequently, the membrane was rinsed with 10 ml diluted TBS-Tween (1:50 in water). In order to elute the antibody, the strip was gently soaked with 1 ml 100 mM glycine-HCl pH 2.5, 100 mM NaCl for 30 seconds and the eluate was collected in an Eppendorf tube containing 300 µl of 1 M Tris-HCl pH 7.5 to reach a final pH of 7. This elution step was repeated three times. All eluates were kept separately. After the final elution step, the strip was washed twice with 10 ml 1x PBS and stored in 10 ml 1x PBS, 1 mg/mL BSA, 0.02 % sodium azide at 4°C. Finally, the eluates were tested for detection of mSYD1A overexpressed and endogenous protein on Western-Blot.

4.2.2 Other antibodies used in this study

Anti-pan-neuroligin was described previously (Taniguchi et al, 2007). Rabbit anti-munc18 was a gift from Matthijs Verhage (de Vries et al, 2000) and rabbit anti-liprin-α3 was a gift from Casper Hoogenraad (Spangler et al, 2011) Other antibodies were purchased from commercial sources: mouse anti-actin (clone AC-40, Sigma-Aldrich), rabbit anti-histone H3 (#96715, Cell Signaling), mouse anti-PSD95 (#73-028, Neuromab), mouse anti-VAMP2 (clone 69.1, Synaptic Systems), anti-vesicular glutamate transporter 1 (vGluT1, #1353303, Synaptic Systems), rabbit anti-GAPDH (#E1C604, Enogene), mouse anti-CASK (#75-000, Neuromab), rabbit anti-munc13-1 (#126103, Synaptic Systems), mouse anti-beta-tubulin (E7, DSHB), rabbit anti-ELKS 1b/2 (#143003, Synaptic Systems), rat anti-HA (clone 3F10, Roche Applied Science), rabbit anti-c-myc (#sc-789,Santa-Cruz), mouse anti-flag (#F1804, Sigma), rabbit anti-homer (#160003, Synaptic Systems), mouse anti-bassoon (#GTX13249, GeneTex), mouse anti-VAMP2 (#104211, Synaptic Systems), mouse anti-NeuN (#MAB377, Chemicon), rabbit anti-calbindin D28K (CB-38, Swant). Secondary antibodies conjugated to cyanine dyes or Alexa 488 or 643 (Jackson ImmunoResearch and Invitrogen) were used for visualization in immunostainings.

4.3 Cell and tissue lysis and detection of proteins by Western-Blot

All lysates of cultured cells or mouse brains were prepared on ice in 20 mM Tris-HCl pH 8.0, 1 % Triton X-100, 0.1 % SDS, 10 % glycerol, 150 mM NaCl and complete protease inhibitor (Roche Applied Science) unless indicated differently. Samples were loaded on SDS-PAGE and transferred onto nitrocellulose membranes by Western-Blotting. Membranes were blocked in 5 % milk in 1x TBS, containing 0.1 % Tween-20 (TBS-Tween). Primary antibodies were incubated over night in 5 % milk in TBS-Tween. Secondary antibodies were applied for 1 h at room temperature. Membranes were incubated with ECL substrate (Pierce ECL Western Blotting Substrate, Thermo Scientific or WesternBright Quantum Western blotting

detection kit, advansta). Signals were acquired using an image analyzer (LAS-3000; Fujifilm).

4.4 Biochemical fractionation methods

4.4.1 Brain subcellular fractionation

Brains of mice at postnatal day 2 (P2) were dissected on ice and lysed in 10 volumes of buffer A [10 mM HEPES pH 7.4, 2 mM EDTA, 1 mM $MgCl_2$, 1 mM DTT, complete protease inhibitor (Roche Applied Science)]. The homogenate was centrifuged (2900 x g for 20 min) to yield post-nuclear supernatant (PNS) and pellet P1, containing nuclei, mitochondria and unbroken cells. PNS was centrifuged (100,000 x g, 2 h) resulting in pellet P2 (insoluble and membrane-associated proteins) and supernatant S2 (cytosolic proteins).

4.4.2 Synaptosome preparation

Three adult mouse brains were homogenized with a motor driven homogenizer in 0.32 M sucrose, 1 mM $NaHCO_3$, 1mM $MgCl_2$, 0.5 mM $CaCl_2$, containing complete protease inhibitor (Roche) (10 ml / 1 g of tissue). The homogenate (H) was centrifuged (1400 x g, 10 min) resulting in the pellet P1 and the supernatant S1. Centrifugation of S1 (13,800 x g, 10 min) resulted in the crude synaptosomal pellet (P2) and a cytosolic supernatant. P2 was resuspended in 1 mM $NaHCO_3$, 0.32 M sucrose and loaded on top of a sucrose gradient (0.8 M, 1 M, 1.2 M sucrose) and centrifuged at 82,500 x g for 2 h. The synaptic plasma membranes (SPM) were collected at the interface between the 1.0 M and 1.2 M sucrose layers. The SPM fraction was extracted for 15 min at 4 °C in 12 mM Tris-HCl pH 8.1, 0.32 M sucrose, 1 % Triton X-100 and centrifuged at 32,800 x g for 1 h to yield Triton X-100 soluble and insoluble fractions.

4.5 FRET sensor assay

HEK293T cells were seeded on 6-well plates and transfected with the RhoA sensor (Pertz et al, 2006) and an mSYD1A expression construct or an empty control vector (mock) in a ration of 1:4. After 48 h, the culture medium was taken off, cells were washed once with 1x PBS and 100 µl of 2x Trypsin was added to each well. After 1 min, 900 µl of 1x PBS was added to each well and the cell suspension was transferred into Eppendorf tubes and kept on ice. For the FRET measurements, the cell suspension was transferred into a quartz cuvette and the emission spectrum between 450 and 600 nm after excitation with 430 nm light was measured in a Fluorescence Spectrophotometer (F-4500, Hitachi or FP-6500,

Jasco). After the measurement, cells were pelleted, the supernatant was discarded and the cells were resuspended in Cell Lysis Buffer [20 mM Tris-HCl pH 8.0, 10 % Glycerol, 150 mM NaCl, 1 % Triton X-100, 0.1 % SDS and complete protease inhibitor (Roche Applied Science)]. The cell lysates were analyzed for expression of the RhoA sensor and co-expressed proteins by Western-Blot analysis. The RhoA sensor was detected with a homemade anti-GFP antibody (rabbit; 1:1000), whereas tagged-mSYD1A proteins were either detected with an anti-HA (rat; 1:1000; Roche Applied Science) or an anti-Myc (rabbit; 1:500; Santa Cruz) antibody. All Western-Blots were tested for equal loading of the protein lysates by staining for actin (mouse, 1:5000; Sigma).

4.6 Co-immunoprecipitation

HEK293T cells were transiently transfected (Fugene, Roche) with different combinations of expression constructs for the proteins of interest. After 48 h, cells were washed once with ice-cold 1x PBS and lysed in Cell Lysis Buffer [20 mM Tris-HCl pH 8.0, 1 % Triton X-100, 0.1 % SDS, 10 % Glycerol, 150 mM NaCl, complete protease inhibitor (Roche Applied Sciences)]. Lysates were pelleted at 13,200 rpm for 10 min and the soluble supernatant was transferred into a new Eppendorf tube. Two-thirds of the lysate were mixed with 2 volumes of Dilution buffer [20 mM Tris-HCl pH 8.0, 150 mM NaCl, 10 % glycerol, complete (Roche Applied Science)]. Antibody (0.5 µl anti-HA, 1 µl anti-Flag or 0.5 µl anti-munc18) was added and the mixture was incubated for 90 min on ice. After the incubation the lysate-antibody-mix was centrifuged at 13,000 rpm, 4 °C for 10 min and the supernatant transferred into a new tube. Protein A sepharose (GE Healthcare) for anti-Flag and anti-munc18 antibodies or anti-rat IgG (Sigma) for anti-HA was added to the samples and the mix was incubated with overhead rotation at 4 °C over night. The next morning the sepharose/agarose beads were precipitated at 1000 rpm in an Eppendorf tabletop centrifuge and washed three times in Wash buffer (20 mM Tris-HCl pH 8.0, 200 mM NaCl, 10 % glycerol, 0.2 % Triton X-100). After the last wash step beads were resuspended in 2x SDS-sample buffer (200 mM DTT, 100 mM Tris-HCl pH 6.8, 4 % SDS, 20 % glycerol, 0.05 % bromphenolblue). Proteins were resolved on SDS-PAGE, transferred to a nitrocellulose membrane and immunoblotted for the proteins of interest.

4.7 Pull-Down assays

The following proteins were purified from *E. coli* and coupled to Glutathione Sepharose (GE Healthcare) or Ni-NTA (Qiagen) Agarose beads: GST-Liprin-α1-CC, GST-Liprin-α2-CC,

GST-Liprin-α4-CC, 6xHis-Liprin-α2-SAM, 6xHis-Liprin-α2-SAM ΔPQ or GST-neurexin (cytoplasmic domain). HEK293T cells were transiently transfected (Fugene, Roche) with the protein of interest and cell lysates were lysed in 50 mM HEPES pH 7.4, 1 % Triton X-100, 0.1 % SDS, 10 % glycerol, 1.5 mM $MgCl_2$, 1 mM EDTA, 100 mM NaF, 1 mM Na_3VO_4 and complete protease inhibitor (for pull down with liprin-CC and GST-neurexin) or 20 mM Tris-HCl pH 8.0, 1 % Triton X-100, 10 % glycerol, 100 mM NaCl and complete protease inhibitor (for pull-down with liprin-SAM). The lysates were centrifuged at 13,200 rpm for 10 min at 4 °C in an Eppendorf tabletop centrifuge and soluble components were transferred into a new tube. Lysates were diluted 1:6 in Dilution buffer: Dilution Buffer liprin-CC and GST-neurexin: 20 mM HEPES pH 7.4, 50 mM NaCl, 10 % glycerol, 1 mM EDTA, 1.5 mM $MgCl_2$, 1 mM NaF, 1 mM Na_3VO_4. Dilution Buffer liprin-SAM: 20 mM Tris-HCl pH 8.0, 10 % glycerol, 100 mM NaCl, 5 mM imidazole pH 8.0. 10 µl of beads coupled to the recombinant proteins were incubated with the lysate for 5 h at 4 °C. The beads were precipitated at 1000 rpm and washed three times in Wash buffer: Wash Buffer liprin-CC and GST-neurexin: 20 mM HEPES pH 7.4, 200 mM NaCl, 0.2 % Triton X-100, 10 % glycerol, 1 mM EDTA, 1.5 mM $MgCl_2$, 1 mM NaF, 1 mM Na_3VO_4. Wash Buffer liprin-SAM: 20 mM Tris-HCl pH 8.0, 0.2 % Triton X-100, 200 mM NaCl, 10 mM Imidazole pH 8.0. After the last wash the beads were resuspended in 2x SDS-sample buffer and bound proteins analyzed by immunoblotting.

4.8 COS cell recruitment assay

For co-aggregation experiments, COS7 cells were seeded on coverslips in 24-well plates and transiently transfected (Fugene, Roche) with different combinations of Myc-liprin-α2, HA-LAR and Flag-mSYD1A. After 48 h, cells were fixed with 4 % PFA, 4 % sucrose in 100 mM sodium phosphate buffer (pH 7.4) for 15 min at room temperature. After three washes with 1x PBS, cells were blocked and permeabilized with 10 % donkey serum, containing 0.1 % Triton X-100 in 1x PBS for 1 h at room temperature. Incubation with the primary antibody (rabbit anti-Myc 1:500, rat anti-HA 1:1000, mouse anti-Flag 1:500) was carried out in blocking buffer at 4 °C over night. The next day, coverslips were washed three times in 1x PBS and the secondary antibody (donkey anti-rat Cy3, 1:500; donkey anti-mouse Cy2, 1:200; donkey anti-rabbit Cy5, 1:500, Jackson Immunoresearch) was applied in blocking buffer for 2 h at room temperature. Subsequently, cells were washed in 1x PBS and mounted with Fluoromount G (Southern Biotech).

4.9 Preparation of cerebellar granule cells and siRNA mediated knockdown

Dissociated cultures of mouse cerebellar granule cells were prepared from P5-P7 pups as previously described (Dean et al, 2003). Cells were dissociated with 0.05 % Trypsin (Gibco) in the presence of DNaseI (Roche Applied Science). Cerebellar granule cells were purified by size exclusion using centrifugation through a 40 % Percoll cushion and a 4 % BSA cushion. After purification, cells were transfected in suspension with Lipofectamine 2000 (Invitrogen). Cells were plated on 12 mm coverslips [coated previously with Poly-D-Ornithine (10 µg/ml) and Laminin (10 µg/ml)] in 24-well plates in a density of 150,000 cells per 12 mm coverslip. Cells were maintained in Neurobasal medium (Gibco) containing 2 % B27 (Invitrogen) supplement, 2 mM Glutamax (Invitrogen) and brain derived neurotrophic factor (10 ng/ml, PeproTech). Knockdown of *msyd-1a* was performed on day 1 (replenished at day 4) with 0.75 µM Accell SMART pool siRNA against *msyd1a* or a non-target control siRNA (Dharmacon). At day 7, cells were fixed with 4 % paraformaldehyde, containing 4 % sucrose in 100 mM phosphate buffer (pH 7.4). After 3 washes with 1x PBS, cells were blocked and permeabilized in 10 % donkey serum, containing 0.1 % Triton X-100 for 1 h at room temperature. Incubation with primary antibody was carried out in blocking solution over night at 4 °C. Coverslips were incubated with secondary antibody for 2 h at room temperature and mounted with ProLong (Invitrogen).

4.10 Electrophysiology

Whole cell patch clamp recordings were performed on DIV 8-11 cerebellar granule cell cultures. For knockdown of mSYD1A, 0.75 µM Accell SMART pool siRNA against *msyd1a* or a non-target control siRNA (Dharmacon) was added at DIV 1 and 4. For rescue, the lentivirus (lenti-hSYD1A or lenti-GFP as control) was added at DIV 3. The extracellular solution (pH 7.3) contained the following: 145 mM NaCl, 5 mM KCl, 2 mM $CaCl_2$, 1 mM $MgCl_2$, 5 mM Glucose, 25 mM Sucrose and 5 mM HEPES. For all the experiments 300 nM TTX, 0.1 mM Picrotoxin and 0.1 mM AP5 were used in the solution. The internal solution contained the following: 130 mM CsCl, 10 mM HEPES, 10 mM EGTA, 10 mM Phosphocreatine, 2 mM MgATP, 5 mM NaCl, pH 7.25 and 298 mOsm. Data was analyzed using Axograph X software and the mEPSCs were detected using a template based detection algorithm package.

4.11 Image acquisition and analysis

Images were acquired on a LSM5 confocal microscope (Zeiss, Germany) and assembled using Adobe Photoshop and Illustrator software. For the analysis of dendritic arborization, soma and dendrites of the neurons were traced and analyzed with Neurolucida (MBF Bioscience). Co-localization analysis of proteins in COS cells was performed by the Pearson's coefficient method computed on fluorograms, using the JaCOP plugin in ImageJ (Bolte & Cordelieres, 2006). Quantification of pre- and postsynaptic proteins in granule cells was performed by a wavelet-based segmentation method, using the Multidimensional Image Analysis module (Izeddin et al, 2012; Racine et al, 2006), run in Metamorph software (Molecular Devices, USA). Some images for figures were processed by deconvolution using a theoretical PSF, a signal/noise ratio of 10 for each channel and 30 iterations of the deconvolution algorithm (Huygens remote manager v2.1.2).

4.12 Statistical analysis

Statistical Analysis was done with Prism software (GraphPad software). Data was tested for normality using the Kolmogorov-Smirnov normality test. Normally distributed data was analyzed for statistical differences with the t-test (pairwise comparisons) or ANOVA and Tukey's for multiple comparisons. For data that was not normally distributed, non-parametric ANOVA and Dunn's multiple comparison test were used.

4.13 Generation of mSYD1A knockout mice

We bought mouse mutant embryonic stem (ES) cell clones for Syde1 from the European Conditional Mouse Mutagenesis Program (EUCOMM ID: 82373). The mutant ES cells contain a lacZ and neomycin expression cassette with a 5' splice acceptor that has been inserted between exon 1 and 2 of the *msyd1a* gene. The cells were thawed in the Transgenic Mouse Facility of the Biozentrum, injected into blastocysts and transplanted into pregnant Balb/c mice. Chimeric offspring were crossed with Balb/c mice and the litters were genotyped for detection of germline transmission. Mice carrying this transgene represent the first generation of mSYD1A KO mice (line name: SYD1A-loxP-lacZ). These mice were crossed with mice carrying the Flip recombinase to delete the lacZ and neomycin expression cassette. The resulting mice carry two loxP sites (between exon 1 and 2 and exon 4 and 5) and belong to the line SYD1A-loxP. These mice have the potential to create conditional knockout mice by crossing them with mice containing the Cre recombinase.

4.14 Generation of mSYD1B knockout mice

We commissioned the University of Connecticut Gene Targeting and Transgenic Facility for cloning and creation of mice carrying two loxP insertions in the *msyd1b* (*syde2*) gene. The 5' loxP site was inserted in intron 2 the 3' loxP site in intron 4. mSyd1B flox mice were crossed with mice carrying a Cre recombinase transgene expressed under control of the CMV promoter (Cre-deleter), giving rise to mSYD1B knockout mice.

4.15 Immunohistochemistry on mSYD1A KO mice

Two adult littermates (WT and mSYD1A homozygous KO) were sacrificed and perfused with 4 % PFA in 0.1 M phosphate buffer (pH 7.4). The brain was post-fixed over night in 4 % PFA and cut on a vibratome (Leica VT1000S) into 50 µm sections. For immunostaining, the sections were washed in 1x PBS and blocked and permeabilized in 10 % donkey serum in 1x PBS, containing 0.1 % Triton X-100. The primary antibody was applied in blocking buffer over night at room temperature (mouse anti-NeuN 1:500 and rabbit anti-calbindin 1:10,000). The next day, sections were washed in 1x PBS and the secondary antibodies were applied in blocking buffer for 2 h at room temperature in the dark (donkey anti-mouse Cy2 1:200 and donkey anti-rabbit Cy5 1:500, Jackson Immunoresearch). Sections were mounted with Fluoromount-G (Southern Biotech).

5. Appendix

5.1 Additional figures

SYD-1

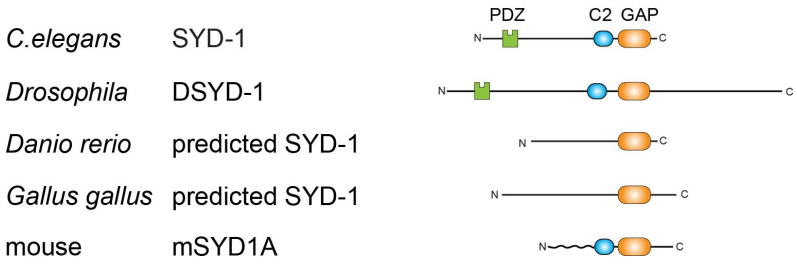

liprin-α

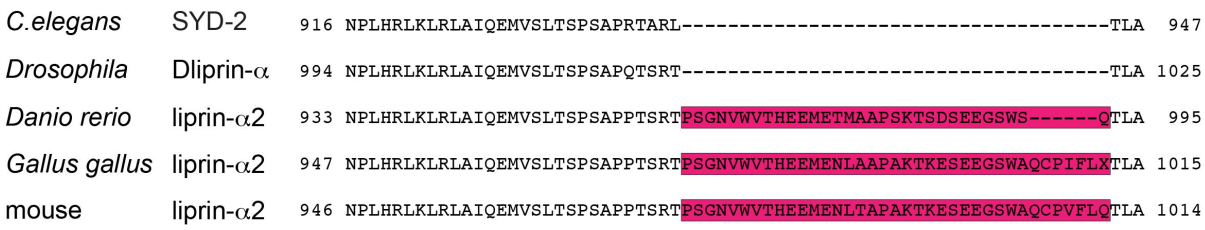

Figure 25 – Sequence comparison of SYD-1 and liprin-α for different species
C.elegans and *Drosophila* SYD-1 have a predicted PDZ domain, whereas in the predicted SYD-1 sequences of *Danio rerio* and *Gallus gallus*, as well as in mouse mSYD1A, no PDZ domain is present (domain predictions: http://pfam.sanger.ac.uk/search/sequence). The SYD-2/liprin-α sequences of *C.elegans* and *Drosophila* do not contain a PQ-loop insertion, whereas the PQ-loop is present in *Danio rerio*, *Gallus gallus* and mouse liprin-α2 (highlighted in pink) (sequence alignment: http://www.tcoffee.org/).

5.2 Additional tables

5.2.1 Analysis of genotype distribution in the SYD1A-lacZ-loxP mouse line

Table 2 – The division of genotypes in SYD1A-lacZ-loxP

heterozygous breedings	litter (DOB)	number of pups with the respective genotype		
		+/+	d/+	d/d
4 (d/+) X 6 (d/+)	09.05.12	4	3	6
	02.06.12	5	5	4
	29.06.12	2	5	7
	23.07.12	6	7	1
	19.08.12	2	6	3
	13.09.12	2	6	2
47 (d/+) X 60 (d/+)	17.06.12	1	3	1
	14.07.12	4	5	1
	25.08.12	2	4	3
	22.09.12	2	6	2
31 (d/+) X 51 (d/+)	28.06.12	5	4	2
	11.08.12	3	7	1
	06.09.12	1	6	4
total number of animals		39	67	37
ratio		**1.1**	**1.9**	**1**
expected mendelian ratio		**1**	**2**	**1**

5.2.2 Analysis of postnatal death in the SYD1A-lacZ-loxP mouse line

Table 3 – Analysis of postnatal death in SYD1A-lacz-loxP

genotype		+/+	d/+	d/d
total number of animals born		**61**	**104**	**37**
no. of animals that died at	**1 week**		1	
	2 weeks	1		3
	3 weeks	2	14	3
	4 weeks	1	3	2
	5 weeks			
	6 weeks		3	
	7 weeks			
	8 weeks			
	9 weeks			
	10 weeks			
	11 weeks		1	
total number that died		**4**	**22**	**8**
percentage (died animals of total that were born)		**6.6**	**21.2**	**21.6**

5.3 Index of figures

5.4 Index of tables

5.5 Abbreviations

aa	amino acid
bp	base pair
C.elegans	*Caenorhabditis elegans*
CAZ	cytomatrix of the active zone
CMV	cytomegalovirus
CNS	central nervous system
DIV	day in vitro
E1	embryonic day 1
ECL	enhanced chemi luminescence
EPSC	excitatory postsynaptic current
EUCOMM	European Conditional Mouse Mutagenesis Program
F-actin	filamentous actin
FRET	Förster resonance energy transfer
GAP	GTPase-activating protein
GFP	green fluorescent protein
GEF	guanine nucleotide exchange factor
HRP	horseradish peroxidase
IRES	internal ribosomal entry site
KD	knockdown
KO	knockout
LIS	liprin-interaction sequence
NMJ	neuromuscular junction
NTD	N-terminal domain

P1	postnatal day 1
PTV	piccolo-bassoon transport vesicle
RNAi	RNA interference
rpm	rounds per minute
RRP	readily-releasable pool
RT	room temperature
STV	synaptic vesicle protein transport vesicle
SV	synaptic vesicle
VGCC	voltage-gated calcium channel
WB	Western-Blot
WT	wildtype
Y2H	yeast-2-hybrid

6. References

Abbott LF, Regehr WG (2004) Synaptic computation. *Nature* **431:** 796-803

Ahmari SE, Buchanan J, Smith SJ (2000) Assembly of presynaptic active zones from cytoplasmic transport packets. *Nat Neurosci* **3:** 445-451

Aiga M, Levinson JN, Bamji SX (2011) N-cadherin and neuroligins cooperate to regulate synapse formation in hippocampal cultures. *The Journal of biological chemistry* **286:** 851-858

Altrock WD, tom Dieck S, Sokolov M, Meyer AC, Sigler A, Brakebusch C, Fassler R, Richter K, Boeckers TM, Potschka H, Brandt C, Loscher W, Grimberg D, Dresbach T, Hempelmann A, Hassan H, Balschun D, Frey JU, Brandstatter JH, Garner CC, Rosenmund C, Gundelfinger ED (2003) Functional inactivation of a fraction of excitatory synapses in mice deficient for the active zone protein bassoon. *Neuron* **37:** 787-800

Aravamudan B, Fergestad T, Davis WS, Rodesch CK, Broadie K (1999) Drosophila UNC-13 is essential for synaptic transmission. *Nat Neurosci* **2:** 965-971

Arikkath J, Reichardt LF (2008) Cadherins and catenins at synapses: roles in synaptogenesis and synaptic plasticity. *Trends in neurosciences* **31:** 487-494

Astigarraga S, Hofmeyer K, Farajian R, Treisman JE (2010) Three Drosophila liprins interact to control synapse formation. *The Journal of neuroscience : the official journal of the Society for Neuroscience* **30:** 15358-15368

Atasoy D, Schoch S, Ho A, Nadasy KA, Liu X, Zhang W, Mukherjee K, Nosyreva ED, Fernandez-Chacon R, Missler M, Kavalali ET, Südhof TC (2007) Deletion of CASK in mice is lethal and impairs synaptic function. *Proceedings of the National Academy of Sciences of the United States of America* **104:** 2525-2530

Augustin I, Rosenmund C, Südhof TC, Brose N (1999) Munc13-1 is essential for fusion competence of glutamatergic synaptic vesicles. *Nature* **400:** 457-461

Bagshaw RD, Callahan JW, Mahuran DJ (2006) The Arf-family protein, Arl8b, is involved in the spatial distribution of lysosomes. *Biochemical and biophysical research communications* **344:** 1186-1191

Ball RW, Warren-Paquin M, Tsurudome K, Liao EH, Elazzouzi F, Cavanagh C, An BS, Wang TT, White JH, Haghighi AP (2010) Retrograde BMP Signaling Controls Synaptic Growth at the NMJ by Regulating Trio Expression in Motor Neurons. *Neuron* **66:** 536-549

Bamji SX, Shimazu K, Kimes N, Huelsken J, Birchmeier W, Lu B, Reichardt LF (2003) Role of beta-catenin in synaptic vesicle localization and presynaptic assembly. *Neuron* **40:** 719-731

Baudouin S, Scheiffele P (2010) SnapShot: Neuroligin-neurexin complexes. *Cell* **141:** 908, 908 e901

Benson DL, Tanaka H (1998) N-cadherin redistribution during synaptogenesis in hippocampal neurons. *The Journal of neuroscience : the official journal of the Society for Neuroscience* **18:** 6892-6904

Biederer T, Sara Y, Mozhayeva M, Atasoy D, Liu XR, Kavalali ET, Südhof TC (2002) SynCAM, a synaptic adhesion molecule that drives synapse assembly. *Science* **297:** 1525-1531

Biederer T, Südhof TC (2001) CASK and protein 4.1 support F-actin nucleation on neurexins. *The Journal of biological chemistry* **276:** 47869-47876

Bolte S, Cordelieres FP (2006) A guided tour into subcellular colocalization analysis in light microscopy. *Journal of Microscopy-Oxford* **224:** 213-232

Borg J-P, Straight SW, Kaech SM, de Taddeo-Borg M, Kroon DE, Karnak D, Turner RS, Kim SK, Margolis B (1998) Identification of an evolutionary conserved heterotrimeric protein complex involved in protein targeting. *Journal of Biological Chemistry* **273:** 31633 - 31636

Borg JP, Lopez-Figueroa MO, de Taddeo-Borg M, Kroon DE, Turner RS, Watson SJ, Margolis B (1999) Molecular analysis of the X11-mLin-2/CASK complex in brain. *The Journal of neuroscience : the official journal of the Society for Neuroscience* **19:** 1307-1316

Brose N, Hofmann K, Hata Y, Südhof TC (1995) Mammalian homologues of Caenorhabditis elegans unc-13 gene define novel family of C2-domain proteins. *The Journal of biological chemistry* **270:** 25273-25280

Burgoyne RD, Barclay JW, Ciufo LF, Graham ME, Handley MT, Morgan A (2009) The functions of Munc18-1 in regulated exocytosis. *Annals of the New York Academy of Sciences* **1152:** 76-86

Bury LA, Sabo SL (2011) Coordinated trafficking of synaptic vesicle and active zone proteins prior to synapse formation. *Neural Dev* **6:** 24

Butz S, Okamoto M, Südhof TC (1998) A tripartite protein complex with the potential to couple synaptic vesicle exocytosis to cell adhesion in brain. *Cell* **94:** 773-782

Canagarajah B, Leskow FC, Ho JY, Mischak H, Saidi LF, Kazanietz MG, Hurley JH (2004) Structural mechanism for lipid activation of the Rac-specific GAP, beta2-chimaerin. *Cell* **119:** 407-418

Cases-Langhoff C, Voss B, Garner AM, Appeltauer U, Takei K, Kindler S, Veh RW, De Camilli P, Gundelfinger ED, Garner CC (1996) Piccolo, a novel 420 kDa protein associated with the presynaptic cytomatrix. *European journal of cell biology* **69:** 214-223

Chi P, Greengard P, Ryan TA (2003) Synaptic vesicle mobilization is regulated by distinct synapsin I phosphorylation pathways at different frequencies. *Neuron* **38:** 69-78

Chia PH, Patel MR, Shen K (2012) NAB-1 instructs synapse assembly by linking adhesion molecules and F-actin to active zone proteins. *Nat Neurosci* **15:** 234-242

Christopherson KS, Ullian EM, Stokes CC, Mullowney CE, Hell JW, Agah A, Lawler J, Mosher DF, Bornstein P, Barres BA (2005) Thrombospondins are astrocyte-secreted proteins that promote CNS synaptogenesis. *Cell* **120:** 421-433

Cingolani L, Goda, Y (2008) Actin in action: the interplay between the actin cytoskeleton and synaptic efficacy. *Nature* **9:** 344 - 356

Cingolani LA, Goda Y (2008) Actin in action: the interplay between the actin cytoskeleton and synaptic efficacy. *Nature reviews Neuroscience* **9:** 344-356

Colicos MA, Collins BE, Sailor MJ, Goda Y (2001) Remodeling of synaptic actin induced by photoconductive stimulation. *Cell* **107:** 605-616

Craig AM, Kang Y (2007) Neurexin-neuroligin signaling in synapse development. *Curr Opin Neurobiol* **17:** 43-52

Crump JG, Zhen M, Jin Y, Bargmann CI (2001) The SAD-1 kinase regulates presynaptic vesicle clustering and axon termination. *Neuron* **29:** 115-129

Dabrowski A, Umemori H (2011) Orchestrating the synaptic network by tyrosine phosphorylation signalling. *Journal of biochemistry* **149:** 641-653

Dai Y, Taru H, Deken SL, Grill B, Ackley B, Nonet ML, Jin Y (2006) SYD-2 Liprin-a organizes presynaptic active zone formation through ELKS. *Nature Neuroscience* **9:** 1479 - 1487

Dai Z, Peng HB (1996) Dynamics of synaptic vesicles in cultured spinal cord neurons in relationship to synaptogenesis. *Molecular and cellular neurosciences* **7:** 443-452

Dalva MB, Takasu MA, Lin MZ, Shamah SM, Hu L, Gale NW, Greenberg ME (2000) EphB receptors interact with NMDA receptors and regulate excitatory synapse formation. *Cell* **103:** 945-956

Darcy KJ, Staras K, Collinson LM, Goda Y (2006) Constitutive sharing of recycling synaptic vesicles between presynaptic boutons. *Nat Neurosci* **9:** 315-321

de Vries KJ, Geijtenbeek A, Brian EC, de Graan PN, Ghijsen WE, Verhage M (2000) Dynamics of munc18-1 phosphorylation/dephosphorylation in rat brain nerve terminals. *The European journal of neuroscience* **12:** 385-390

Dean C, Scholl FG, Choih J, DeMaria S, Berger J, Isacoff E, Scheiffele P (2003) Neurexin mediates the assembly of presynaptic terminals. *Nat Neurosci* **6:** 708-716

Deken SL, Vincent R, Hadwiger G, Liu Q, Wang ZW, Nonet ML (2005) Redundant localization mechanisms of RIM and ELKS in Caenorhabditis elegans. *The Journal of neuroscience : the official journal of the Society for Neuroscience* **25:** 5975-5983

Deng L, Kaeser PS, Xu W, Südhof TC (2011) RIM proteins activate vesicle priming by reversing autoinhibitory homodimerization of Munc13. *Neuron* **69:** 317-331

DiAntonio A, Haghighi AP, Portman SL, Lee JD, Amaranto AM, Goodman CS (2001) Ubiquitination-dependent mechanisms regulate synaptic growth and function. *Nature* **412:** 449-452

Dick O, tom Dieck S, Altrock WD, Ammermuller J, Weiler R, Garner CC, Gundelfinger ED, Brandstatter JH (2003) The presynaptic active zone protein bassoon is essential for photoreceptor ribbon synapse formation in the retina. *Neuron* **37:** 775-786

Drugan JK, Rogers-Graham K, Gilmer T, Campbell S, Clark GJ (2000) The Ras/p120 GTPase-activating protein (GAP) interaction is regulated by the p120 GAP pleckstrin homology domain. *Journal of Biological Chemistry* **275:** 35021-35027

Dunah AW, Hueske E, Wyszynski M, Hoogenraad CC, Jaworski J, Pak DT, Simonetta A, Liu G, Sheng M (2005) LAR receptor protein tyrosine phosphatases in the development and maintenance of excitatory synapses. *Nat Neurosci* **8:** 458-467

Dyson HJ, Wright PE (2005) Intrinsically unstructured proteins and their functions. *Nature Reviews Molecular Cell Biology* **6:** 197-208

Elste AM, Benson DL (2006) Structural basis for developmentally regulated changes in cadherin function at synapses. *The Journal of comparative neurology* **495:** 324-335

Evans LL, Lee AJ, Bridgman PC, Mooseker MS (1998) Vesicle-associated brain myosin-V can be activated to catalyze actin-based transport. *Journal of cell science* **111 (Pt 14):** 2055-2066

Fegan A, White B, Carlson JC, Wagner CR (2010) Chemically controlled protein assembly: techniques and applications. *Chemical reviews* **110:** 3315-3336

Fejtova A, Davydova D, Bischof F, Lazarevic V, Altrock WD, Romorini S, Schone C, Zuschratter W, Kreutz MR, Garner CC, Ziv NE, Gundelfinger ED (2009) Dynein light chain regulates axonal trafficking and synaptic levels of Bassoon. *The Journal of cell biology* **185:** 341-355

Fenster SD, Chung WJ, Zhai R, Cases-Langhoff C, Voss B, Garner AM, Kaempf U, Kindler S, Gundelfinger ED, Garner CC (2000) Piccolo, a presynaptic zinc finger protein structurally related to bassoon. *Neuron* **25:** 203-214

Fenster SD, Kessels MM, Qualmann B, Chung WJ, Nash J, Gundelfinger ED, Garner CC (2003) Interactions between Piccolo and the actin/dynamin-binding protein Abp1 link vesicle endocytosis to presynaptic active zones. *The Journal of biological chemistry* **278:** 20268-20277

Fox MA, Umemori H (2006) Seeking long-term relationship: axon and target communicate to organize synaptic differentiation. *Journal of neurochemistry* **97:** 1215-1231

Frank CA, Pielage J, Davis GW (2009) A presynaptic homeostatic signaling system composed of the Eph receptor, Ephexin, Cdc42 and Ca2.1 Calcium Channels. *Neuron* **61:** 556 - 569

Friedman HV, Bresler T, Garner CC, Ziv NE (2000) Assembly of new individual excitatory synapses: time course and temporal order of synaptic molecule recruitment. *Neuron* **27:** 57-69

Fu Z, Washbourne P, Ortinski P, Vicini S (2003) Functional excitatory synapses in HEK293 cells expressing neuroligin and glutamate receptors. *Journal of neurophysiology* **90:** 3950-3957

Garner CC, Zhai RG, Gundelfinger ED, Ziv NE (2002) Molecular mechanisms of CNS synaptogenesis. *Trends in neurosciences* **25:** 243-251

Gascon S, Paez-Gomez JA, Diaz-Guerra M, Scheiffele P, Scholl FG (2008) Dual-promoter lentiviral vectors for constitutive and regulated gene expression in neurons. *Journal of neuroscience methods* **168:** 104-112

Govek EE, Newey SE, Van Aelst L (2005) The role of the Rho GTPases in neuronal development. *Genes Dev* **19:** 1-49

Graf ER, Zhang X, Jin SX, Linhoff MW, Craig AM (2004) Neurexins induce differentiation of GABA and glutamate postsynaptic specializations via neuroligins. *Cell* **119:** 1013-1026

Graham DL, Eccleston JF, Lowe PN (1999) The conserved Arginine in Rho-GTPas-activating protein is essential for efficient catalysis but not for complex formation with RhoGDP and Aluminium Fluoride. *Biochemistry* **38:** 985 - 991

Guan R, Dai H, Rizo J (2008) Binding of the Munc13-1 MUN domain to membrane-anchored SNARE complexes. *Biochemistry* **47:** 1474-1481

Hall AC, Lucas FR, Salinas PC (2000) Axonal remodeling and synaptic differentiation in the cerebellum is regulated by WNT-7a signaling. *Cell* **100:** 525-535

Hall DH, Hedgecock EM (1991) Kinesin-related gene unc-104 is required for axonal transport of synaptic vesicles in C. elegans. *Cell* **65:** 837-847

Hallam SJ, Goncharov A, McEwen J, Baran R, Jin Y (2002) SYD-1, a presynaptic protein with PDZ, C2 and rhoGAP-like domains, specifies axon identity in C. elegans. *Nat Neurosci* **5:** 1137-1146

Hallermann S, Fejtova A, Schmidt H, Weyhersmuller A, Silver RA, Gundelfinger ED, Eilers J (2010) Bassoon speeds vesicle reloading at a central excitatory synapse. *Neuron* **68:** 710-723

Hata Y, Butz S, Südhof TC (1996) CASK: a novel dlg/PSD95 homolog with an N-terminal calmodulin-dependent protein kinase domain identified by interaction with neurexins. *The Journal of neuroscience : the official journal of the Society for Neuroscience* **16:** 2488-2494

Hibino H, Pironkova R, Onwumere O, Vologodskaia M, Hudspeth AJ, Lesage F (2002) RIM binding proteins (RBPs) couple Rab3-interacting molecules (RIMs) to voltage-gated Ca(2+) channels. *Neuron* **34:** 411-423

Hirokawa N, Sobue K, Kanda K, Harada A, Yorifuji H (1989) The cytoskeletal architecture of the presynaptic terminal and molecular structure of synapsin 1. *The Journal of cell biology* **108:** 111-126

Hofmann I, Munro S (2006) An N-terminally acetylated Arf-like GTPase is localised to lysosomes and affects their motility. *Journal of cell science* **119:** 1494-1503

Hoogenraad CC, Feliu-Mojer MI, Spangler SA, Milstein AD, Dunah AW, Hung AY, Sheng M (2007) Liprina1 degradation by calcium/calmodulin-dependent protein kinase II regulates LAR receptor tyrosine phosphatase distribution and dendrite development. *Developmental Cell* **12:** 587 - 602

Huang ZJ, Scheiffele P (2008) GABA and neuroligin signaling: linking synaptic activity and adhesion in inhibitory synapse development. *Curr Opin Neurobiol* **18:** 77-83

Inoue T, Heo WD, Grimley JS, Wandless TJ, Meyer T (2005) An inducible translocation strategy to rapidly activate and inhibit small GTPase signaling pathways. *Nature methods* **2:** 415-418

Itoh RE, Kurokawa K, Ohba Y, Yoshizaki H, Mochizuki N, Matsuda M (2002) Activation of rac and cdc42 video imaged by fluorescent resonance energy transfer-based single-molecule probes in the membrane of living cells. *Molecular and cellular biology* **22:** 6582-6591

Izeddin I, Boulanger J, Racine V, Specht CG, Kechkar A, Nair D, Triller A, Choquet D, Dahan M, Sibarita JB (2012) Wavelet analysis for single molecule localization microscopy. *Opt Express* **20:** 2081-2095

Jin Y, Garner CC (2008) Molecular mechanisms of presynaptic differentiation. *Annu Rev Cell Dev Biol* **24:** 237-262

Jordan R, Lemke EA, Klingauf J (2005) Visualization of synaptic vesicle movement in intact synaptic boutons using fluorescence fluctuation spectroscopy. *Biophysical journal* **89:** 2091-2102

Jullien N, Sampieri F, Enjalbert A, Herman JP (2003) Regulation of Cre recombinase by ligand-induced complementation of inactive fragments. *Nucleic acids research* **31:** e131

Kaeser PS, Deng L, Chavez AE, Liu X, Castillo PE, Südhof TC (2009) ELKS2alpha/CAST deletion selectively increases neurotransmitter release at inhibitory synapses. *Neuron* **64:** 227-239

Kaeser PS, Deng L, Wang Y, Dulubova I, Liu X, Rizo J, Südhof TC (2011) RIM proteins tether Ca2+ channels to presynaptic active zones via a direct PDZ-domain interaction. *Cell* **144:** 282-295

Kaufmann N, DeProto J, Ranjan R, Wan H, Van Vactor D (2002) Drosophila liprin-alpha and the receptor phosphatase Dlar control synapse morphogenesis. *Neuron* **34:** 27-38

Kayser MS, McClelland AC, Hughes EG, Dalva MB (2006) Intracellular and trans-synaptic regulation of glutamatergic synaptogenesis by EphB receptors. *The Journal of neuroscience : the official journal of the Society for Neuroscience* **26:** 12152-12164

Kennedy MJ, Hughes RM, Peteya LA, Schwartz JW, Ehlers MD, Tucker CL (2010) Rapid blue-light-mediated induction of protein interactions in living cells. *Nature methods* **7:** 973-975

Kim S, Ko J, Shin H, Lee JR, Lim C, Han JH, Altrock WD, Garner CC, Gundelfinger ED, Premont RT, Kaang BK, Kim E (2003) The GIT family of proteins forms multimers and associates with the presynaptic cytomatrix protein Piccolo. *The Journal of biological chemistry* **278:** 6291-6300

Kittel RJ, Wichmann C, Rasse TM, Fouquet W, Schmidt M, Schmid A, Wagh DA, Pawlu C, Kellner RR, Willig KI, Hell SW, Buchner E, Heckmann M, Sigrist SJ (2006) Bruchpilot promotes active zone assembly, Ca2+ channel clustering, and vesicle release. *Science* **312:** 1051-1054

Klassen MP, Wu YE, Maeder CI, Nakae I, Cueva JG, Lehrman EK, Tada M, Gengyo-Ando K, Wang GJ, Goodman M, Mitani S, Kontani K, Katada T, Shen K (2010) An Arf-like small G protein, ARL-8, promotes the axonal transport of presynaptic cargoes by suppressing vesicle aggregation. *Neuron* **66:** 710-723

Ko J, Kim S, Valtschanoff JG, Shin H, Lee JR, Sheng M, Premont RT, Weinberg RJ, Kim E (2003a) Interaction between liprin-alpha and GIT1 is required for AMPA receptor targeting. *The Journal of neuroscience : the official journal of the Society for Neuroscience* **23:** 1667-1677

Ko J, Na M, Kim S, Lee JR, Kim E (2003b) Interaction of the ERC family of RIM-binding proteins with the liprin-alpha family of multidomain proteins. *The Journal of biological chemistry* **278:** 42377-42385

Koushika SP, Richmond JE, Hadwiger G, Weimer RM, Jorgensen EM, Nonet ML (2001) A post-docking role for active zone protein Rim. *Nat Neurosci* **4:** 997-1005

Kraszewski K, Mundigl O, Daniell L, Verderio C, Matteoli M, De Camilli P (1995) Synaptic vesicle dynamics in living cultured hippocampal neurons visualized with CY3-conjugated antibodies directed against the lumenal domain of synaptotagmin. *The Journal of neuroscience : the official journal of the Society for Neuroscience* **15:** 4328-4342

Kwon S-K, Woo J, Kim S-Y, Kim H, Kim E (2010) Trans-synaptic adhesions between Netrin-G Ligand-3 (NGL-3) and receptor tyrosine phosphatases LAR, protein-tyrosine phosphatase d (PTPd), and PTPs via specific domains regulate excitatory synapse formation. *Journal of Biological Chemistry* **285:** 13966 - 13978

Leal-Ortiz S, Waites CL, Terry-Lorenzo R, Zamorano P, Gundelfinger ED, Garner CC (2008) Piccolo modulation of Synapsin1a dynamics regulates synaptic vesicle exocytosis. *The Journal of cell biology* **181:** 831-846

Linhoff MW, Lauren J, Cassidy RM, Dobie FA, Takahashi H, Nygaard HB, Airaksinen MS, Strittmatter SM, Craig AM (2009) An Unbiased Expression Screen for Synaptogenic Proteins Identifies the LRRTM Protein Family as Synaptic Organizers. *Neuron* **61:** 734-749

Lucido AL, Suarez Sanchez F, Thostrup P, Kwiatkowski AV, Leal-Ortiz S, Gopalakrishnan G, Liazoghli D, Belkaid W, Lennox RB, Grutter P, Garner CC, Colman DR (2009) Rapid assembly of functional presynaptic boutons triggered by adhesive contacts. *The Journal of neuroscience : the official journal of the Society for Neuroscience* **29:** 12449-12466

Luo L (2000) Rho GTPases in neuronal morphogenesis. *Nature reviews Neuroscience* **1:** 173-180

Maas C, Torres VI, Altrock WD, Leal-Ortiz S, Wagh D, Terry-Lorenzo RT, Fejtova A, Gundelfinger ED, Ziv NE, Garner CC (2012) Formation of Golgi-derived active zone precursor vesicles. *The Journal of neuroscience : the official journal of the Society for Neuroscience* **32:** 11095-11108

Maruyama IN, Brenner S (1991) A phorbol ester/diacylglycerol-binding protein encoded by the unc-13 gene of Caenorhabditis elegans. *Proceedings of the National Academy of Sciences of the United States of America* **88:** 5729-5733

Matus A, Ackermann M, Pehling G, Byers HR, Fujiwara K (1982) High actin concentrations in brain dendritic spines and postsynaptic densities. *Proceedings of the National Academy of Sciences of the United States of America* **79:** 7590-7594

Maximov A, Südhof TC, Bezprozvanny I (1999) Association of neuronal calcium channels with modular adaptor proteins. *The Journal of biological chemistry* **274:** 24453-24456

Miller KE, DeProto J, Kaufmann N, Patel BN, Duckworth A, Van Vactor D (2005) Direct observation demonstrates that liprin-alpha is required for trafficking of synaptic vesicles. *Current Biology* **15:** 684-689

Moskwa P, Paclet MN, Dagher MC, Ligeti E (2005) Autoinhibition of p50 Rho GTPase-activating protein (GAP) is released by prenylated small GTPases. *Journal of Biological Chemistry* **280:** 6716-6720

Mukherjee K, Yang X, Gerber SH, Kwon HB, Ho A, Castillo PE, Liu X, Südhof TC (2010) Piccolo and bassoon maintain synaptic vesicle clustering without directly participating in vesicle exocytosis. *Proceedings of the National Academy of Sciences of the United States of America* **107:** 6504-6509

Nyanguile O, Uesugi M, Austin DJ, Verdine GL (1997) A nonnatural transcriptional coactivator. *Proceedings of the National Academy of Sciences of the United States of America* **94:** 13402-13406

O'Brien RJ, Xu D, Petralia RS, Steward O, Huganir RL, Worley P (1999) Synaptic clustering of AMPA receptors by the extracellular immediate-early gene product Narp. *Neuron* **23:** 309-323

Ohtsuka T, Takao-Rikitsu E, Inoue E, Inoue M, Takeuchi M, Matsubara K, Deguchi-Tawarada M, Satoh K, Morimoto K, Nakanishi H, Takai Y (2002) CAST: a novel protein of the cytomatrix at the active zone of synapses that forms a ternary complex with RIM1 and Munc13-1. *Journal of Cell Biology* **158:** 577-590

Okada Y, Yamazaki H, Sekine-Aizawa Y, Hirokawa N (1995) The neuron-specific kinesin superfamily protein KIF1A is a unique monomeric motor for anterograde axonal transport of synaptic vesicle precursors. *Cell* **81:** 769-780

Olsen O, Moore KA, Fukata M, Kazuta T, Trinidad JC, Kauer FW, Streuli M, Misawa H, Burlingame AL, Nicoll RA, Bredt DS (2005) Neurotransmitter release regulated by a MALS-Liprin-a presynaptic complex. *Journal of Cell Biology* **170:** 1127 - 1134

Owald D, Fouquet W, Schmidt M, Wichmann C, Mertel S, Depner H, Christiansen F, Zube C, Quentin C, Körner J, Urlaub H, Mechtler K, Sigrist SJ (2010) A Syd-1 homologue regulates pre- and postsynaptic maturation in Drosophila. *The Journal of cell biology* **188:** 565-579

Owald D, Khorramshahi O, Gupta VK, Banovic D, Depner H, Fouquet W, Wichmann C, Mertel S, Eimer S, Reynolds E, Holt M, Aberle H, Sigrist SJ (2012) Cooperation of Syd-1 with Neurexin synchronizes pre- with postsynaptic assembly. *Nat Neurosci* **15:** 1219-1226

Patel MR, Lehrman EK, Poon VY, Crump JG, Zhen M, Bargmann CI, Shen K (2006) Hierarchical assembly of presynaptic components in defined C. elegans synapses. *Nat Neurosci* **9:** 1488-1498

Patel MR, Shen K (2009) RSY-1 Is a Local Inhibitor of Presynaptic Assembly in C. elegans. *Science* **323:** 1500-1503

Pawson C, Eaton BA, Davis GW (2008) Formin-Dependent Synaptic Growth: Evidence That Dlar Signals via Diaphanous to Modulate Synaptic Actin and Dynamic Pioneer Microtubules. *Journal of Neuroscience* **28:** 11111-11123

Pertz O (2010) Spatio-temporal Rho GTPase signaling - where are we now? *Journal of cell science* **123:** 1841-1850

Pertz O, Hodgson L, Klemke RL, Hahn KM (2006) Spatiotemporal dynamics of RhoA activity in migrating cells. *Nature* **440:** 1069-1072

Racine V, Sachse M, Salamero J, Fraisier V, Trubuil A, Sibarita J-B (2006) Visualization and quantification of vesicle trafficking on a three-dimensional cytoskeleton network in living cells. *Journal of Microscopy* **225:** 214 - 228

Rankin CH, Beck CD, Chiba CM (1990) Caenorhabditis elegans: a new model system for the study of learning and memory. *Behavioural brain research* **37:** 89-92

Rizzoli SO, Betz WJ (2005) Synaptic vesicle pools. *Nature reviews Neuroscience* **6:** 57-69

Rosenberger G, Kutsche K (2006) AlphaPIX and betaPIX and their role in focal adhesion formation. *European journal of cell biology* **85:** 265-274

Rosenmund C, Sigler A, Augustin I, Reim K, Brose N, Rhee JS (2002) Differential control of vesicle priming and short-term plasticity by Munc13 isoforms. *Neuron* **33:** 411-424

Sabo SL, Gomes RA, McAllister AK (2006) Formation of presynaptic terminals at predefined sites along axons. *The Journal of neuroscience : the official journal of the Society for Neuroscience* **26:** 10813-10825

Samuels BA, Hsueh YP, Shu T, Liang H, Tseng HC, Hong CJ, Su SC, Volker J, Neve RL, Yue DT, Tsai LH (2007) Cdk5 promotes synaptogenesis by regulating the subcellular distribution of the MAGUK family member CASK. *Neuron* **56:** 823-837

Sankaranarayanan S, Atluri PP, Ryan TA (2003) Actin has a molecular scaffolding, not propulsive, role in presynaptic function. *Nature Neuroscience* **6:** 127 - 135

Schaefer AM, Hadwiger GD, Nonet ML (2000) rpm-1, a conserved neuronal gene that regulates targeting and synaptogenesis in C. elegans. *Neuron* **26:** 345-356

Scheffzek K, Ahmadian MR (2005) GTPase activating proteins: structural and functional insights 18 years after discovery. *Cell Mol Life Sci* **62:** 3014-3038

Scheiffele P, Fan J, Choih J, Fetter R, Serafini T (2000) Neuroligin expressed in nonneuronal cells triggers presynaptic development in contacting axons. *Cell* **101:** 657-669

Schoch S, Castillo PE, Jo T, Mukherjee K, Geppert M, Wang Y, Schmitz F, Malenka RC, Südhof T (2002) Rim1alpha forms a protein scaffold for regulating neurotransmitter release at the active zone. *Nature* **415:** 321 - 326

Schoch S, Mittelstaedt T, Kaeser PS, Padgett D, Feldmann N, Chevaleyre V, Castillo PE, Hammer RE, Han W, Schmitz F, Lin W, Südhof TC (2006) Redundant functions of RIM1alpha and RIM2alpha in Ca(2+)-triggered neurotransmitter release. *The EMBO journal* **25:** 5852-5863

Serra-Pagès C, Kedersha NL, Fazikas L, Medley Q, Debant A, Streuli M (1995) The LAR transmembrane protein tyrosine phosphatase and a coiled-coil LAR-interacting protein co-localize at focal adhesions. *EMBO Journal* **14:** 2827 - 2838

Serra-Pagès C, Medley, QG, Tang, M, Hart, A and Streuli, M (1998) Liprins, a family of LAR transmembrane protein-tyrosine phosphatase-interacting proteins. *Journal of Biological Chemistry* **273:** 15611 - 15620

Shapira M, Zhai RG, Dresbach T, Bresler T, Torres VI, Gundelfinger ED, Ziv NE, Garner CC (2003) Unitary assembly of presynaptic active zones from Piccolo-Bassoon transport vesicles. *Neuron* **38:** 237-252

Shapiro L, Fannon AM, Kwong PD, Thompson A, Lehmann MS, Grubel G, Legrand JF, Als-Nielsen J, Colman DR, Hendrickson WA (1995) Structural basis of cell-cell adhesion by cadherins. *Nature* **374:** 327-337

Shen K, Scheiffele P (2010) Genetics and cell biology of building specific synaptic connectivity. *Annual review of neuroscience* **33:** 473-507

Shin H, Wyszynski M, Huh KH, Valtschanoff JG, Lee JR, Ko J, Streuli M, Weinberg RJ, Sheng M, Kim E (2003) Association of the kinesin motor KIF1A with the multimodular protein liprin-alpha. *The Journal of biological chemistry* **278:** 11393-11401

Shupliakov O, Bloom O, Gustafsson JS, Kjaerulff O, Low P, Tomilin N, Pieribone VA, Greengard P, Brodin L (2002) Impaired recycling of synaptic vesicles after acute perturbation of the presynaptic actin cytoskeleton. *Proceedings of the National Academy of Sciences of the United States of America* **99:** 14476-14481

Sieburth D, Ch'ng Q, Dybbs M, Tavazoie M, Kennedy S, Wang D, Dupuy D, Rual J-F, Hill DE, Vidal M, Ruvkun G, Kaplan JM (2005) Systemic analysis of genes required for synapse structure and function. *Nature* **436:** 510 - 517

Sigrist SJ, Schmitz D (2011) Structural and functional plasticity of the cytoplasmic active zone. *Curr Opin Neurobiol* **21:** 144-150

Singh S, Narang AS, Mahato RI (2011) Subcellular fate and off-target effects of siRNA, shRNA, and miRNA. *Pharmaceutical research* **28:** 2996-3015

Skarnes WC, Rosen B, West AP, Koutsourakis M, Bushell W, Iyer V, Mujica AO, Thomas M, Harrow J, Cox T, Jackson D, Severin J, Biggs P, Fu J, Nefedov M, de Jong PJ, Stewart AF, Bradley A (2011) A conditional knockout resource for the genome-wide study of mouse gene function. *Nature* **474:** 337-342

Spangler SA, Jaarsma D, De Graaff E, Wulf PS, Akhmanova A, Hoogenraad CC (2011) Differential expression of liprin-alpha family proteins in the brain suggests functional diversification. *The Journal of comparative neurology* **519:** 3040-3060

Spencer DM, Wandless TJ, Schreiber SL, Crabtree GR (1993) Controlling signal transduction with synthetic ligands. *Science* **262:** 1019-1024

Stan A, Pielarski KN, Brigadski T, Wittenmayer N, Fedorchenko O, Gohla A, Lessmann V, Dresbach T, Gottmann K (2010) Essential cooperation of N-cadherin and neuroligin-1 in the transsynaptic control of vesicle accumulation. *Proceedings of the National Academy of Sciences of the United States of America* **107:** 11116-11121

Stavoe AK, Colon-Ramos DA (2012) Netrin instructs synaptic vesicle clustering through Rac GTPase, MIG-10, and the actin cytoskeleton. *The Journal of cell biology* **197:** 75-88

Su Q, Cai Q, Gerwin C, Smith CL, Sheng ZH (2004) Syntabulin is a microtubule-associated protein implicated in syntaxin transport in neurons. *Nature cell biology* **6:** 941-953

Su SC, Seo J, Pan JQ, Samuels BA, Rudenko A, Ericsson M, Neve RL, Yue DT, Tsai LH (2012) Regulation of N-type Voltage-Gated Calcium Channels and Presynaptic Function by Cyclin-Dependent Kinase 5. *Neuron* **75:** 675-687

Südhof TC (2012) The presynaptic active zone. *Neuron* **75:** 11-25

Sun Y, Aiga M, Yoshida E, Humbert PO, Bamji SX (2009) Scribble interacts with beta-catenin to localize synaptic vesicles to synapses. *Molecular biology of the cell* **20:** 3390-3400

Sun Y, Bamji SX (2011) beta-Pix modulates actin-mediated recruitment of synaptic vesicles to synapses. *The Journal of neuroscience : the official journal of the Society for Neuroscience* **31:** 17123-17133

Tahirovic S, Bradke F (2009) Neuronal polarity. *Cold Spring Harb Perspect Biol* **1:** a001644

Takahashi H, Arstikaitis P, Prasad T, Bartlett TE, Wang YT, Murphy TH, Craig AM (2011) Postsynaptic TrkC and Presynaptic PTPsigma function as a bidirectional excitatory synaptic organizing complex. *Neuron* **69:** 287 - 303

Takahashi H, Katayama K, Sohya K, Miyamoto H, Prasad T, Matsumoto Y, Ota M, Yasuda H, Tsumoto T, Aruga J, Craig AM (2012) Selective control of inhibitory synapse development by Slitrk3-PTPdelta trans-synaptic interaction. *Nat Neurosci* **15:** 389-398, S381-382

Takao-Rikitsu E, Mochida S, Inoue E, Deguchi-Tawarada M, Inoue M, Ohtsuka T, Takai Y (2004) Physical and functional interaction of the active zone proteins, CAST, RIM1, and Bassoon, in neurotransmitter release. *The Journal of cell biology* **164:** 301-311

Tanaka H, Shan W, Phillips GR, Arndt K, Bozdagi O, Shapiro L, Huntley GW, Benson DL, Colman DR (2000) Molecular modification of N-cadherin in response to synaptic activity. *Neuron* **25:** 93-107

Taniguchi H, Gollan L, Scholl FG, Mahadomrongkul V, Dobler E, Limthong N, Peck M, Aoki C, Scheiffele P (2007) Silencing of neuroligin function by postsynaptic neurexins. *The Journal of neuroscience : the official journal of the Society for Neuroscience* **27:** 2815-2824

Taru H, Jin YS (2011) The Liprin Homology Domain Is Essential for the Homomeric Interaction of SYD-2/Liprin-alpha Protein in Presynaptic Assembly. *Journal of Neuroscience* **31:** 16261-16268

Tolias KF, Duman JG, Um K (2011) Control of synapse development and plasticity by Rho GTPase regulatory proteins. *Prog Neurobiol* **94:** 133-148

tom Dieck S, Sanmarti-Vila L, Langnaese K, Richter K, Kindler S, Soyke A, Wex H, Smalla KH, Kampf U, Franzer JT, Stumm M, Garner CC, Gundelfinger ED (1998) Bassoon, a novel zinc-finger CAG/glutamine-repeat protein selectively localized at the active zone of presynaptic nerve terminals. *The Journal of cell biology* **142:** 499-509

Tompa P (2002) Intrinsically unstructured proteins. *Trends Biochem Sci* **27:** 527-533

Toonen RF, de Vries KJ, Zalm R, Sudhof TC, Verhage M (2005) Munc18-1 stabilizes syntaxin 1, but is not essential for syntaxin 1 targeting and SNARE complex formation. *Journal of neurochemistry* **93:** 1393-1400

Tucker CL (2012) Manipulating cellular processes using optical control of protein-protein interactions. *Progress in brain research* **196:** 95-117

Umemori H, Linhoff MW, Ornitz DM, Sanes JR (2004) FGF22 and its close relatives are presynaptic organizing molecules in the mammalian brain. *Cell* **118:** 257-270

Vallee RB, Williams JC, Varma D, Barnhart LE (2004) Dynein: An ancient motor protein involved in multiple modes of transport. *Journal of neurobiology* **58:** 189-200

van Roessel P, Elliott DA, Robinson IM, Prokop A, Brand AH (2004) Independent regulation of synaptic size and activity by the anaphase-promoting complex. *Cell* **119:** 707-718

Wagh DA, Rasse TM, Asan E, Hofbauer A, Schwenkert I, Durrbeck H, Buchner S, Dabauvalle MC, Schmidt M, Qin G, Wichmann C, Kittel R, Sigrist SJ, Buchner E (2006) Bruchpilot, a protein with homology to ELKS/CAST, is required for structural integrity and function of synaptic active zones in Drosophila. *Neuron* **49:** 833-844

Waites CL, Leal-Ortiz SA, Andlauer TF, Sigrist SJ, Garner CC (2011) Piccolo regulates the dynamic assembly of presynaptic F-actin. *The Journal of neuroscience : the official journal of the Society for Neuroscience* **31:** 14250-14263

Wang X, Hu B, Zimmermann B, Kilimann MW (2001) Rim1 and Rabphilin-3 bind Rab3-GTP by composite determinants partially related through N-terminal a-helix motifs. *The Journal of biological chemistry* **276:** 32480 - 32588

Wang XH, Zheng JQ, Poo MM (1996) Effects of cytochalasin treatment on short-term synaptic plasticity at developing neuromuscular junctions in frogs. *The Journal of physiology* **491 (Pt 1):** 187-195

Wang Y, Okamoto M, Schmitz F, Hofmann K, Südhof TC (1997) Rim is a putative Rab3 effector in regulating synaptic-vesicle fusion. *Nature* **388:** 593-598

Wang Y, Südhof TC (2003) Genomic definition of RIM proteins: evolutionary amplification of a family of synaptic regulatory proteins(small star, filled). *Genomics* **81:** 126-137

Watanabe M, Nomura K, Ohyama A, Ishikawa R, Komiya Y, Hosaka K, Yamauchi E, Taniguchi H, Sasakawa N, Kumakura K, Ushiki T, Sato O, Ikebe M, Igarashi M (2005) Myosin-Va regulates exocytosis through the submicromolar Ca2+-dependent binding of syntaxin-1A. *Molecular biology of the cell* **16:** 4519-4530

Wei Z, Zheng S, Spangler SA, Yu C, Hoogenraad CC, Zhang M (2011) Liprin-mediated large signaling complex organization revealed by the Liprin-a/CASK and Liprin-a/Liprin-b complex structures. *Molecular Cell* **43:** 586 - 598

Williams RW, Herrup K (1988) The control of neuron number. *Annual review of neuroscience* **11:** 423-453

Woo J, Kwon SK, Choi S, Kim S, Lee JR, Dunah AW, Sheng M, Kim E (2009) Trans-synaptic adhesion between NGL-3 and LAR regulates the formation of excitatory synapses. *Nature Neuroscience* **12:** 428-437

Wyszynski M, Kim E, Dunah AW, Passafaro M, Valtschanoff JG, Serra-Pages C, Streuli M, Weinberg RJ, Sheng M (2002) Interaction between GRIP and liprin-alpha/SYD2 is required for AMPA receptor targeting. *Neuron* **34:** 39-52

Yao J, Qi J, Chen G (2006) Actin-dependent activation of presynaptic silent synapses contributes to long-term synaptic plasticity in developing hippocampal neurons. *The Journal of neuroscience : the official journal of the Society for Neuroscience* **26:** 8137-8147

Yoshida T, Yasumura M, Uemura T, Lee S-J, Ra M, Taguchi R, Iwakura Y, Mishina M (2011) IL-1 receptor accessory protein-like 1 associated with mental retardation an autism mediates synapse formation by trans-synaptic interaction with protein tyrosine phosphatese delta. *Journal of Neuroscience* **31:** 13485 - 13499

Zhai RG, Vardinon-Friedman H, Cases-Langhoff C, Becker B, Gundelfinger ED, Ziv NE, Garner CC (2001) Assembling the presynaptic active zone: a characterization of an active one precursor vesicle. *Neuron* **29:** 131-143

Zhang W, Benson DL (2001) Stages of synapse development defined by dependence on F-actin. *The Journal of neuroscience : the official journal of the Society for Neuroscience* **21:** 5169-5181

Zhen M, Jin Y (1999) The liprin protein SYD-2 regulates the differentiation of presynaptic termini in C. elegans. *Nature* **401:** 371-375

Ziv NE, Garner CC (2004) Cellular and molecular mechanisms of presynaptic assembly. *Nature reviews Neuroscience* **5:** 385-399

Zürner M, Mittelstaedt T, Dieck ST, Becker A, Schoch S (2011) Analysis of the spatiotemporal expression and subcellular localization of Liprin-alpha proteins. *The Journal of comparative neurology* **519:** 3019 - 3039

Zürner M, Schoch S (2009) The mouse and human Liprin-alpha family of scaffolding proteins: genomic organization, expression profiling and regulation by alternative splicing. *Genomics* **93:** 243-253

Acknowledgements

First of all, I would like to thank my advisor Peter Scheiffele, for his ongoing support during the last years. His enthusiasm for science has always been contagious and has motivated me many times to take a second look and discover exciting findings that would have remained unseen otherwise. We had very fruitful discussions and his good ideas repeatedly brought the project forward and out of situations that seemed to be dead ends at first. But also I would like to thank him for giving me the freedom to pursue my own ideas. Finally I am grateful for all the lab skiing and hiking trips that we did during the last years, which were always a lot of fun and contributed to an enjoyable lab atmosphere.

In particular, I am very thankful to Julia Sommer, who allowed me to join in on her project. As a starting PhD student, I was very lucky to be able to work with her and learn from her. She was a great teacher for me, always very supportive and enthusiastic about my first results, which meant a lot to me. During our work together, I learned how important it is to discuss your results and your problems with someone else, how much easier it is to cope with disappointments if they are shared and how much nicer it is to share success. Finally, I also would like to thank her for her friendship outside work, for our runs together and for making my first months in Basel very enjoyable.

I am grateful to all members of the Scheiffele lab. Everyone has been very helpful and supportive throughout the years, which has contributed to a nice lab atmosphere and made me enjoy every single day at work. In particular, I would like to thank Fatiha Boukhtouche, for many, many explanations about lab techniques, mouse breedings, brain development etc., for listening to me and keeping my morals up during difficult situations, for her friendship that means a lot to me, for all the amazing dinners that she organized and finally for taking me to a very special party during my first week in Basel ☺. I would like to thank Stephane Baudouin for his support on image analysis, that was very important for my work, for all the fruitful discussions, for his friendship and finally for very helpful comments on this manuscript. I want to thank Harald Witte for his help with various techniques, lab reagents, the plasmid database ☺ and his friendship and Dietmar Schreiner for good advice and sharing his plasmids with me. I also would like to thank Laetitia Hatstatt for help with mice work and last minute biopsies for genotyping and for her help with perfusions. Finally, I am grateful to Ramya Nair, who introduced me to the world of electrophysiology and who made an important contribution to this manuscript.

I was very fortunate to get a lot of help from Adeline Stiefvater, who made a heroic effort to purify all these recombinant proteins that were so important for this work. Together, we generated over 75 different DNA constructs. She also helped me in all the mouse work,

taught me how to handle the mice and saved me a lot of time and worries by keeping a close eye on my mouse colonies.

I am grateful to my committee members Yves-Alain Barde and Olivier Pertz for their good ideas, ongoing support and reagents. The fact that not only their door but also the door of their lab members was always open for me was very important for the success of my project. I got a lot of good advice and reagents from everyone.

I am also thankful to Mingjie Zhang, Eunjoon Kim, Matthijs Verhage, Casper Hoogenraad and Susanne Schoch for providing us with valuable reagents. Furthermore, I would like to thank Stephan Sigrist and his lab members for sharing their results on *Drosophila* DSYD-1 with us and helpful discussion and comments. I also would like to thank Tim Sharpe from the Biophysics Facility of the Biozentrum for providing fast help with a new Fluorimeter that suddenly replaced the old one that I had used before and was the reason for a lot of worries during the last weeks of my studies.

Also, I would like to thank the Transgenic Mouse Facility at the Biozentrum for the generation of the mSYD1A knockout mice, which I unfortunately did not have time to analyze in this study, but which will be the beginning of an exciting new project.

I would like to thank the Werner-Siemens Foundation for their financial support during my PhD.

Ich möchte meinen Eltern und meinem Bruder für ihre fortwährende Unterstützung danken. Ohne eure Hilfe wäre ich nicht hier und wäre diese Arbeit nicht möglich gewesen. Ich weiß, dass ihr mich oft entbehren musstet in den letzten Jahren und ich weiß es sehr zu schätzen, dass ihr immer für mich da seid, wenn ich euch brauche.

Finalmente voglio ringraziare il mio ragazzo Stefano per tutto il suo appoggio e amore. Ero molto fortunata di averti incontrato nella mia prima settimana in Basilea. Mi hai incoraggiato tante volte quando ero delusa o triste. Abbiamo passato tante fine settimane eccezionale e emozionante insieme che significano molto per me e che dimenticherò mai. Primo di averti incontrato non ho creduto che esiste il vero amore.